MOUNTAIN-PLAINS CONSORTIUM

MPC 24-517 | B.R. Cox, T. Jackson, and N.Dawadi

CALIBRATING GROUND RESPONSE ANALYSES BENEATH AN INSTRUMENTED BRIDGE USING THE I-15 BOREHOLE ARRAY AND GROUND MOTIONS FROM THE 2020 M5.7 MAGNA EARTHQUAKE

MOUNTAIN-PLAINS CONSORTIUM REGION 8

A University Transportation Center sponsored by the U.S. Department of Transportation serving the Mountain-Plains Region. Consortium members:

Colorado State University
North Dakota State University
South Dakota State University
University of Colorado Denver
University of Denver
University of Utah
Utah State University
University of Wyoming

Technical Report Documentation Page

1. Report No.	2. Government Accession No.	3. Recipient's Catalog No.
MPC-694		

4. Title and Subtitle	5. Report Date
Calibrating Ground Response Analyses Beneath an Instrumented Bridge using the I-15 Borehole Array and Ground Motions from the 2020 M5.7 Magna Earthquake	March 2024
	6. Performing Organization Code

7. Author(s)	8. Performing Organization Report No.
Brady R. Cox, Ph.D., P.E. Tyler Jackson, B.S. Nishkarsha Dawadi, M.S.	MPC 24-517

9. Performing Organization Name and Address	10. Work Unit No. (TRAIS)
Dept. of Civil and Environmental Engineering Utah State University 4110 Old Main Hill Logan, UT 84322-4110	11. Contract or Grant No.

12. Sponsoring Agency Name and Address	13. Type of Report and Period Covered
Mountain-Plains Consortium North Dakota State University PO Box 6050, Fargo, ND 58108	Final Report
	14. Sponsoring Agency Code

15. Supplementary Notes

Supported by a grant from the US DOT, University Transportation Centers Program

16. Abstract

The I-15 Downhole Array (I15DA) is located near the intersection of I-15 and I-80 in Salt Lake City, Utah. This downhole array is installed in soft soil deposited by Lake Bonneville, where depth to bedrock is expected to be at a considerable depth. The soil conditions at the I15DA are representative of other sites in deep, sediment-filled valleys throughout the state (e.g., the Utah, Salt Lake, and Cache valleys), and understanding the seismic response at the downhole array is crucial to determine how to conduct numerical site response analyses at other locations across the state. The I15DA recorded a number of aftershocks following the 2020 M5.7 Magna Earthquake, and these ground motion records have been used to calibrate numerical site response analyses. This report details single- and multi-dimensional site response studies aimed at calculating theoretical transfer functions that capture the empirical transfer functions produced by small-strain ground motions recorded by horizontal components of sensors in the I15DA. We investigate the importance of accounting for spatial variability in shear wave velocity (Vs) during site response modeling using Vs obtained from invasive methods, non-invasive methods (i.e., surface wave inversion-derived Vs profiles), and a pseudo-3D Vs model developed using the H/V geostatistical approach.

17. Key Word	18. Distribution Statement
boreholes, bridges, calibration, earthquakes, instrumentation, seismicity	Public distribution

19. Security Classif. (of this report)	20. Security Classif. (of this page)	21. No. of Pages	22. Price
Unclassified	Unclassified	105	n/a

Form DOT F 1700.7 (8-72) Reproduction of completed page authorized

Calibrating Ground Response Analyses Beneath an Instrumented Bridge using the I-15 Borehole Array and Ground Motions from the 2020 M5.7 Magna Earthquake

Brady R. Cox, Ph.D., P.E.
Tyler Jackson, B.S.
Nishkarsha Dawadi, M.S.

Department of Civil and Environmental Engineering
Utah State University

March 2024

Acknowledegments

We would like to thank Mr. Jon Rusho, Dr. Kristine Pankow, and Dr. Keith Koper from the University of Utah Seismographs Stations for their help with obtaining the ground motions recorded by the Interstate-15 Downhole Array (I15DA) during the aftershock sequence of the 2020 M5.7 Magna Earthquake.

Disclaimer

The contents of this report reflect the views of the authors, who are responsible for the facts and the accuracy of the information presented. This document is disseminated under the sponsorship of the Department of Transportation, University Transportation Centers Program, in the interest of information exchange. The U.S. Government assumes no liability for the contents or use thereof.

ABSTRACT

The I-15 Downhole Array (I15DA) is located near the intersection of I-15 and I-80 in Salt Lake City, Utah. This downhole array is installed in soft soil deposited by Lake Bonneville, where depth to bedrock is expected to be at a considerable depth. The soil conditions at the I15DA are representative of other sites in deep, sediment-filled valleys throughout the state (e.g., the Utah, Salt Lake, and Cache valleys), and understanding the seismic response at the downhole array is crucial to determine how to conduct numerical site response analyses at other locations across the state. The I15DA recorded a number of aftershocks following the 2020 M5.7 Magna Earthquake, and these ground motion records have been used to calibrate numerical site response analyses. This report details single- and multi-dimensional site response studies aimed at calculating theoretical transfer functions that capture the empirical transfer functions produced by small-strain ground motions recorded by horizontal components of sensors in the I15DA. We investigate the importance of accounting for spatial variability in shear wave velocity (Vs) during site response modeling using Vs obtained from invasive methods, non-invasive methods (i.e., surface wave inversion-derived Vs profiles), and a pseudo-3D Vs model developed using the H/V geostatistical approach.

TABLE OF CONTENTS

LIST OF FIGURES

LIST OF TABLES

EXECUTIVE SUMMARY

The I-15 Downhole Array (I15DA) is located near the south intersection of I-15 and I-80 in South Salt Lake City, which is a seismically active region of Utah. This downhole array was installed in 2003 (Youd and Briggs, 2003) and largely sat dormant without recording any significant earthquake ground motions until the 2020 M5.7 Magna Earthquake. Unfortunately, due to loss of power at the site and other unforeseen technical issues, the main shock of the Magna Earthquake was only partially recorded by the array. However, a number of important aftershocks were fully recorded. This report provides details about the I15DA, and attempts made to calibrate single- and multi-dimensional (i.e., 1D and 2D) seismic site response analyses for the site using the ground motions recorded at the surface and at the deepest (120 m) reference sensor.

The I15DA site is installed in soft soil deposited by Lake Bonneville, where depth to bedrock is expected to be at a considerable depth. The soil conditions at the I15DA are representative of soil conditions in deep, sediment-filled valleys throughout the state of Utah (e.g., the Utah, Salt Lake, and Cache valleys), and understanding the site response of the downhole array is crucial to determine how to properly conduct site response at other locations across the state. Furthermore, the I15DA is located close to an instrumented bridge at the interchange between I-15 and I-80 (Halling and Petty, 2001). Thus, this site provides a unique opportunity for future studies aimed at understanding soil-foundation-structure interaction (SFSI) effects using the ground motions recorded simultaneously by the downhole array and the bridge instrumentation.

This report details 1D and 2D numerical site response modeling efforts at the I15DA. Specifically, theoretical transfer functions (TTFs) obtained from numerical site response modeling are compared with empirical transfer functions (ETFs) calculated from the small-strain ground motions recorded by horizontal components of sensors in the array. We investigate the importance of accounting for spatial variability in shear-wave velocity (Vs) for site response modeling through: (1) 1D site response modeling using an invasive Vs profile measured in a borehole of the I15DA, (2) 1D site response modeling using several Vs profiles inverted from non-invasive surface wave testing, and (3) 2D site response modeling using a pseudo-3D Vs model obtained from a horizontal-to-vertical (H/V) spectral ratio geostatistical approach.

From the results of site response modeling obtained in this study, it is clear that properly incorporating spatial variability produces TTFs that more closely match the ETFs recorded by the I15DA. All site response models produced estimates of the fundamental resonant frequency that are quite similar to the fundamental resonance of the median ETF. However, the 1D site response analyses based on the invasive- and surface wave inversion-derived Vs profiles tend to produce estimates of amplification at the fundamental mode that are 15 to 20 times greater than the amplification exhibited by the median ETF. The amplification estimated by the 2D site response is more accurate but still 10 to 12 times greater than the median ETF. This over-prediction of amplification is consistent with the results of 1D and 2D site response analyses at other downhole array sites in the United States and throughout the world (e.g., Hallal et al. 2022). It is hoped that future 3D site response analyses based on the psuedo-3D Vs model derived herein for the I15DA will be able to produce estimates of TTFs that better fit the ETF.

1. I15DA SITE INFORMATION

The I-15 Downhole Array (I15DA) is located near the south intersection of I-15 and I-80 in South Salt Lake City, Utah. This is a seismically active area of Utah that is approximately 5 km west of the Salt Lake City section of the Wasatch Fault zone and approximately 4 km east of the Taylorsville section of the West Valley Fault zone. The downhole array is installed in soft soil deposited by Lake Bonneville, where depth to bedrock is expected to be at a considerable depth. The soil conditions at the I15DA are representative of soil conditions in deep, sediment-filled valleys throughout the state of Utah (e.g., the Utah, Salt Lake, and Cache valleys). Work to install the array began in April of 2002 and finished in April of 2003 (Youd and Briggs, 2003).

The array is made up of five, three-component force-balance accelerometers (FBA). One of the sensors was installed on the surface, and the other sensors were installed at depths of 7.6, 18.3, 48.8, and 119.8 m. The depth-locations of these sensors are shown schematically in Figure 1.1. The boreholes for all the sensors were cased with PVC and grouted in place. In this report, each sensor in the I15DA is referred to as DH (downhole) and sequentially numbered 0 through 4 based on the depth of the sensor. The surface sensor is called DH_0, the 7.6-m sensor is DH_1, the 18.3-m sensor is DH_2, the 48.8-m sensor is DH_3, and the 119.8-m sensor is DH_4. The sensors were set to continuously monitor and were triggered to store data when any sensor in the array sensed accelerations greater than 0.01 g. Unfortunately, due to a loss of power and data buffering/telemetry issues at the site, none of these sensors fully captured the main shock of the 2020 M5.7 Magna Earthquake. However, sensors DH_0 and DH_4 recorded data during a portion of the aftershocks following the main event.

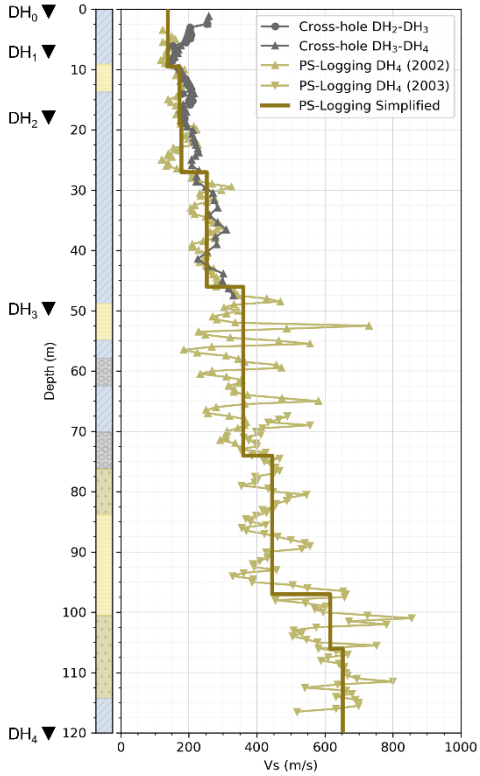

Figure 1.1 Lithologic soil log, invasive Vs profiles, and downhole sensor locations for the I15DA. The red profile shows the PS-logging profile simplified to nine layers. Each downhole sensor is shown at its as-built depth to the left of the lithologic log.

Though they are not used in this study, an additional nine FBAs were installed on Bridge C-846 above the I15DA site (Halling and Petty, 2001). Similarly, none of these sensors recorded the main shock of the 2020 M5.7 Magna earthquake, though some sensors recorded data during aftershocks following the event. These data can be used in future studies to model the soil-foundation-structure interaction (SFSI) of the bridge site.

As detailed in Youd and Briggs (2003), multiple invasive tests were performed to characterize the shear-wave velocity (Vs) profile of the subsurface. Cross-hole seismic testing was performed by Dr. James Bay from Utah State University between the boreholes for the DH_2 and DH_3 sensors, and between the boreholes for the DH_3 and DH_4 sensors. These profiles only extend to a depth of 50 m. Robert Steller from GEOVision performed two PS-logging tests in the borehole for the DH_4 sensor: (1) one test in 2002 to a depth of approximately 76 m, and (2) one test in 2003 from approximately 65 m to 116 m. As shown in Figure 1.1, the cross-hole and PS-logging results are quite similar to one another over the top 50 m. Since the PS-logging data capture the complete Vs profile between the DH_0 and DH_4 sensors, it is appropriate to use this profile in 1D site response analyses

between the two sensors. The measured Vs profile from PS-logging was simplified to nine layers before use in site response. The simplified PS-logging Vs profile, as well as a lithologic log compiled from soil cuttings in the DH_4 borehole, are shown in Figure 1.1.

2. EMPIRICAL TRANSFER FUNCTIONS

This section discusses the ground motion processing and empirical transfer function (ETF) calculations for aftershock events recorded by the I15DA following the 2020 M5.7 Magna Earthquake. As noted above, the mainshock was not recorded due to loss of power and data buffering/telemetry issues at the site. Thus, only the smaller strain ground motions from various events in the aftershock sequence are available. The ground motions used for calculating the ETF were provided by the University of Utah Seismograph Stations (UUSS; Jon Rusho, personal communication).

A total of 61 aftershock events with magnitudes greater than 2.0 were included in the continuous data stream recordings provided by the UUSS. The continuous data spanned from 18 March 2020 at 18:30 UTC (note that the main shock happened at approximately 13:00 UTC) to 26 March 2020 at 19:15 UTC. The 61 events had magnitudes that ranged from 2.0 to 4.57 and PGA values for the surface sensor that ranged from less than 0.001 to 0.132 g's. Because the largest magnitude event induced a relatively high PGA on the surface sensor (0.132 g), it was temporarily excluded from consideration when calculating the ETFs for small-strain ground motions. After removing this event, the magnitudes ranged from 2.88 to 3.94 with PGA values for the surface sensor that ranged from 0.002 to 0.032 g's. Unfortunately, after processing, only seven of the events generated high enough signal-to-noise ratios (SNR) on both the surface and 120-m sensors over a bandwidth large enough to capture the first four modes (i.e., fundamental frequency and first-, second-, and third-higher modes) of the ETF. The ground motion processing and ETF calculations are described in detail below.

2.1 Aftershock Time Histories

The ground motions were provided in their rawest form in a continuous data stream (not triggered). The raw data were first sorted by sensor depth and component of interest. For this particular study, only the horizontal components (both north and east) recorded by the DH_0 and DH_4 sensors were considered. Records with the prefix of "40" were recorded by the DH_4 sensor at a depth of 120 m, while records with the prefix "F0" were recorded by the DH_0 sensor on the ground surface. A list of aftershocks from the Magna Earthquake was obtained using the "Search Earthquake Catalog" tool provided by the ANSS Comprehensive Catalog (ComCat) on the United States Geological Survey (USGS) website. Using this list, the continuous data streams for each component of each sensor were parsed to extract each aftershock event. The ground motion records were trimmed with a buffer of 40 seconds before and 90 seconds after the ComCat catalog event start time to make sure the pre-event noise and the total signal was captured in the event specific traces.

2.2 Ground Motion Processing

After isolating the aftershock events for each station and component of interest, each component and station for each aftershock event was processed following the procedures presented in Goulet et. al. (2021) for processing ground motions in the PEER NGA-East database. First, a visual inspection was conducted on the raw time histories to ensure the ground motion's time history was distinguishable from the sensor background noise. Time histories where the ground motion could not clearly be distinguished were omitted from further consideration.

The raw ground motion time histories then underwent the following pre-processing procedure. First, the time histories were converted to engineering units of acceleration (g's) using the digitizer and sensor response data provided by the UUSS. After visual inspection, the time history was trimmed again, if necessary, to remove errant noise around the ground motion signal. A constant "de-meaning" method was then used to detrend the entire time history. Next, the trace was filtered in the time domain using a 5th

order Butterworth high-pass filter at a low-cut frequency of 0.01 Hz to remove undesirable low-frequency data. The trace was integrated twice to obtain displacement, and a 6th order polynomial baseline correction detrending was applied to the displacement time history. Finally, the time history was differentiated twice to produce the pre-processed acceleration time history.

The pre-processed acceleration time histories from the deep DH_4 sensor, also referred to as the "base" sensor, were then divided into corresponding ground motion signal windows and pre-event noise windows based on the following procedure (refer to Figure 2.1). First, the beginning of the base signal window, t_{Bi}, was visually determined based on the P-wave's first arrival time. The end of the base signal window, t_{Bf}, was determined by the time to 98% of the Arias Intensity, I_a, relative to the start time t_{Bi}. Thus, the signal/event duration was equal to $t_{Bf} - t_{Bi}$. The noise window was determined by taking the catalog event start time (which was consistently before the P-wave arrival) as the end time for the noise window, and the noise start time was determined by subtracting the length of the signal window ($t_{Bf} - t_{Bi}$) from the catalog event time (refer to Figure 2.1b). This resulted in signal and noise windows for the deep DH_4 sensor of equivalent length.

In an effort to capture the complete ground motion event recorded by the base sensor on the surface sensor, the surface time history from sensor DH_0 was divided into corresponding signal windows and pre-event noise windows using the following procedure. First, for simplicity, the surface signal start time, t_{Si}, was set equal to the same time as t_{Bi}. Then, the Vs travel time between the base sensor and the surface sensor was accounted for using the simplified PS-logging Vs profile shown in Figure 1.1. This was done by adding the mean Vs travel time from a depth of 120 m to the surface (Δt_{SH}), which was 0.4 s, to the t_{Bf} in order to get the surface signal end time, t_{Sf}. If this Δt_{SH} adjustment was not accounted for, the entire event recorded on the base sensor would not be captured on the surface sensor. Of course, this resulted in surface windows that were 0.4 s longer than base windows. This challenge was overcome through zero padding to make the base and surface time histories the same length, as discussed below. The beginning of the surface noise window was calculated by subtracting the length of the surface signal window (t_{Sf} - t_{Si}) from the catalog event start time (refer to Figure 2.1a). This resulted in signal and noise windows for the surface DH_0 sensor of equivalent length.

After dividing the time histories into signal and noise windows, the base and surface sensors were processed in the same manner. A Tukey cosine taper with a width of 5% of the time history was applied on both ends of the signal and noise windows. The trailing end of the window was then padded with zeros to the next-greater power of two to force the surface and deepest sensor windows to the same length. Using a Fourier transformation, the Fourier amplitude spectrum (FAS) was calculated for each window. This FAS was resampled from frequencies of 0.1 to 100 Hz on a logarithmic scale with a total of 512 points. It was then smoothed using a Konno and Ohmachi smoothing window with a bandwidth of 40 (Konno and Ohmachi 1998). An example of the processed signal and noise window FAS for the 120-m sensor is shown in Figure 2.2a.

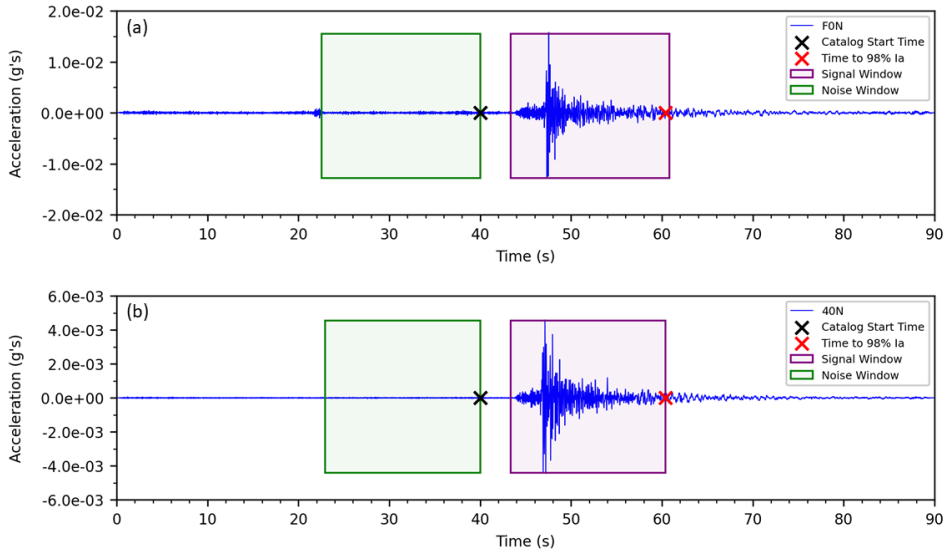

Figure 2.1 Illustration of the signal and noise windows for USGS Event ID uu60364822 recorded by the I15DA. Plot (a) shows the surface sensor windows for the north component (F0N), and plot (b) shows the base sensor (120 m) windows for the north component.

After smoothing, the SNR was calculated by dividing the signal FAS by the noise FAS (see Figure 2.2b). The usable bandwidth of the FAS for each base and surface station during each event was determined to be where the SNR was greater than 3.0. At this stage, the ground motions that produced limited usable bandwidth on either the base or surface sensors due to a low SNR across the FAS were discarded. The final suite of ground motions consists of seven events recorded on each horizontal component (north and east) with a usable bandwidth of 0.5 to 10 Hz. These events had magnitudes that ranged from 2.88 to 3.94 and PGA values that ranged from 0.002 to 0.032 g's. Additional information about the ground motions used to calculate the ETFs for the site are tabulated in 0.

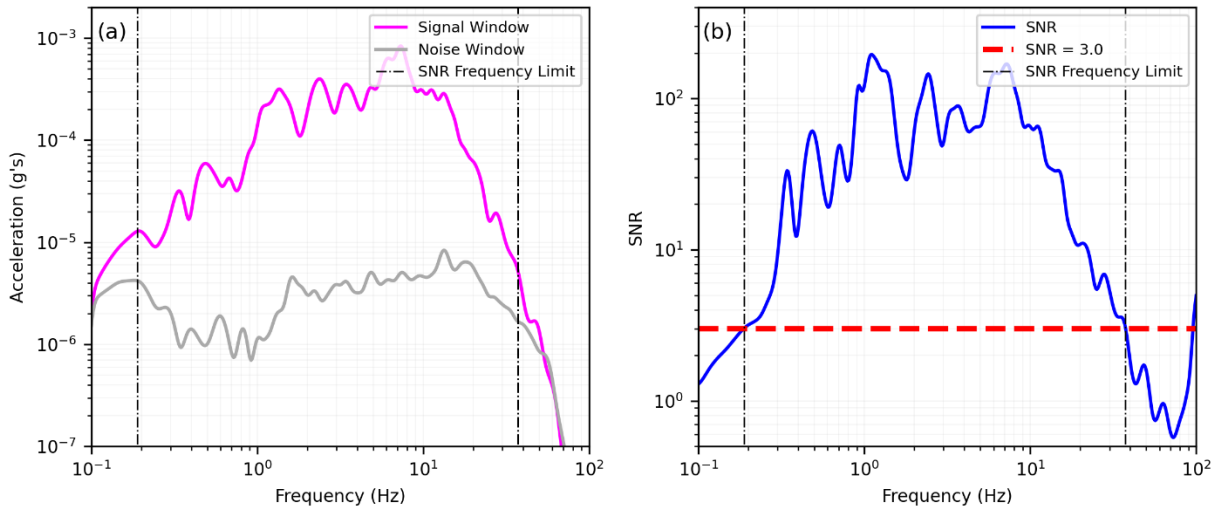

Figure 2.2 (a) North component FAS and (b) SNR for processed USGS Event ID uu60364822 recorded by the 120-m downhole sensor at the I15DA. The dotted red line on the SNR plot signifies a SNR of 3.0, and the dotted black lines on both plots show the frequency bandwidth for the time history based on the SNR of 3.0.

2.3 Calculating the Empirical Transfer Function

After determining which recorded ground motion events had a large enough common bandwidth on the base and surface sensors, the individual empirical transfer functions (ETFs) were then calculated by dividing the FAS of the surface signal window for a given horizontal component by the corresponding FAS of the base signal window for the same horizontal component. Since the individual ETFs from the north and east components of the I15DA sensors were found to be similar for any given event, the ETFs for each component were combined by calculating the geometric mean of both components (the square root of the product of the north and east components) in the frequency domain. The representative ETFs for each individual event, the lognormal median ETF from all events, LM_{ETF}, and the associated standard deviation across events, $\sigma_{ln,ETF}$, were calculated by taking the lognormal median and lognormal standard deviation of the horizontal component-combined ground motion ETFs. The LM_{ETF} and the individual component ETFs are displayed in Figure 2.3. The fundamental frequency of the ETF, $f_{0,ETF}$, and associated lognormal standard deviation, $\sigma_{f_{0,ETF}}$, was calculated by taking the lognormal median of the frequencies associated with the highest peak from each individual north and east component ETF from 0.6 to 1.0 Hz. From the final suite of small-strain ground motions, the $f_{0,ETF}$ is 0.80 Hz with a $\sigma_{f_{0,ETF}}$ of 0.22.

Since the LM_{ETF} curve was calculated from small-strain ground motions at the site, the results of single- and multi-dimensional linear-viscoelastic site response modeling will be compared to this curve to judge accuracy of each theoretical model. It is important to note that this LM_{ETF} represents the ETF between the base sensor (DH_4, installed at a depth of 120 m) to the surface sensor (DH_0). The theoretical transfer functions from site response will be calculated over the same depth range.

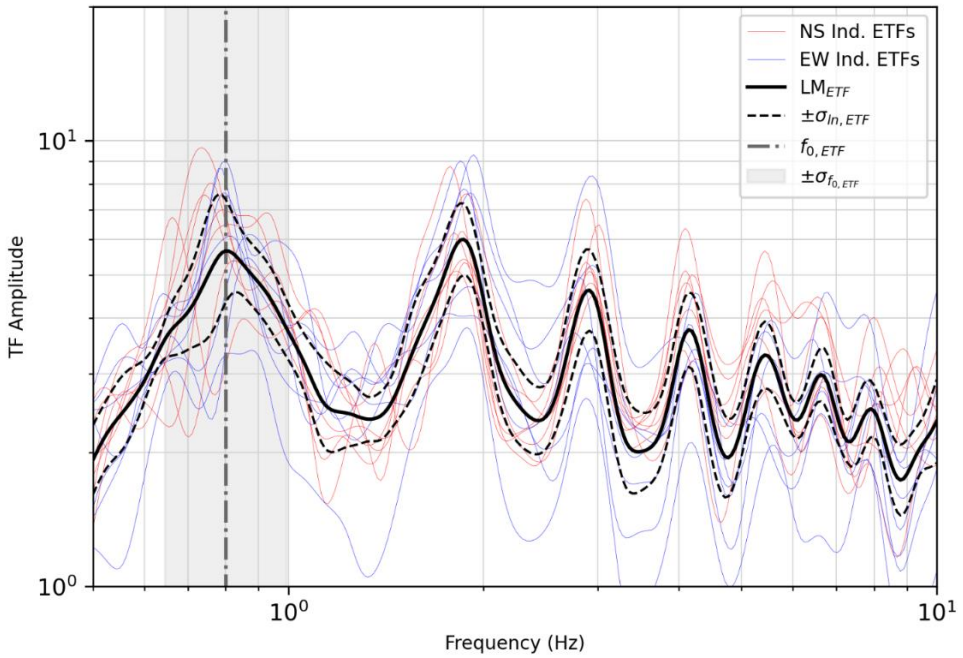

Figure 2.3 Empirical transfer function (ETF) from 120 m to the surface based on small-strain ground motions recorded by the I15DA. The $\boldsymbol{LM_{ETF}}$ is calculated from combining the individual north/south (red) and east/west (blue) ETFs using a geometric mean, and then calculating the lognormal median of the combined ETFs. The fundamental frequency, $\boldsymbol{f_{0,ETF}}$, and its associated lognormal standard deviation, $\boldsymbol{\sigma_{f_{0,ETF}}}$, are shown in gray.

3. PS-LOGGING 1D SITE RESPONSE MODELING

This section discusses the one-dimensional (1D) site response modeling for the nine-layer simplified PS-logging profile (refer to Figure 1.1) at the I15DA using the a 1D linear-viscoelastic ground response analysis (GRA) Python script developed within the Cox research group, which has been validated against the 1D viscoelastic GRA calculations in the program "DEEPSOIL" (Hashash et al. 2020).

3.1 PS-logging Soil Model

The Cox Research Group's Python script was chosen to compute the 1D linear-viscoelastic theoretical transfer function (TTF) for the simplified PS-logging profile because of its simple interface and ability to easily assign small-strain minimum damping (D_{min}) values to each soil layer. The soil layering and properties required to calculate D_{min} (e.g., unit weights, plasticity indices, over-consolidation ratios, etc.) were assumed based on a log of soil cuttings obtained during drilling of the 120-m borehole (Youd and Briggs, 2003). A simplified representation of this boring log is provided in Figure 1.1. Layers that classified as sandy clays were assigned a plasticity index of 30, while layers classified as clayey sands were assigned a plasticity index of 10. Unit weights for each layer were calculated using a relationship based on the Vs of each layer (Mayne 2001). An over-consolidation ratio of 1.5 was assigned to the surface layer, and the over-consolidation ratios assigned to deeper layers gradually decreased to a ratio of 1.0 where the soil contained gravel (approximately 50 m). The assumed layer properties were used to calculate D_{min} for each layer using the relationships provided in Darendelli 2001. These D_{min} values ranged from 2.0% near the surface to 0.7% near the base sensor. It is important to note that Vs layer boundaries and the layer boundaries from the borehole lithology log were not at consistent depths. Consequently, the full 1D ground profile for the model was a combination of all the layer boundaries between the soil lithology profile and the PS-logging simplified Vs profile. To match the frequency sampling of the LM_{ETF}, the TTF was calculated from 0.5 to 10 Hz with 256 points. As the ETF for the borehole was calculated between 120 m and the surface, "within" conditions were specified for calculating the theoretical transfer function. The 1D TTF for the simplified PS-logging Vs profile is shown in Figure 3.1.

3.2 Comparing the PS-logging Vs TTF with the ETF

Visually, the TTF obtained from the nine-layer simplified PS-logging Vs profile appears to fit the LM_{ETF} moderately well. The Vs profile captures the frequencies of the first two peaks/modes of the LM_{ETF} quite well but does not capture the third and fourth modes as well. Also, while the frequencies for the first two modes of the TTF and LM_{ETF} agree very well, the amplitudes of the TTF are significantly higher than the amplitudes of the individual ETFs and LM_{ETF}. This problem has been noted in many prior site response studies at borehole array sites (e.g., Hallal et al. 2022). In addition to qualitative comparisons, it is desirable to quantitatively compare the TTF with the LM_{ETF} as a means to determine how well the TTF produced by the PS-logging Vs profile captures the LM_{ETF}.

Teague et al. (2018) discussed two relationships to quantify the goodness-of-fit of the TTFs to the LM_{ETF}: the Pearson correlation coefficient, r, and the transfer function misfit, m_{TF}. The calculation of r quantifies how well the shapes of the TTF and LM_{ETF} align, and the calculation of m_{TF} better quantifies how many standard deviations the amplitude of the TTF is from the LM_{ETF}. Higher r values represent better fits, while lower m_{TF} values represent better fits. Hallal et al. (2022) state that these statistical quantifications should be performed between a lower-bound frequency determined from the absolute half-amplitude of the first mode ETF peak and an upper-bound frequency determined from the absolute half-

amplitude of the fourth mode ETF peak. These limits, denoted by dotted red lines, are shown in Figure 3.1.

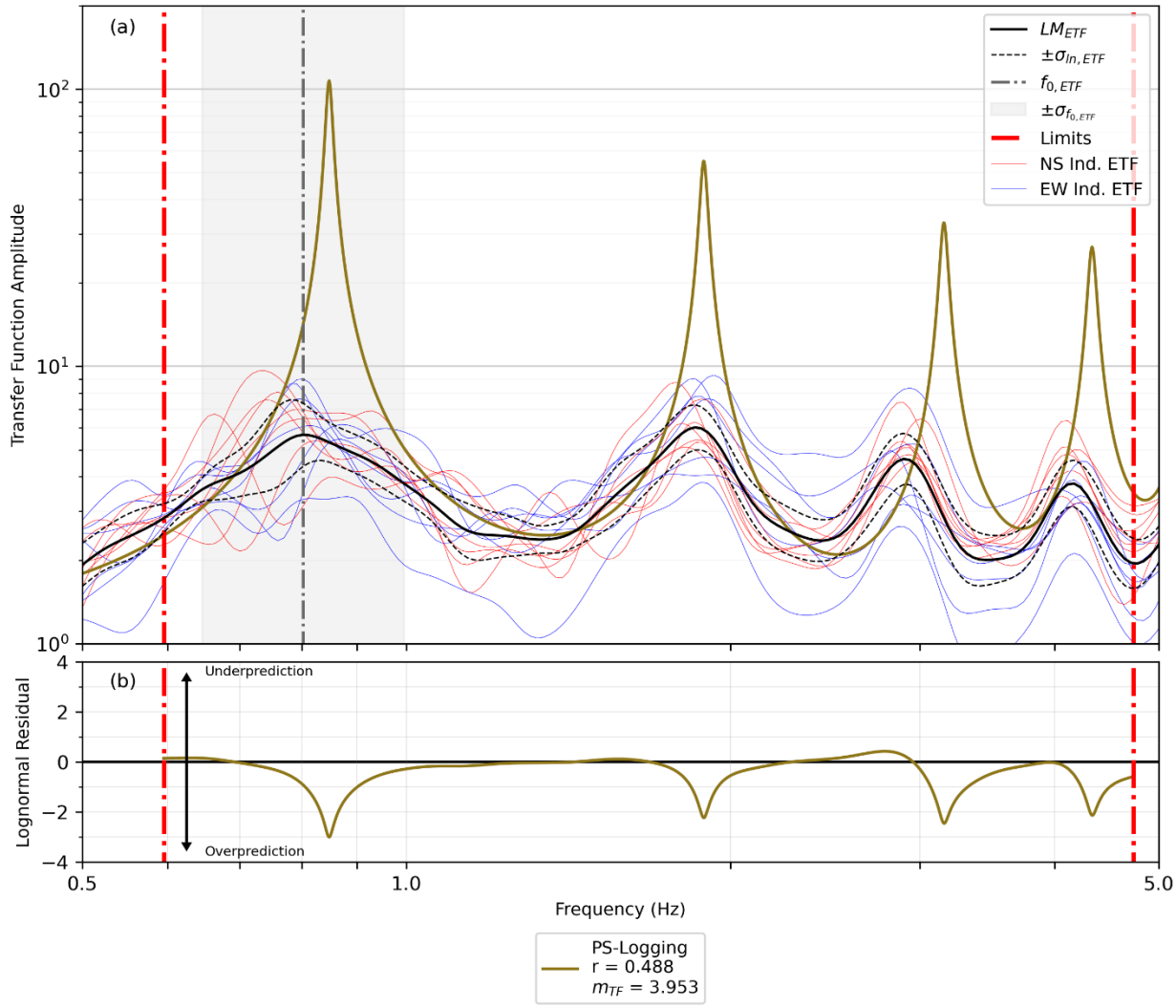

Figure 3.1 Comparison of ETFs from small-strain recorded ground motions and the TTF from 1D linear-viscoelastic GRA for the simplified PS-logging Vs profile at the I15DA site. Plot (a) shows the individual ETFs from each ground motion, the $\boldsymbol{LM_{ETF}}$ curve, and the TTF. Plot (b) displays the lognormal residual of the TTF to the $\boldsymbol{LM_{ETF}}$. The Pearson correlation coefficient, $\boldsymbol{r}$, and transfer function misfit, $\boldsymbol{m_{TF}}$, values are displayed in the legend at the bottom of the figure. Note that all goodness-of-fit parameters were calculated between the frequency range denoted by the dotted red lines.

Quantitatively, the TTF calculated from the simplified PS-logging profile has an r of 0.488 and an m_{TF} of 3.953. According to Thompson et al. (2012), r values greater than 0.6 indicate sites that are well-modeled using 1D site response. Since the r of this TTF is less than 0.6, the PS-logging profile's 1D GRA does not model the site response for the I15DA well, which indicates a need to explore GRA methods that incorporate spatial variability of Vs near the site. Additionally, the m_{TF} value is quite high, indicating that, on average, the TTF amplitudes are more than 4 standard deviations outside of the ETF range. In particular, the TTF amplitudes are particularly high at the fundamental and higher modes, as indicated by

the lognormal residual values between the TTF and the median ETF that range between approximately -3.0 to 0.3 for each of the first four modes (refer to Figure 3.1). These goodness-of-fit parameters confirm that while the TTF is able to capture the frequencies of the first two peaks/modes quite well, the TTF does not capture the frequencies of the third and fourth peaks/modes as well, and it estimates the amplitudes of these peaks as significantly higher than the LM_{ETF}.

The PS-logging Vs profile serves as a singular point measurement at the I15DA, and the site response approach discussed above does not account for any spatial variability at the site. Hallal et al. (2022) examined multiple approaches used to incorporate spatial variability into 1D site response analyses. The surface wave approach and pseudo-3D Vs models determined from an H/V geostatistical approach produced TTFs that tended to better fit the LM_{ETF} at multiple downhole array sites. Thus, we chose to investigate these approaches as a means to account for spatial variability at the I15DA.

4. SEISMIC SITE CHARACTERIZATION DATA AQUSITION

To characterize the near-surface and deep Vs structure for the I15DA, a combination of active-source and passive wavefield array-based surface wave testing was performed in conjunction with single station horizontal-to-vertical spectral ratio (H/V) noise measurements. These tests were performed by Dr. Brady R. Cox and five graduate students from Utah State University between 29 September 2022 and 01 October 2022. The multi-channel analysis of surface waves (i.e., MASW) method was employed for active-source testing and two-dimensional (2D) microtremor array measurements (i.e., MAM) were used for passive-source testing. Additionally, to characterize the lateral variability in the resonant frequency (f_0) near the downhole array, a total of 96 H/V measurements were collected across the I15DA site.

4.1 Multi-Channel Analysis of Surface Waves (MASW)

Figure 4.1 shows a plan view of the active-source MASW test location. MASW testing was performed using 4.5-Hz vertical geophones (Geospace Technologies GS-ONE installed in PC803 land cases) coupled to the parking lot surface with aluminum tripod bases. A single line of 24 geophones was placed in a linear array with a spacing of 2 m between successive geophones, resulting in an array length of 46 m. Vertical geophones were used to record wavefields with strong Rayleigh wave content that was actively generated by striking vertically on a circular aluminum strike-plate with a 7.3-kg sledgehammer at three distinct "shot" locations offset 5, 10, and 20 m relative to the first geophone on each side of the array. Five distinct blows were recorded per shot location for subsequent stacking to increase SNR. Wavefields were recorded for 1.0 second with a 0.25-second pre-trigger delay using a sampling rate (Δt) of 1.0 ms.

4.2 Microtremor Array Measurements (MAM)

MAM testing was performed using one circular array and two L-shaped arrays (refer to Figure 4.1). The arrays are referred to by their approximate maximum aperture (i.e., diameter or longest leg/side); that is, 60 m for the C60 MAM array, and 300 m and 1000 m for the L300 and L1000 MAM arrays, respectively. All three MAM arrays were comprised of 10 broadband seismometers. Note that the C60 and L300 arrays shared two common receiver locations, namely C60-L300-06 and C60-L300-10. Note also that the L300 and L1000 arrays shared four common receiver locations, namely L300-L1000-01, L300-L1000-03, L300-L1000-05, and L300-L1000-08. Three-component broadband seismometers with a flat frequency response between 120 seconds and 100 Hz (Nanometrics Inc. Trillium Compact Horizon 120s) were used to record ambient vibrations. Seismometers were oriented to magnetic north and buried where possible to provide better coupling with the ground surface. Where it was not possible to bury, sensors were placed on tripod leveling bases and covered with a weighted bucket to mitigate the effects of wind vibrations and temperature fluctuations. Acquisition systems for the Trillium Compact 120s seismometers were Nanometrics Inc. Pegasus digitizers (24-bit ADC, 135 dB dynamic range, internal clock, and GPS receiver accurate to <100 μs).

Coordinates for all broadband seismometer locations used in MAM arrays are provided in Appendix B. MAM stations were used to record ambient vibrations for periods between 1.5 hours to 3 hours, depending on the size of the array, with longer recording times corresponding to the larger arrays. Data were recorded with a sampling frequency of 100 Hz.

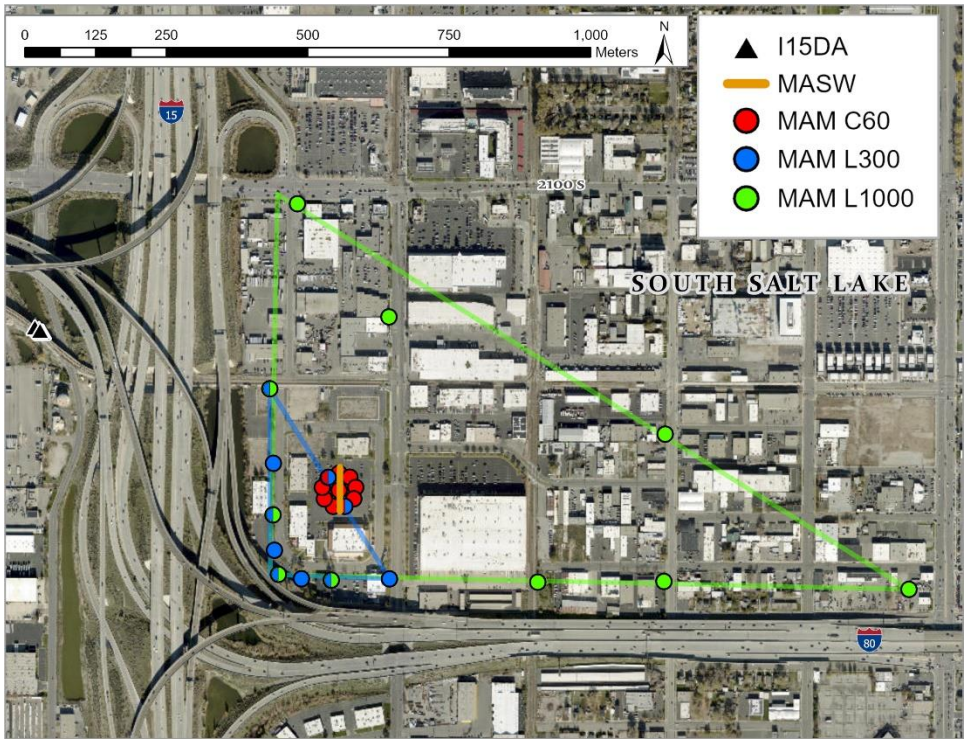

Figure 4.1 Plan view of the multi-channel analysis of surface waves (i.e., MASW) and microtremor array measurement (i.e., MAM) test locations at the I15DA site.

4.3 Horizontal-To-Vertical Spectral Ratio (HVSR)

In addition to the 30 ambient noise measurements collected for MAM testing, 96 single-station 30-minute ambient noise records were collected around the site (refer to Figure 4.2) to characterize the lateral variability in whatever notable impedance contrast governs resonance around the site and to estimate the corresponding resonant frequency from the H/V measurements ($f_{0,H/V}$) collected around the site. The single-station H/V measurements were collected roughly on a 200-m x 200-m grid, spanning a total distance of approximately 2 km x 2 km and centered on the I15DA. H/V spectral noise ratios were computed for all single-station ambient noise measurements and all stations used in MAM testing. If an H/V curve exhibits a well-defined peak, the frequency corresponding to the lowest frequency peak ($f_{0,H/V}$) can be used to estimate the fundamental shear wave resonant frequency of the site (f_{0_S}) (Lermo and Chávez-García 1993; Lachet and Bard 1994; SESAME 2004) and/or the lowest-frequency peak of the fundamental mode Rayleigh wave ellipticity (f_{0_R}) (Malischewsky and Scherbaum 2004; Poggi and Fah 2010). When a strong impedance contrast is present at a site, $f_{0,H/V}$, f_{0_S}, and f_{0_R} are approximately equal to one another. When a more moderate impedance contrast is present, $f_{0,H/V}$ may be more representative of f_{0_S} than f_{0_R} (Bonnefoy-Claudet 2004).

At each broadband station location, H/V data were processed following the procedures documented in Cox et al. (2020) and Cheng et al. (2020), wherein a frequency-domain window-rejection algorithm

(FDWRA) is used to reject contaminated time windows, and a lognormal distribution is used to calculate statistics for both the lognormal median H/V curve (LM_{curve}) and the individual $f_{0,i}$ values from each time window (i.e., LM_{f_0}). As noted in Cox et al. (2020), the FDWRA tends to bring the statistical values of LM_{f_0} into better alignment with the peak values from the LM_{curve} (i.e., $f_{0,mc}$). In this study, the peak values from the LM_{curve} (i.e.,$f_{0,mc}$) were used to estimate the fundamental resonance peak of the H/V curve within the expected peak range indicated by the empirical transfer function (i.e., $f_{0,ETF}$; refer to Figure 3.1).

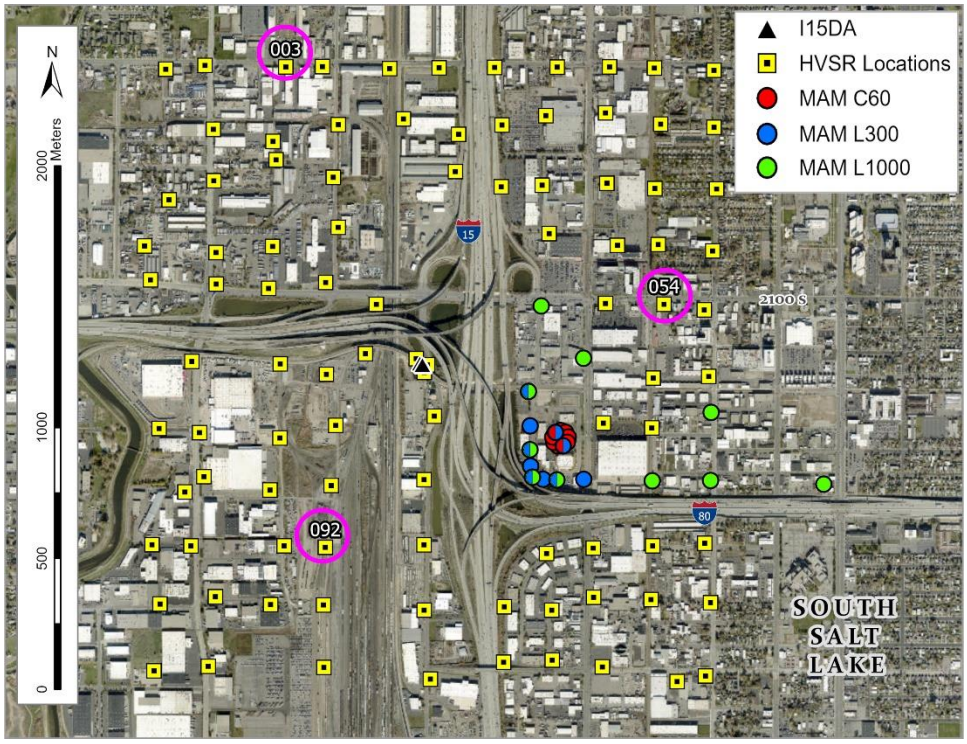

Figure 4.2 Plan view of the single-station ambient noise measurement locations used for horizontal-to-vertical (H/V) spectral ratio calculations across the I15DA site. Note that example locations 003, 054, and 092 are circled in blue.

The open-source Python package *hvsrpy* (Vantassel 2020), which was developed within the Cox research group, was used for all H/V analyses. Ambient noise records were divided into 60-s long time windows and the north and east components were combined by taking the geometric mean (the square root of the product of the north and east components). Konno and Ohmachi (1998) smoothing with a smoothing constant (b) of 40 was utilized to remove spurious spikes in the Fourier spectra obtained from each time window. After smoothing, contaminated time windows were rejected using the FDWRA and two standard deviations (i.e., n = 2). Figure 4.3 shows an example of the H/V processing results for ambient noise recording locations 003, 054, and 092.

Some H/V data, like the data shown for ambient noise location 003, produced a single clear peak near $f_{0,ETF}$ (refer to Figure 4.3a). In this example, the $f_{0,mc}$ was simply chosen as the highest amplitude peak above 0.5 Hz. However, other ambient noise locations produced multiple peaks and/or fewer clear peaks in the H/V data (refer to Figure 4.3b and 4.3c). Where there was no clear single peak, $f_{0,ETF}$ was used as a guide to visually estimate $f_{0,mc}$. This process was subjective, and several iterations were performed. In most instances, the peak with the highest amplitude on the LM_{curve} was chosen. However, in some cases,

the peak with a slightly lower amplitude was chosen when it was observed closer to the $f_{0,ETF}$ range. Ambient noise records that produced no significant peak in H/V data were discarded. The individual $f_{0,mc}$ values from all ambient noise time histories that produced reliable H/V data from frequencies between 0.5 and 1.5 Hz are tabulated in Appendix B.

It is important to note that we refer to the resonance in H/V at $f_{0,mc}$ as the "fundamental" resonance of the site, as this is where the $f_{0,mc}$ peak values are between the range of $f_{0,ETF}$. These values may or may not represent the true fundamental site resonance, but they do represent resonances that occur between the DH_4 sensor at 120 m and the ground surface in the I15DA. These $f_{0,mc}$ values are used to build a pseudo-3D Vs model for use in multi-dimensional site response (refer to Section 0). Based on shear-wave velocity profiles inverted from the MASW and MAM dispersion data (refer to Section 5.3 of this report), the depth to bedrock is likely greater than 1 km. Thus, it is somewhat unlikely that the $f_{0,mc}$ peak values from H/V testing represent the true fundamental frequency of the site. However, currently, it is difficult to resolve H/V data at frequencies lower than approximately 0.2 Hz, and the expected resonant frequency values for the deeper rock impedance may fall at or below 0.2 Hz. Thus, the peaks chosen as $f_{0,mc}$ are sufficient to capture the site response between the DH_4 sensor and the surface, which allows for direct comparison of the estimated site response to LM_{ETF}. Hereafter, for simplicity, the resonance peak around the $f_{0,mc}$ values and $f_{0,ETF}$ (i.e., the first peak of the ETF) shall be referred to as the fundamental resonance peak at the I15DA.

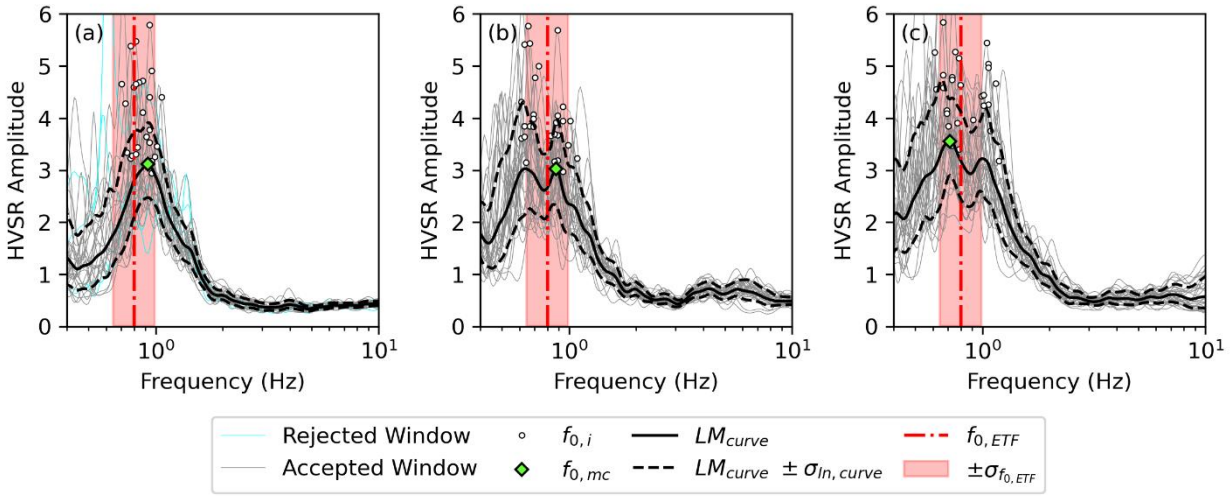

Figure 4.3 Examples of H/V curves processed with *hvsrpy*: (a) ambient noise location 003, (b) ambient noise location 054, and (c) ambient noise location 078. For each location shown, the peak $\boldsymbol{f_{0,mc}}$ from the $\boldsymbol{LM_{curve}}$ H/V curve is the highest clear single peak near $\boldsymbol{f_{0,ETF}}$.

5. SURFACE WAVE TESTING DATA INVERSION

This section discusses data processing and analysis techniques employed to obtain Vs profiles from the collected MASW and MAM data. This involves processing the raw waveforms to characterize the experimental Raleigh wave dispersion data, inverting the Raleigh wave dispersion data to obtain Vs profiles, and comparing the inversion-derived Vs profiles with prior invasive site characterization information at the site.

5.1 Dispersion Processing

MASW data were analyzed using the frequency domain beamformer method (Zywicki 1999) coupled with the multiple source-offset technique for identifying near-field contamination and quantifying dispersion uncertainty (Cox and Wood 2011; Vantassel and Cox 2022). Rayleigh dispersion data influenced by near-field effects and/or significant offline noise were interactively trimmed prior to calculating dispersion statistics.

Three-component beamforming (Wathelet et al. 2018) was used to generate Rayleigh wave dispersion data for each of the MAM arrays. Recordings from each array were divided into time windows, with the smallest array using shorter window lengths (30 s) and the largest arrays using longer window lengths (150 s). For each array, window lengths were selected such that there was a minimum of 30 cycles per window for the lowest frequency targeted. Spurious dispersion data stemming from high-amplitude noise in the near-field (e.g., traffic noise close to the sensors) and incoherent noise were manually eliminated through a trimming process prior to calculating dispersion statistics (Vantassel and Cox 2022).

Passive dispersion data from all MAM arrays were combined with the active dispersion data obtained from MASW processing, and the combined data were used to compute mean and +/- one standard deviation dispersion estimates (Vantassel and Cox 2022). The mean and +/- one standard deviation Rayleigh wave dispersion data for the I15DA site are shown relative to the individual MASW and MAM dispersion data points in Figure 5.1. In the figure, the dispersion data are plotted as a function of both frequency and wavelength (f and λ, refer to Figure 5.1a and 5.1b respectively) in order to best visualize key aspects of the data. The Rayleigh wave dispersion data were interpreted to include contributions from only the fundamental (R_0) mode.

One must be cautious about using dispersion data at wavenumbers ($k = 2\pi/\lambda$) less than the theoretical array resolution limit associated with the largest array deployed at the site. At wavenumbers less than the theoretical array resolution limit (i.e., $k_{min}/2$, Wathelet et al. 2008), the dispersion data may be negatively influenced by limitations of the array aperture (i.e., the array is not large enough to accurately resolve low frequency, high phase velocity dispersion data whose associated wavenumbers are less than the $k_{min}/2$ resolution limit). In other words, the dispersion data at frequencies below this threshold (wavelengths above this threshold) may be of lower quality and higher uncertainty.

The $k_{min}/2$ resolution limit for the largest MAM array used at the I15DA site (i.e., L1000; refer to Figure 4.1) is shown in Figure 5.1. It should be observed that some of the dispersion data beyond the $k_{min}/2$ line (i.e., at lower frequencies, or equivalently at longer wavelengths) were retained and used to calculate dispersion statistics, as they appeared to be of good quality. While less certain, these data provide guiding information for the inversion about the deeper Vs structure. Without these additional data points, it is believed that the inversions would have underestimated the velocity structure at depth.

During the inversion process (discussed below), the array resolution wavelength ($\lambda_{res} = k_{min}/2$) was used to guide the depth to which the Vs profiles are reported. Based on the largest MAM array geometry used for the I15DA site, $\lambda_{res} = k_{min}/2$ was calculated to be approximately 1,570 m. However, dispersion data extracted from the MAM arrays appeared to be of high quality to much longer wavelengths (~ 5 km). Thus, dispersion statistics were calculated at wavelengths greater than λ_{res}. The R_0 experimental dispersion data targeted during surface wave inversions for the I15DA site are tabulated in Appendix C in terms of mean phase velocity and standard deviation as a function of frequency.

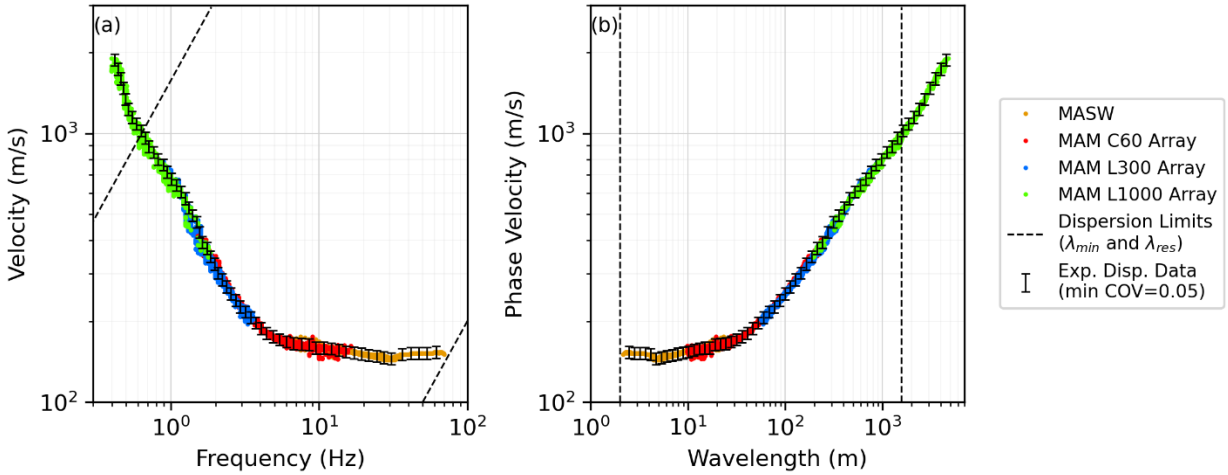

Figure 5.1 Mean and +/- one standard deviation experimental Rayleigh wave dispersion data calculated from the individual MASW (i.e., active-source) and MAM (i.e., passive-wavefield) data collected at the I15DA site and presented in terms of: (a) frequency, and (b) wavelength. $\boldsymbol{\lambda_{min}}$ is controlled by the minimum wavelength recorded by the MASW array (2 m), and $\boldsymbol{\lambda_{res}}$ is controlled by half of the minimum theoretical wavenumber ($\boldsymbol{k_{min}}/2$) recorded by the largest MAM array (1,570 m).

5.2 Inversion Procedure

The inversion of surface wave data involves finding layered earth models whose theoretical dispersion curves, which are computed via the "forward" problem, best match the experimentally measured dispersion data. This process is shown schematically in

Figure **5.2**. The quality of fit between theoretical and experimental data is typically quantified using a "misfit" value (Wathelet et al. 2004; Foti et al. 2009). The forward problem used in this study was the transfer matrix approach developed by Thomson (1950) and Haskell (1953) and later modified by Dunkin (1965) and Knopoff (1964). The inversion was performed using the open-source software Geopsy, which uses a neighborhood algorithm (Sambridge 1999) to locate earth models within a pre-defined parameterization that yield the lowest possible misfit values between the theoretical and experimental data. Misfit values for this study were computed using Equation 5.1 (modified from Wathelet et al. 2004).

$$m_d = \sqrt{\sum_{i=1}^{n_f} \frac{(X_{di} - X_{ci})^2}{\sigma_i^2 n_f}} \qquad \text{Eq. (5.1)}$$

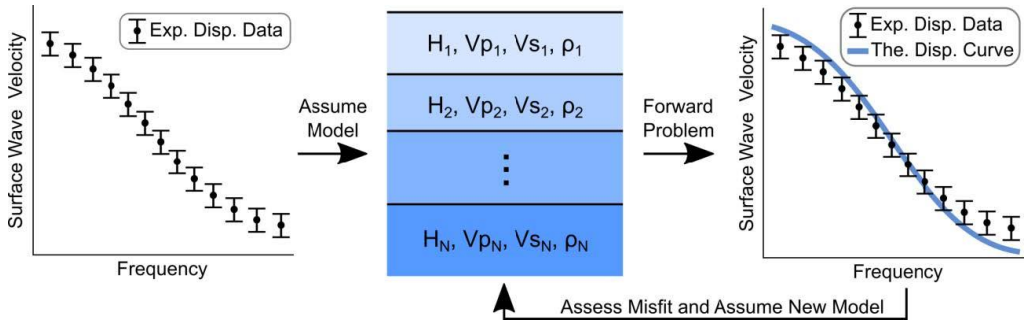

Figure 5.2 Schematic representation of the forward and inverse problems.

In Equation 5.1, m_d is the misfit value based only on dispersion data; x_{di} represents the Rayleigh wave phase velocity of the experimental dispersion data at frequency f_i; X_{ci} is the calculated/theoretical Rayleigh wave phase velocity computed for the trial layered earth model at frequency f_i; σ_i is the standard deviation associated with the experimental dispersion data at frequency f_i; and n_f is the number of frequency samples considered for the misfit calculation.

While there are no universally "good" or "bad" misfit values (Cox and Teague 2016), m_d values less than 1.0 indicate that, on average (i.e., across the frequency band considered), the theoretical dispersion curve falls within the +/- one standard deviation bounds of the experimental data. Thus, m_d values far in excess of 1.0 suggest a poor fit of the experimental dispersion data, and low m_d values indicated models that fit the mean dispersion data well across the entire bandwidth.

The inverse problem involved in obtaining a realistic layered earth model from surface wave dispersion data is inherently ill-posed, nonlinear, and mix-determined and without a unique solution. If detailed borehole data and/or geologic information are available, they can and should be used to help constrain the inversions and thereby limit the solution's non-uniqueness (Teague et al., 2018a). The use of supporting/a-priori information during inversion is the best approach for retrieving Vs profiles that are consistent with the actual subsurface layering. As described in more detail below, some boring log information was used to inform the inversions. However, the boring logs did not extend deep enough to provide information about soil properties to completely constrain the inversions. Thus, in the absence of a-priori information, or for cases where a-priori information does not extend deep enough, the analyst must decide on an appropriate number of layers to use for the inversion and the ranges for their corresponding inversion parameters (i.e., thicknesses, shear wave velocities, compression wave velocities, and mass densities). The selection of these parameters has been shown to significantly impact the results of an inversion. Thus, uncertainties due to the choice of inversion parameterization should be considered. To do this in a systematic fashion, the "layering ratio" (LR) approach was utilized to methodically invert the experimental data using several trial subsurface models with different numbers of layers (Cox and Teague, 2016; Vantassel and Cox, 2021).

For the LR inversion parameterization approach, each trial inversion parameterization is defined by a unique layering ratio (Ξ), representing a multiplier that systemically increases each layer's *potential* thickness in the inversion parameterization based on the *potential* thickness of the layer directly above it (Cox and Teague 2016). Low values of the layering ratio parameter Ξ result in trial subsurface models with more layers and typically weaker impedance contrasts, while higher values of the layering ratio parameter Ξ result in trial subsurface models with fewer layers and typically stronger impedance contrasts. Considering multiple layering parameterizations allows for the quantification of uncertainty in the derived Vs profiles. Irrespective of which LR parameterization was used, the shear wave velocities were constrained to minimum and maximum values of 80 m/s and 3,500 m/s, respectively.

The number of trial models necessary to search the entire parameter space during inversion and obtain a large number of acceptable models is controlled by the experimental data and model parameterization (i.e., it is site-specific). We searched approximately 60,000 trial layered earth models for each considered LR parameterization using Geopsy's optimization algorithm, with the goodness of fit for each trial model being calculated using Equation 5.1. While it may appear reasonable to extract all Vs profiles with misfit values less than 1.0 for each parameterization, the number of profiles with misfits below 1.0 varies considerably between parameterizations, and in some cases, is not computationally manageable. For consistency, the 100 lowest misfit Vs profiles obtained from each inversion parameterization were extracted for further analysis and used to quantify Vs uncertainty**.** These profiles are presented and discussed below.

5.3 Inversion Results

Surface waves at a given wavelength are generally capable of profiling to a maximum depth of 1/3 to 1/2 of their wavelength (Foti et al. 2015; Garofalo et al. 2016). Thus, Vs profiles obtained from inversion are considered most reliable at depths less than approximately $\lambda_{res}/2$. In other words, the resolution depth (d_{res}) for Vs profiles derived from surface wave inversion is approximately $\lambda_{res}/2$. At depths greater than d_{res}, the Vs profiles are constrained by less reliable dispersion data and should be used with caution. Vs profiles at depths greater than d_{res} are reported herein because, while less certain, they provide guiding information about the deep Vs structure that is more reliable than simply guessing. We clearly delineate the d_{res} depth in all Vs figures and tables presented below.

Numerous layering parameterizations were considered during the inversion process for the I15DA. However, four layering parameterizations (i.e., LR = 1.5, LR = 2.0, LR = 3.0 and 5.0) were ultimately considered to yield acceptable results with low dispersion misfit values. The LR = 1.5, 2.0, 3.0, and 5.0 parameterizations had 18, 12, 8, and 7 layers, respectively. The inversion results are summarized in Figure 5.3. Theoretical Rayleigh wave dispersion curves associated with the best 100 Vs profiles from each LR inversion parameterization are shown in Figure 5.3.

It is clear from inspection that all theoretical dispersion curves visually match the experimental dispersion data quite well (i.e., within the uncertainty bounds of the experimental data). The numbers in brackets next to the parameterization names in the figure's legend are the ranges in dispersion misfit values for the best 100 Vs profiles for each LR inversion parameterization. The lowest misfit values were achieved using the LR = 5.0 layering parameterization, with m_d values between 0.47 – 0.69. However, misfit values associated with all other parameterizations shown in Figure 5.3 also indicate good fits to the experimental dispersion data. Hence, all of the 400 theoretical dispersion curves shown in Figure 5.3a and 5.3b are deemed to be possible representations of the experimental data and their corresponding uncertainties.

Figure 5.3c shows all 400 inversion-derived Vs profiles to a depth of 150 m to allow for better visualization of the near-surface velocity structure. Figure 5.3d shows these same Vs profiles plotted down to a depth of 1,570 m. Additionally, the resolution depth ($d_{res} = \lambda_{res}/2$) of 785 m (2,575 ft) is also shown on Figure 5.3c. Since the experimental dispersion data were measured over a relatively large footprint, we believe that they capture spatial variability and represent a "site signature" (Teague and Cox 2016; Teague et al. 2018b) that contains important information about small-strain wave propagation across the site. All Vs profiles shown in Figure 5.3, while visually variable, well-capture the site signature. Therefore, in order to realistically account for Vs uncertainty in site response, we believe that a reasonable number of these Vs profiles should be considered for use in subsequent site response analyses.

The median theoretical dispersion curves and median Vs profiles for each LR parameterization are shown in Figure 5.4. These median Vs profiles can be used as reasonable base-case Vs profiles to account for epistemic uncertainty. Appendix C contains each median Vs profile tabulated to a depth of 1,500 m.

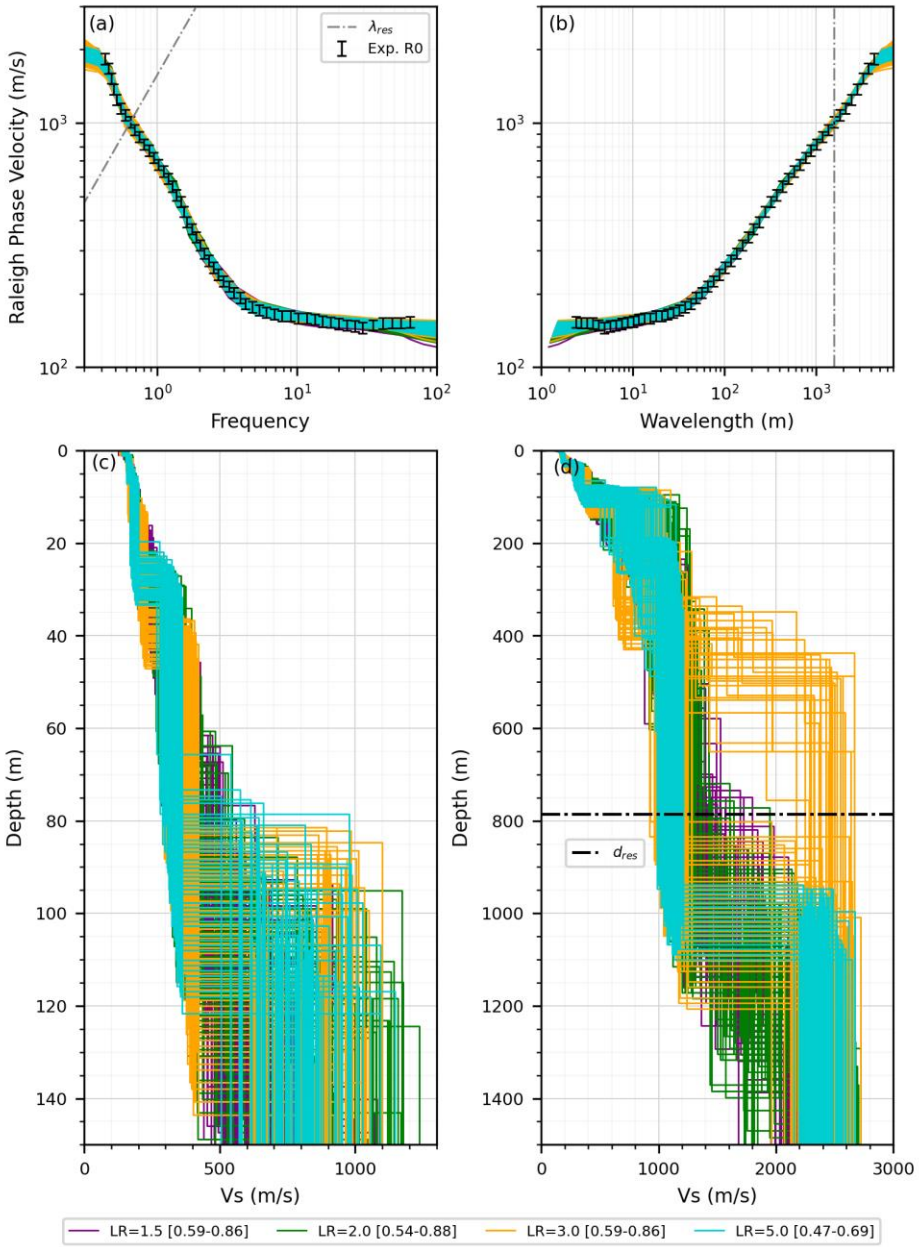

Figure 5.3 Inversion results for the I15DA site based on a fundamental mode interpretation/inversion of the experimental Rayleigh wave dispersion data ($\boldsymbol{R_0}$). Shown for each inversion parameterization (i.e., LR = 1.5, 2.0, 3.0, and 5.0) are the 100 lowest misfit ground models in terms of: (a and b) theoretical fundamental mode Rayleigh wave dispersion curves along with the experimental dispersion data in frequency and wavelength, respectively; and (c and d) Vs profiles shown to depths of 150 m and 1,500 m, respectively. The array resolution depth limit ($\boldsymbol{d_{res} = \lambda_{res}/2}$) is shown at 785 m. The dispersion misfit values for each inversion parameterization are indicated in brackets in the legend.

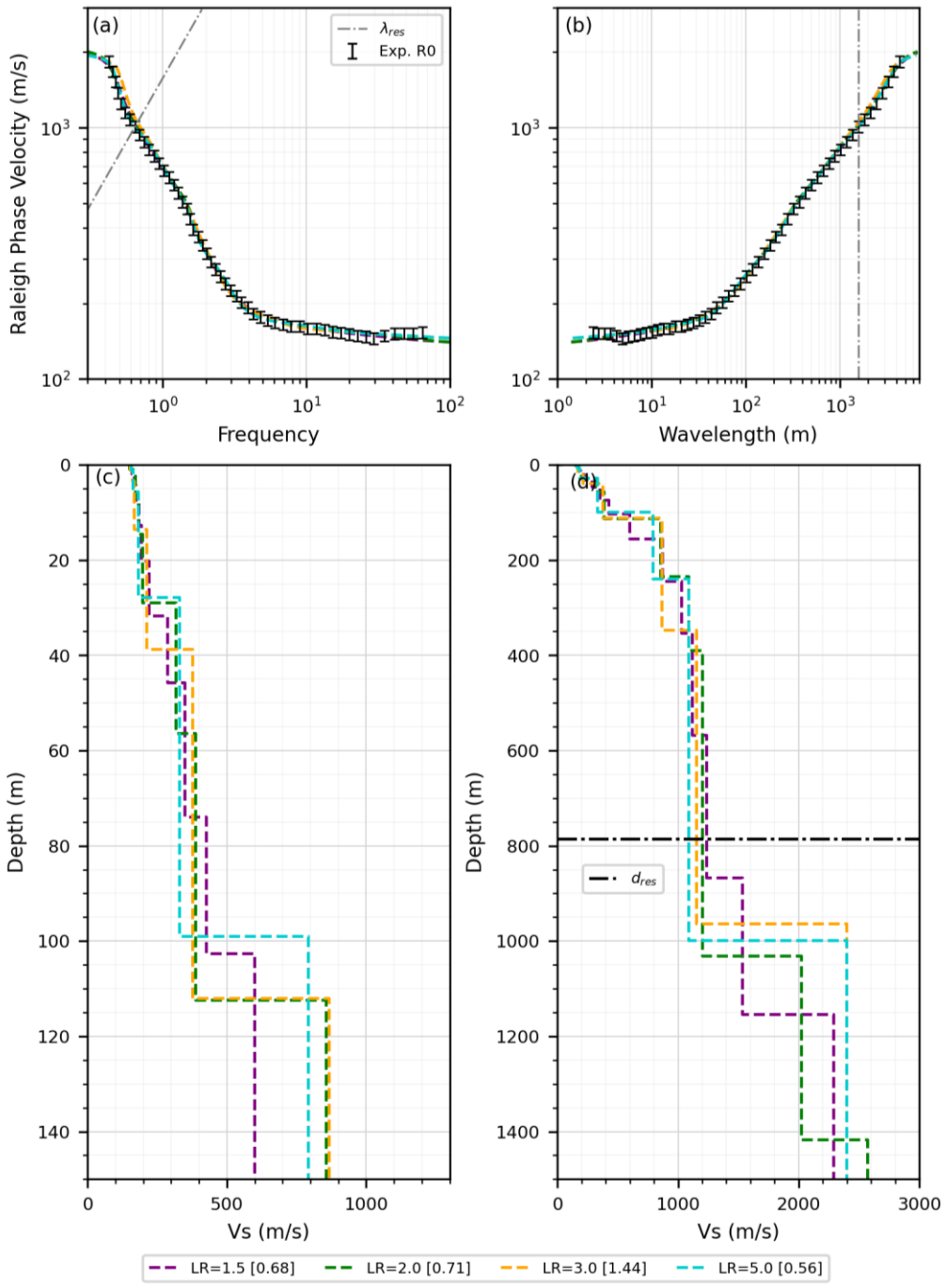

Figure 5.4 Median inversion results for the I15DA site based on a fundamental mode interpretation/inversion of the experimental Rayleigh wave dispersion data ($\boldsymbol{R_0}$). Shown for each inversion parameterization (i.e., LR = 1.5, 2.0, 3.0, and 5.0) are the median ground models in terms of: (a and b) theoretical fundamental Rayleigh wave dispersion curve along with the experimental dispersion data in terms for frequency and wavelength, respectively; and (c and d) Vs profiles shown to depths of 150 m and 1,500 m, respectively. The array resolution depth limit ($\boldsymbol{d_{res} = \lambda_{res}/2}$) is shown at 785 m. The dispersion misfit values for the median Vs profiles for each inversion parameterization are indicated in brackets in the legend.

5.4 Comparison of Invasive and Non-invasive Vs Profiles

As noted above, invasive Vs profiling (i.e., PS-logging and cross-hole seismic testing) was performed at the downhole array site in the PVC-cased boreholes for DH_2, DH_3, and DH_4 prior to the installation of each of the sensors (Youd and Briggs, 2003). When overlaid, the results from the PS-logging and cross-hole seismic testing agree remarkably well with the median surface wave inversion-derived Vs profiles from each of the four LR parameterizations (refer to Figure 5.5). Since the median Vs profiles inverted from each of the four LR parameterizations are variable yet agree quite well with the invasive seismic testing results, we can conclude that it would be appropriate to use each of them to model site response at the I15DA site in an attempt to account for epistemic uncertainty. The site response modeling is discussed below in Sections 6 and 0.

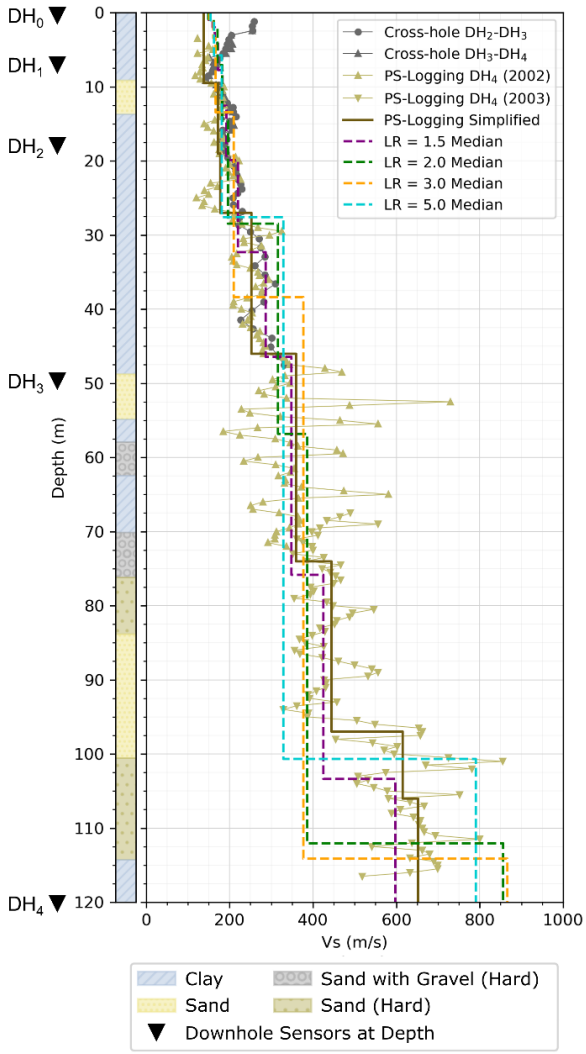

Figure 5.5 Invasive (PS-logging and cross-hole seismic testing) and non-invasive (inversion-derived surface wave testing) Vs profiles over the top 120 m at the I15DA site. Note that Robert Steller from GeoVision completed the PS-logging and Dr. James Bay from Utah State University completed the cross-hole testing. The soil log to the left of the Vs plot was developed from descriptions of soil cuttings during the drilling of the DH_4 sensor at a depth of 120 m (data obtained from Youd and Briggs, 2003). The depths of the DH sensors relative to the Vs profiles are denoted by black triangles.

6. SURFACE WAVE 1D SITE RESPONSE MODELING

As discussed in Section 3, using deep Vs profiles obtained from surface wave testing has been shown to be quite effective for modeling 1D site response at several borehole array sites, provided that uncertainty in the Vs profiles is properly noted (e.g., Teague et al. 2017, Hallal et al. 2022). The successful use of inversion-derived Vs profiles can be partly attributed to the fact that surface wave testing inherently incorporates some of the spatial variability across the site due to the distributed nature of the sensors used in both MASW and MAM testing. To help capture the uncertainty resulting from surface wave testing site characterization, separate models were created from each of the four inversion-derived median Vs profiles from surface wave testing (refer to Figure 5.4). Thus, in addition to the 1D site response conducted for PS-logging (refer to Section 3), additional 1D site response was conducted for each of the four median Vs profiles as described below. Please note that this analysis pertains only to 1D GRAs for each of the four median Vs profiles shown in Figure 5.4. In this report, we did not perform 1D GRAs using all 400 of the Vs profiles shown in Figure 5.3, as described in Hallal et al. 2022, which uses an aggregation of 1D GRAs from a large number of surface wave inversion-derived Vs profiles to account for spatial variability. This approach will be discussed in a later publication.

6.1 Inversion-Derived Vs Models

The 1D GRA Python script was again utilized to compute the 1D linear-viscoelastic TTFs for each of the four inversion-derived median Vs profiles. The same procedures used to calculate TTFs from the PS-logging Vs profile, as described in Section 3, were used for the surface wave inversion-derived Vs profiles. The 1D TTFs for each of the four median Vs profiles from surface wave testing (i.e., LR = 1.5, 2.0, 3.0, and 5.0) are shown in Figure 6.1a.

6.2 Comparing Inversion-Derived Vs TTFs with the ETF

Visually, all of the TTFs obtained from the various inversion-derived Vs profiles appear to fit the LM_{ETF} relatively well. The TTFs from the inversion-derived Vs profiles also agree quite well with the TTF from the PS-logging Vs profile, albeit they have slightly lower amplitudes across the first four modes. Nonetheless, like the TTF previously discussed in regard to the PS-logging Vs profile, the amplitudes of the TTFs derived from the surface wave Vs profiles are still significantly higher than the amplitudes of the individual and LM_{ETF}.

Quantitatively, the TTF calculated from the median Vs profile associated with LR = 2.0 surface wave inversion parameterization fits the LM_{ETF} the closest. It has the highest r of 0.510, the lowest m_{TF} at 3.238, and it tends to have smaller lognormal residual values across the goodness-of-fit range (refer to Figure 6.1b). However, the other 1D Vs profiles produced TTFs that had only marginally lower r values and marginally higher m_{TF} values. Furthermore, while the 1D TTF produced from the LR = 2.0 Vs profile results in the best fit of all the Vs profiles used in 1D site response, it still results in estimates of ground motion amplification at the first transfer function mode that overpredicts the LM_{ETF} by a factor of 15 to 20. Given that the TTFs from 1D site response tend to overpredict ground motion amplification, it was desirable to attempt multi-dimensional site response analyses as a means to potentially bring down the TTF amplitude values through explicitly modeling subsurface spatial variability (Hallal and Cox 2023). Therefore, the LR = 2.0 median Vs profile was used to create a pseudo-3D Vs model for multi-dimensional site response modeling, as discussed below.

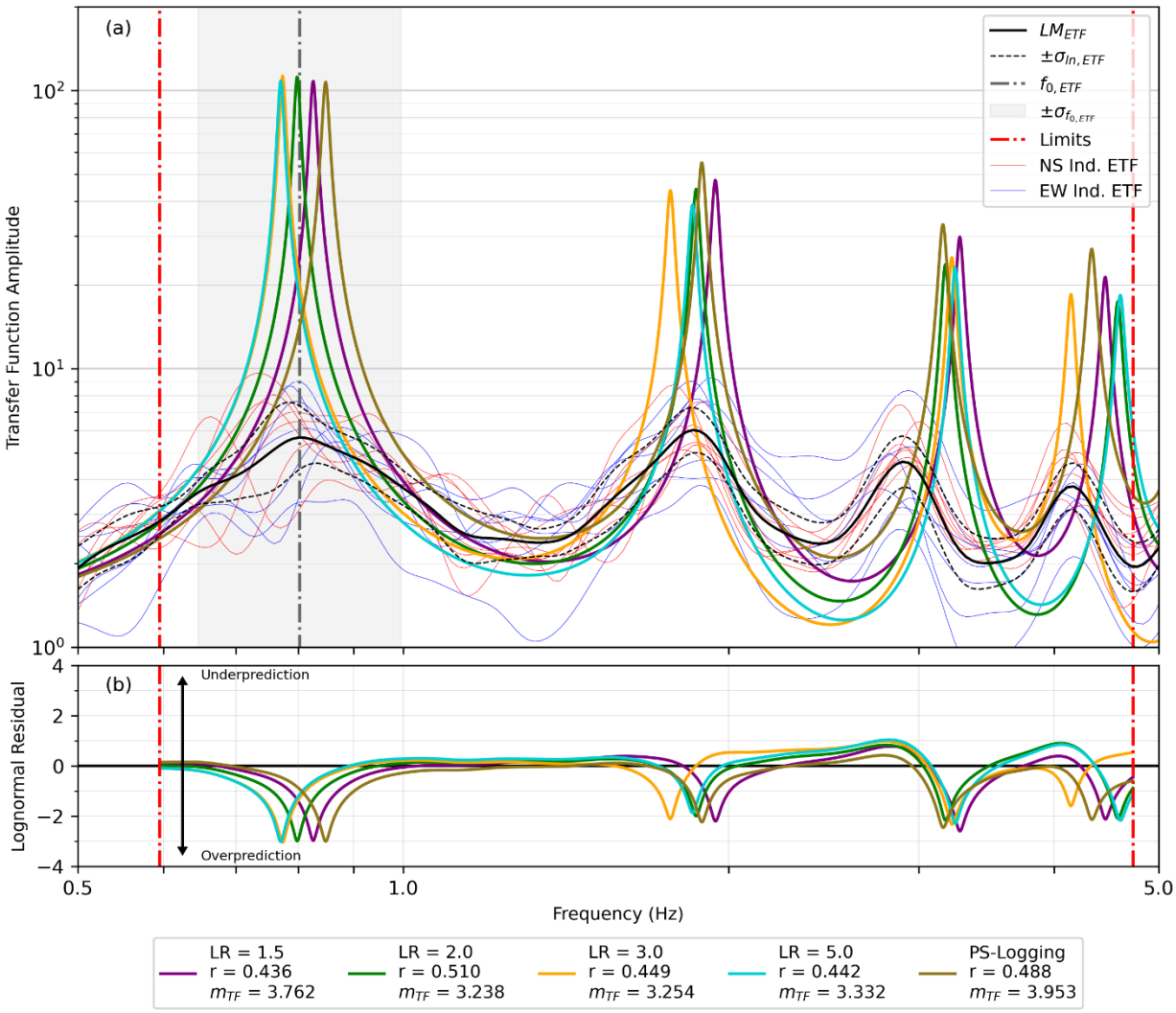

Figure 6.1 Comparison of ETFs from small-strain recorded ground motions and all TTFs from 1D linear-viscoelastic site response for the I15DA site. Plot (a) shows the individual ETFs from each ground motion, the $\boldsymbol{LM_{ETF}}$ curve, and the TTF curves from various 1D Vs profiles. Plot (b) displays the lognormal residual of each TTF to the $\boldsymbol{LM_{ETF}}$. The Pearson Correlation Coefficient, $\boldsymbol{r}$, and transfer function misfit, $\boldsymbol{m_{TF}}$, values are displayed in the legend at the bottom of the figure. Note that all goodness-of-fit parameters were calculated between the frequency range denoted by the dotted red lines.

7. MULTI-DIMENSIONAL SITE RESPONSE MODELING

To begin investigating multi-dimensional site response modeling at the I15DA, a pseudo-3D Vs model (Hallal and Cox 2021) was developed using the LR = 2.0 Vs profile and the spatially distributed H/V measurements performed across the site. The steps in this process involve determining the appropriate model depth, creating a pseudo-3D Vs model using the H/V geostatistical approach to account for spatial variability, and performing 2D site response analyses on cross-sections obtained from various azimuths of the pseudo-3D Vs model.

7.1 Determining the Psuedo-3D Vs Model Depth

It is important to create a pseudo-3D Vs model that extends deep enough to capture the governing impedance contrast for site response across the site. However, as multi-dimensional site response analyses will be conducted for models that extend laterally at least 1 km in each direction around the I15DA, the model should not extend any deeper than necessary to avoid high computational costs. In this case, we are simply trying to model the site response between the deepest sensor in the I15DA (i.e., 120 m) and the ground surface. The governing impedance contrast within this depth range, as observed for the LR = 2.0 median Vs profile, is at a depth of approximately 112 m, where the Vs increases from 390 m/s to 860 m/s (refer to Figure 5.5). This layer, with Vs > 760 m/s (i.e., "engineering rock"), extends with constant velocity to depths greater than 150 m (refer to Figure 5.4b). As discussed below, the layers in the Vs profile will be scaled to shallower and deeper depths based on the spatial variability of the $f_{0,mc}$ values calculated from H/V data across the I15DA site (refer to Section 4.3). Thus, it is possible that the governing impedance contrast may be scaled to depths greater than 120 m in order to capture spatial variability. Therefore, we chose to use a total model depth of 150 m to capture the governing impedance contrast and its presumed spatial variability across the site.

7.2 Pseudo-3D Vs Model from the H/V Geostatistical Approach

To create a pseudo-3D Vs model for the I15DA site, it was necessary to follow the procedures recommended by Hallal et al. (2021a and 2021b). Specifically, spatial interpolation was required to turn the irregularly sampled $f_{0,mc}$ values discussed in Section 4.3 into a uniformly estimated map of $f_{0,mc}$ values. Hallal et al. (2021a) recommended geostatistical kriging to perform the spatial interpolation necessary to create this map. However, the $f_{0,mc}$ values for the I15DA site only range from approximately 0.80 to 1.1 Hz and there is no coherent trend of change in $f_{0,mc}$ with increasing spatial separation (i.e., lag distance) across the site. As a result, it was difficult to obtain reasonable semi-variograms to produce a reliable uniformly estimated map of $f_{0,mc}$ via kriging. To overcome these challenges, we chose to develop the uniformly estimated map of $f_{0,mc}$ by performing natural neighbor interpolation, similar to Perron et al. (2022).

The $f_{0,mc}$ values for each H/V location where clear peaks could be determined are indicated by the color-coded circular symbols in Figure 7.1a. These measured $f_{0,mc}$ values were spatially interpolated using natural neighbor interpolation (Stevens 2018) over a distance of 1,250 m in all directions from the I15DA surface sensor (local coordinate 0,0) using an individual cell size of 10 m. This provided a uniformly estimated map of $f_{0,mc}$ values at every 10-m interval. After obtaining the uniformly estimated map of $f_{0,mc}$ values, the measured $f_{0,mc}$ value closest to the surface sensor (i.e., H/V location 400 with a $f_{0,mc}$ value of 0.92 Hz) was defined as the f_{0,mc,V_s}. This f_{0,mc,V_s} value was divided by the estimated $f_{0,mc}$ value at every cell to obtain a scaling factor (i.e., $S_{f_{0,mc}}$) for every cell at the site (refer to Figure 7.1b). The scaling factors were then used to thin or thicken the layers of the measured Vs profile by multiplying

the layer thicknesses by the scaling factors for each cell. In this manner, a scaled 1D Vs profile was obtained for each cell. These scaled 1D Vs profiles are shown in Figure 7.1c. While presently shown in only 1D, one can visualize their approximate spatial position in a 3D Vs model via the same $f_{0,mc}$ coloring scale used in Figure 7.1a. In other words, Vs profiles with shallower layer boundaries correspond to spatial locations with higher $f_{0,mc}$ values.

In order to build and implement the pesuo-3D Vs model into multi-dimension GRAs, the measured and scaled 1D Vs profiles need to be travel-time interpolated at a depth resolution (i.e., element size) that will allow for high-quality numerical wave propagation simulations at the highest frequency/shortest wavelength of interest. Based on the minimum Vs in the profile of 150 m/s, and a desire to resolve frequencies up to 5 Hz, the scaled LR = 2.0 Vs profiles were discretized through travel-time interpolation to a cell size of 2 m. This determination was made by requiring 15 elements per shortest wavelength for high-quality results (Hallal et al. 2023). This range of frequencies allows us to calculate goodness-of-fit statistics consistent with the absolute half-amplitude range discussed in Section 3.2.

To perform the travel time interpolation for the measured and scaled Vs profiles, a shear wave travel time through each scaled layer was obtained by dividing the thickness of that layer by the layer's Vs. A cumulative travel time curve was then calculated for each scaled Vs profile by summing the travel times of each layer (refer to Figure 7.1d). The cumulative travel time curves were then used to obtain travel-time interpolated curves that were discretized over 2-m intervals. The travel times were determined for every discretized 2-m interval from the cumulative travel time curve by subtracting the cumulative travel time at the bottom of the discretized interval by the cumulative travel time at the top of the discretized interval. The discretized Vs profile was then calculated by dividing the discretized thickness of 2 m by the individual travel times over each interval (refer to Figure 7.1e).

While shown as a stack of 1D Vs profiles, each color-coded travel-time interpolated profile in Figure 7.1e represents a single Vs profile for each surface cell in the 10-m by 10-m uniformly estimated map of $f_{0,mc}$ values (refer to Figure 7.1a). To match the depth interval used for travel-time interpolation (i.e., 2 m) and create cubic elements for numerical modeling, the square 10-m cells of the uniformly estimated $f_{0,mc}$ map were split into 25 equal 2-m by 2-m cells. Each scaled 1D Vs profile was assigned to the corresponding surface cell in the 2-m cell map of uniformly estimated $f_{0,mc}$ to create the final pseudo-3D model for the I15DA, which is shown in Figure 7.2a. In Figure 7.2a, the uniformly estimated $f_{0,mc}$ map is superimposed on top of the pseudo-3D Vs model to aid with visualizing how higher $f_{0,mc}$ values correspond to shallower layer boundaries and lower $f_{0,mc}$ values correspond to deeper layer boundaries.

The open-source software Seismo-VLAB (i.e., SVL; Kusanovic et al. 2022) was used to model multi-dimensional site response for the I15DA. Currently, it is not computationally feasible for us to run 3D site response models in SVL for a model of this size (i.e., 2,500 m x 25,00 m x 150 m) when using 2-m elements (i.e., over 117 million elements). Instead, the pseudo-3D Vs model for the I15DA was sliced to create 2D cross-sections at 15° intervals in the clockwise direction, starting at the north azimuth (0°) and continuing to an azimuth of 165°. The 45° azimuth cross-section is shown in Figure 7.2Figure 7.2b. Each of the 2D cross-sections was used to perform a 2D GRA.

Material properties needed for the linear-viscoelastic 2D GRAs include small-strain Vs, mass density, Poisson's ratio, and small-strain damping ratio. Each cross-section from the pseudo-3D Vs model provides a small-strain Vs for each element. Mass density was fixed at 2000 kg/m^3 for all layers. Additionally, a Poisson's ratio of 0.30 was used for soil above the ground water table, 0.48 for soil layers below the ground water table, and 0.30 for rock layers (Vs > 760 m/s). The water table was set at 20 m based on information provided in the boring logs for the site. Currently, it is not feasible to assign unique

values of small strain damping ratio to each soil layer within SVL. Instead, a small strain damping value D_{min} = 0.88% was assigned to each layer, which is the depth/layer thickness weighted average of the Darendeli (2001) D_{min} values used for the 1D site response.

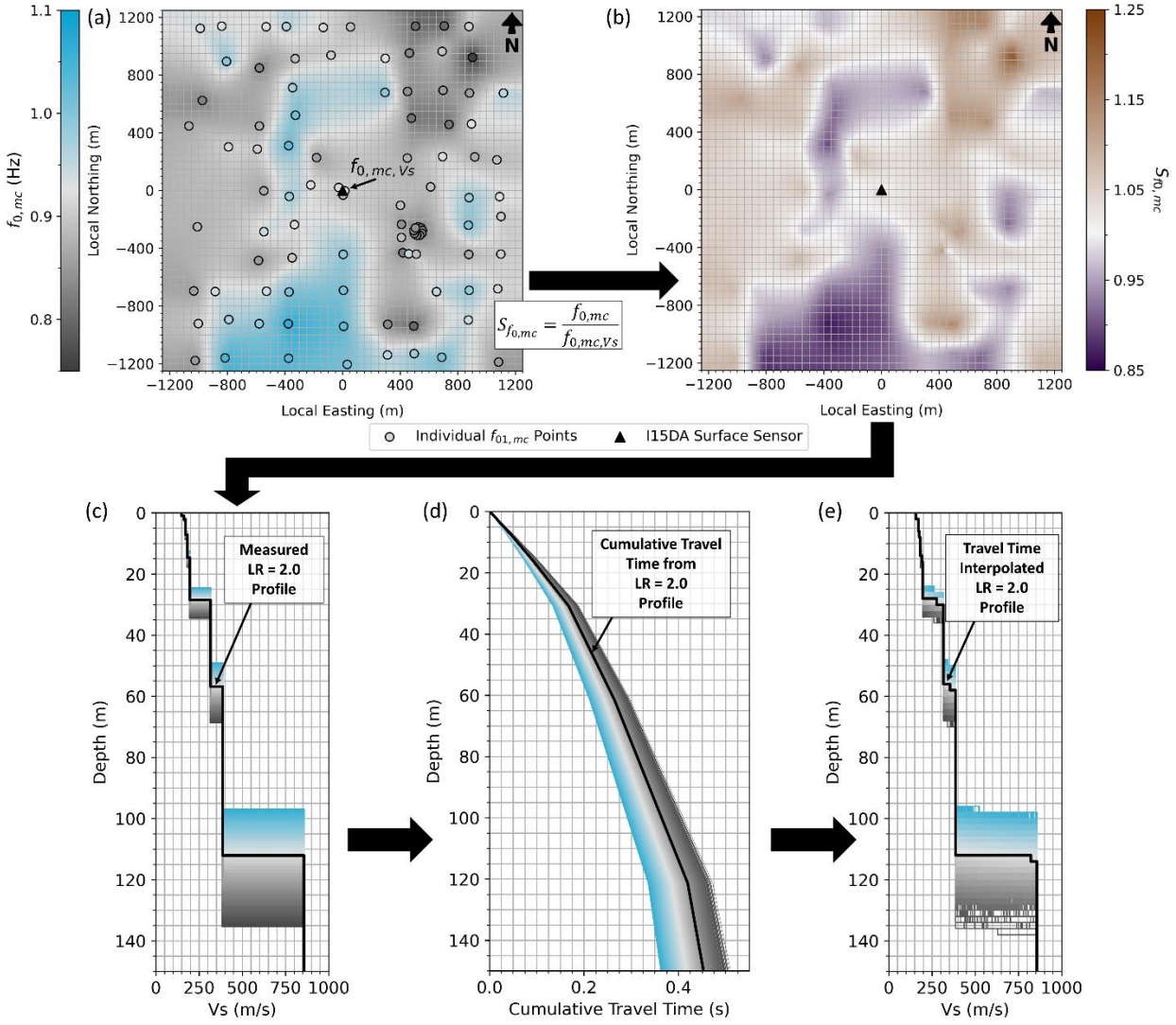

Figure 7.1 Schematic illustrating the steps required to develop a pseudo-3D Vs model for the I15DA using the H/V geostatistical approach: (a) interpolating $\boldsymbol{f_{0,mc}}$ points to obtain a uniformly estimated map of $\boldsymbol{f_{0,mc}}$, (b) calculating the $\boldsymbol{S_{f_{0,mc}}}$ for each cell in the map, (c) scaling the measured Vs profile by $\boldsymbol{S_{f_{0,mc}}}$ at each cell to obtain a scaled Vs profile for each cell, (d) calculating a cumulative travel time profile for each cell, and (e) using the cumulative travel time profile for each cell to determine the travel-time interpolated Vs profiles over a 2-m cell/depth interval

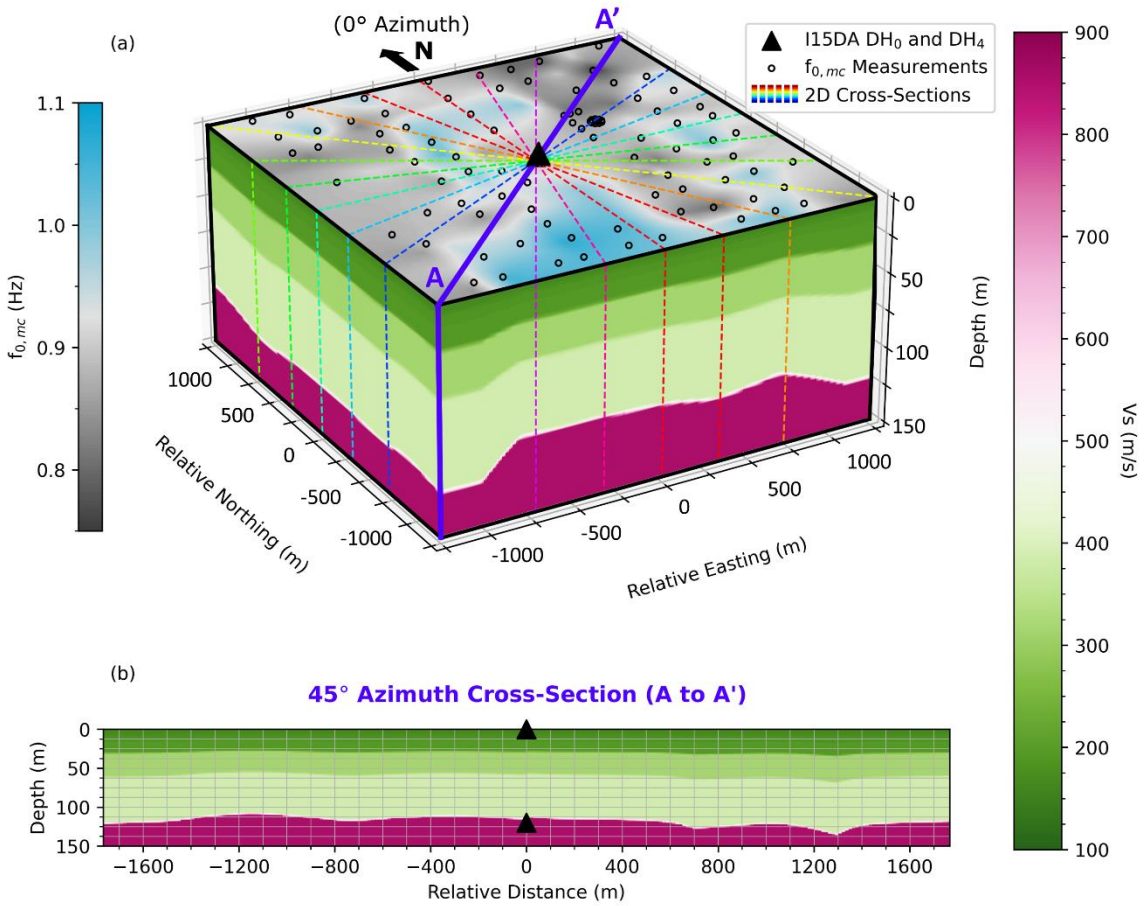

Figure 7.2 Final pseudo-3D Vs model for the I15DA in terms of: (a) an isometric 3D view, and (b) a 45° azimuth cross-section. The location of the I15DA sensors DH_0 and DH_4 are denoted by black triangles. The 45° azimuth cross-section is highlighted in purple on the isometric view of the model.

A vertically propagating plane Ricker wavelet was used as the input excitation at the base of the model (150 m). This wavelet had a dominant frequency of 3.0 Hz with a center time of 2 s (refer to Figure 7.3a). To capture the full wavefield and enable accurate Fourier spectra computations, the total duration of the analysis was extended to 15 s using 1,501 time steps. The 3.0 Hz wavelet has sufficient energy between 0.5 Hz and 5 Hz (refer to Figure 7.3b) to capture the first four modes of the LM_{ETF}. Note that while the excitation is input as a vertically propagating plane wavelet, irregularities in the bedrock and other layer boundaries within the cross-sections will produce non-vertically propagating body waves and surface waves.

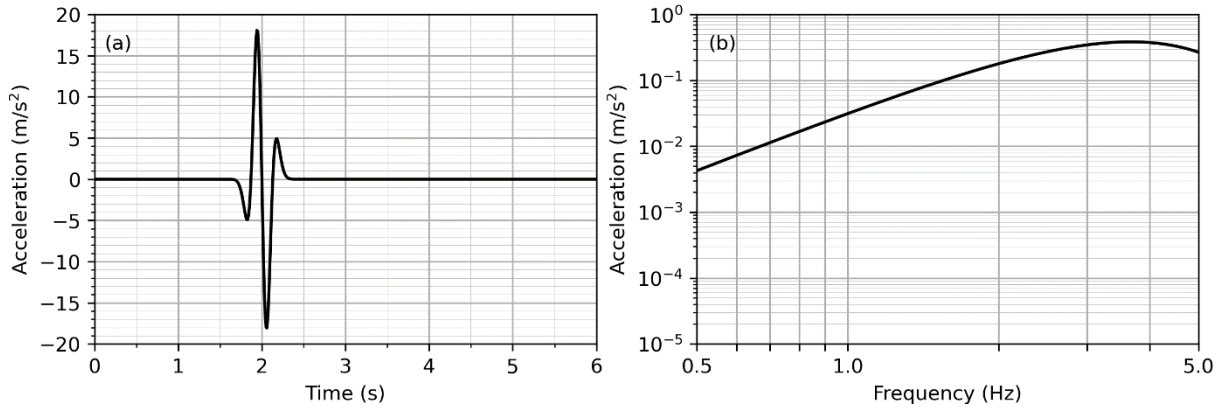

Figure 7.3 Ricker wavelet input excitation for the 2D cross-section GRAs in terms of: (a) acceleration time series, and (b) Fourier amplitude spectrum. This Ricker wavelet was based on a dominant frequency of 3.0 Hz.

Prior to numerical wave propagation, the 2D azimuthal cross-sections were extended to a total length of 3,000 m in each direction from the surface sensor, and free-field boundary conditions were used along the model boundaries. These considerations were made to minimize any potential wave reflections back into the model and were demonstrated to be successful at doing so by Hallal and Cox (2023). The Ricker wavelet was applied as a vertically propagating, horizontally polarized shear wave uniformly across the bottom of the model. Following wave propagation simulations, SVL was used to output horizontal acceleration time histories at the base sensor DH_4 and the surface sensor DH_0. The FAS of each time history was computed, similar to the process described in Section 2.2, and TTFs were calculated by dividing the FAS of the surface time history by the FAS of the base time history. A "within" condition at the depth of the downhole sensor DH_4 was used to calculate the corresponding simulated TTF for each cross-section. The individual TTFs for each azimuth and the mean TTF of all azimuths (i.e., Mean 2D) are displayed in Figure 7.4.

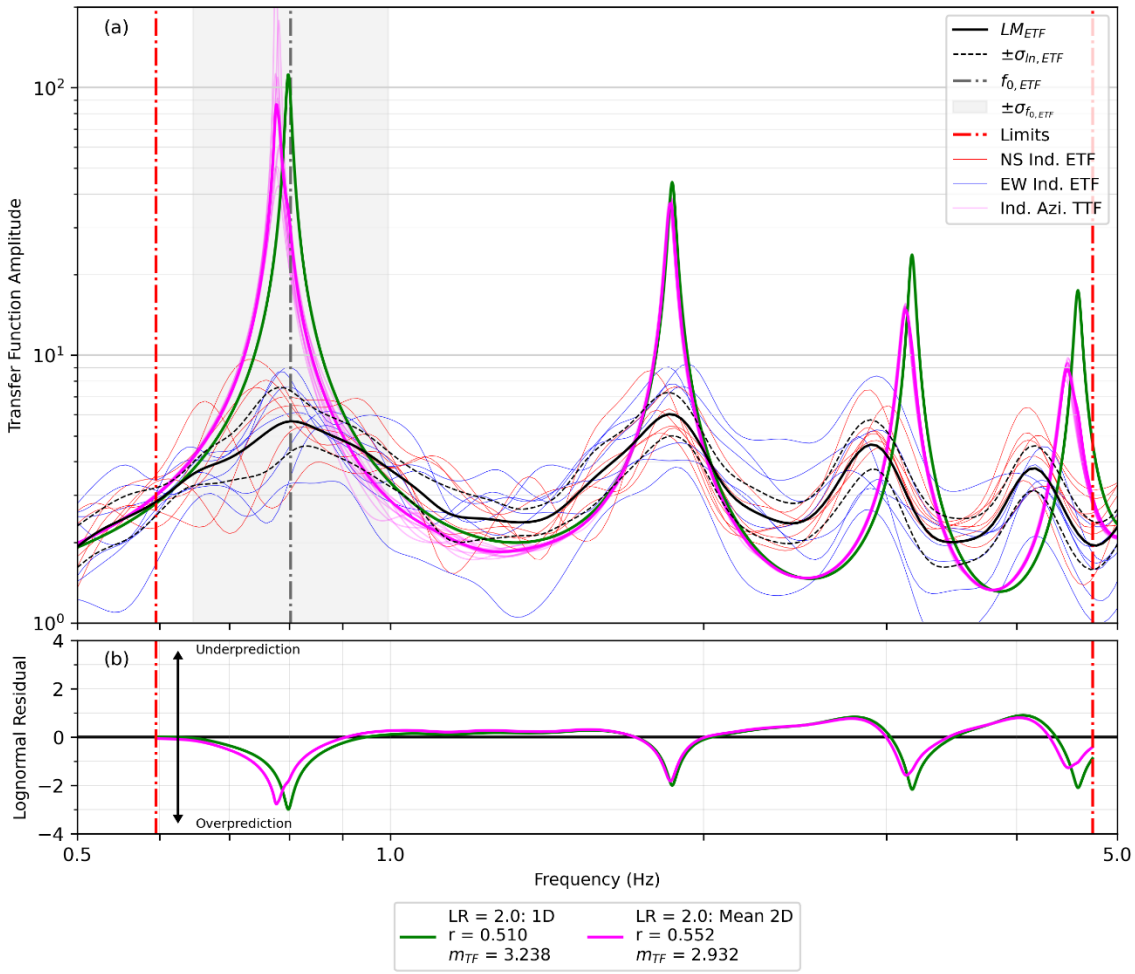

Figure 7.4 Comparison of ETFs from small-strain recorded ground motions with the LR = 2.0 1D linear-viscoelastic TTF and the mean 2D linear-viscoelastic TTF from SVL. Plot (a) shows the individual ETFs, the $\boldsymbol{LM_{ETF}}$ curve, the TTF curve from the LR = 2.0 1D Vs profile, and the individual and mean TTFs from the various 2D Vs cross-sections. Plot (b) displays the lognormal residual of each TTF to the $\boldsymbol{LM_{ETF}}$. The Pearson correlation coefficient, $\boldsymbol{r}$, and transfer function misfit, $\boldsymbol{m_{TF}}$, values are displayed in the legend at the bottom of the figure. Note that all goodness-of-fit parameters were calculated between the frequency range denoted by the dotted red lines.

7.3 Comparing the 2D TTF Goodness-of-Fit

Visually, the azimuthally variable 2D site response analyses produce a mean TTF that better fits the individual and LM_{ETF} curves than the 1D site response analyses based on the LR = 2.0 Vs profile. Specifically, the amplitudes of the first, third, and fourth modes of the 2D mean TTF are lower than the 1D TTF, and the frequencies of the third and fourth peaks in the 2D mean TTF also align slightly better with the LM_{ETF} curve. Quantitatively, the mean 2D TTF produces an r of 0.552 and an m_{TF} of 2.932. The higher r value indicates that the 2D TTF fits the overall shape of the LM_{ETF} curve better, while the lower m_{TF} value indicates that the 2D TTF is fitting the amplitudes better. While these 2D GRA results are promising and indicate better predictive performance than the 1D GRAs, the 2D mean TTF still produces estimates of amplification at the fundamental and first-higher modes that are 10 to 12 times greater than the median ETF.

8. DISCUSSION AND CONCLUSIONS

From the results of the 1D and 2D site response modeling presented in this study, it is clear the 1D TTFs agree better with the individual ETFs than the LM_{ETF}. As more site-specific spatial variability of Vs is explicitly accounted for in the 2D TTFs they become closer to the LM_{ETF}. This is shown in Figure 8.1 where the Pearson correlation coefficient, r, and the transfer function misfit value, m_TF, are plotted for each GRA discussed in this report by Vs profile and GRA type.

The 1D TTF calculated from the simplified nine-layer PS-logging profile is able to generally capture the peaks and shape of the ETF; however, the amplitudes of the TTF are significantly greater than the amplitudes of the LM_{ETF}. In particular, the frequencies of the fundamental and first-higher modes of the LM_{ETF} are very well predicted by the PS-logging 1D TTF. The second- and third-higher mode TTF peaks do not align quite as well with the LM_{ETF} peaks, being biased slightly toward higher frequencies. The PS-logging TTF overestimates the amplification at the fundamental and higher modes of the LM_{ETF} by a factor of 15 to 20. The 1D PS-logging GRA produced a TTF with an r of 0.488 and an m_{TF} of 3.953, which quantitatively indicates that this 1D analysis does not accurately model the small-strain, viscoelastic site response observed at the I15DA described by the LM_{ETF}.

We elected to use the surface wave approach in an attempt to implicitly account for some spatial variability in Vs at the I15DA site. From the surface wave dispersion data derived from MASW and MAM testing, four inversion-derived Vs profiles were produced to account for epistemic uncertainty in the Vs profiles. Subsequently, each inversion-derived Vs profile was used to create an independent 1D site response model. Each model produced TTFs that were both visually and quantitatively similar to the 1D TTF from the simplified PS-logging Vs profile. The TTF from the LR = 2.0 inversion-derived Vs profile proved to fit the LM_{ETF} slightly better than the TTFs from the other inversion-derived Vs profiles and from the PS-logging Vs profile. Nonetheless, the TTF amplification factors at the fundamental and higher modes were still overestimated by a factor of 15 to 20. The LR = 2.0 inversion-derived Vs profile 1D GRA produced a TTF with an r of 0.510 and an m_{TF} of 3.238. While these goodness-of-fit parameters describe a better fit of the TTF to the LM_{ETF} than the 1D PS-logging GRA, these parameters still suggest that this profile does not accurately model the small-strain, viscoelastic site response observed at the I15DA.

To explicitly account for spatial variability of Vs at the I15DA, we used the H/V geostatistical approach to create a pseudo-3D Vs model from H/V ambient noise measurements across the site. A total of 12 cross-sections at various azimuths in the model were used for 2D numerical GRAs. These estimates of 2D site response produced TTFs that visually and quantitatively fit the model frequencies and amplitudes of the LM_{ETF} better than the PS-logging and the surface wave 1D TTFs. Though the estimates of TTF amplification from 2D GRAs are closer to the LM_{ETF}, the amplification is still 10 to 15 times higher than what is shown by the LM_{ETF}. This 2D analysis produced a TTF with an r of 0.552 and an m_{TF} of 2.932, which makes the TTF produced in this analysis the best fitting TTF to the LM_{ETF} produced for the I15DA in this study. Still, these goodness-of-fit parameters indicate that this analysis does not fully capture the LM_{ETF}; thus, other GRA methods like those described in Hallal et al. (2022) should be explored as well, as they may better capture the amplitudes of the LM_{ETF} more accurately.

Overall, each of the 1D and 2D analyses were able to produce TTFs that generally capture the LM_{ETF} modal frequencies; however, none of the site response modeling discussed in this study produced estimates of TTFs that were exceptionally good fits in terms of amplitude. Over-prediction of TTF amplitude is typical of 1D and 2D GRA results at other borehole array sites in the United States and across the world. While attempting to incorporate more spatial variability in Vs has produced better

estimates of site response for the I15DA, the TTF amplitudes are still over-predicted, and more studies are required to determine the cause of this over-amplification.

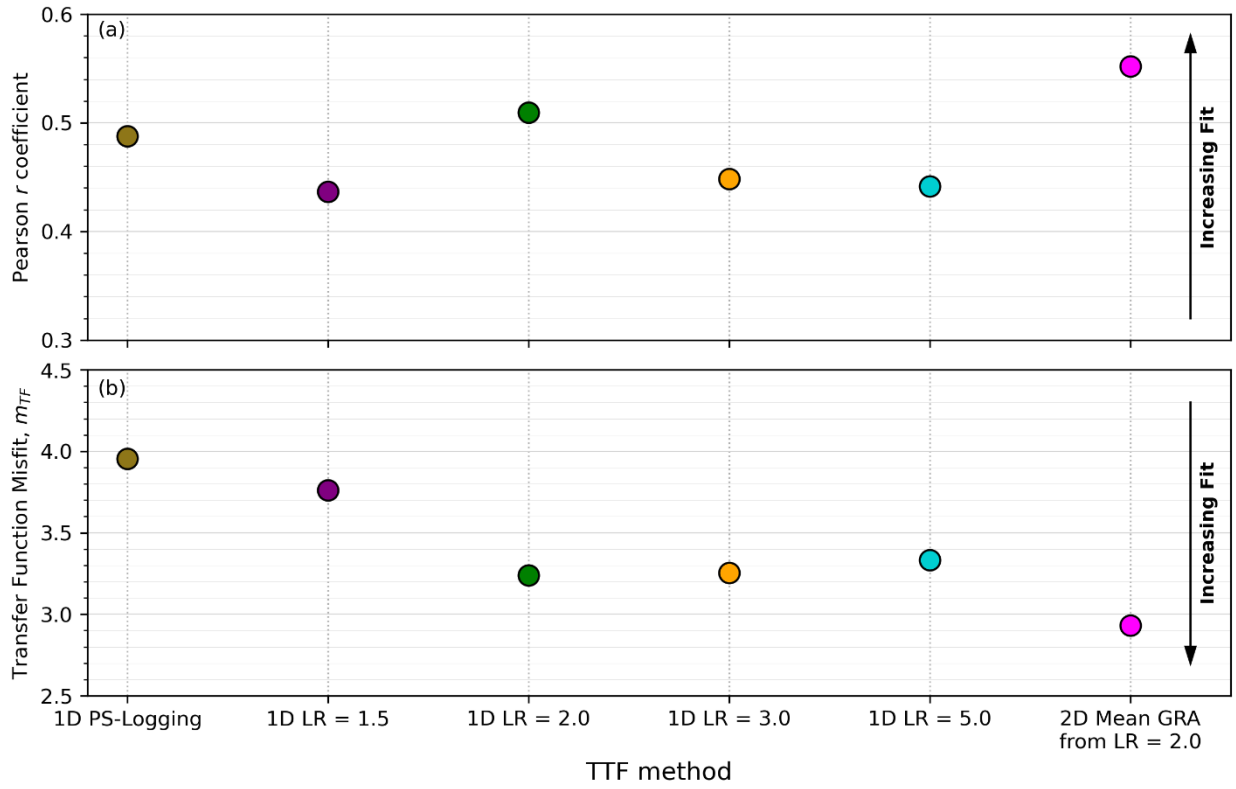

Figure 8.1 Comparison of goodness-of-fit parameters for each 1D and 2D GRA in terms of: (a) Pearson's correlation coefficient, $\boldsymbol{r}$, and (b) transfer function misfit value, $\boldsymbol{m_{TF}}$. Note that the 1D GRA with the best fit is the 1D LR = 2.0 GRA and the overall best fitting GRA is the 2D Mean GRA from the LR = 2.0 Psuedo-3D Vs Model.

Due to software implementation limitations, we were only able to use a single, average estimate of D_{min} for the 2D GRAs. This simplification does not represent the actual in-situ small strain damping, where D_{min} is dependent on layer-specific soil properties and confining stresses. The amplification factors associated with the first four modes of the TTF might be reduced when using soil-type and layer-specific estimates for D_{min}.

As soon as it is computationally feasible, we hope to conduct 3D GRAs on the full psuedo-3D Vs model developed in this study. Note that the 2D GRAs in the present work were performed on cross-sections with 225,000 2-m square elements. However, it will require over 117 million 2-m cubic elements to perform 3D GRAs for the entire pseudo-3D Vs model. 3D GRAs will more naturally account for site-specific wave scattering, hopefully leading to TTFs that better fit the LM_{ETF}, especially in terms of amplification factors at the first four modes. In the future, we also hope to perform non-linear site response analyses at the I15DA and to eventually perform SFSI studies using the calibrated site response model and the ground motions recorded by the instrumented bridge above the I15DA. We believe these types of studies will contribute significantly to better understanding and modeling site response of transportation infrastructure in Utah and beyond.

9. REFERENCES

Bonnefoy-Claudet, S. (2004). "Nature du bruit de fond sismique: implications pour les études des effets de site." Universite Joseph Fourier, Grenoble, France.

Capon, J. (1969). "High-resolution frequency-wavenumber spectrum analysis." Proceedings of the IEEE, 8, 1408–1418.

Capon J. (1969). "High-resolution frequency-wavenumber spectrum analysis." *Proc IEEE* 8:1408–1418. (https://doi.org/10.1109/PROC.1969.7278)

Cheng, T., Cox, B. R., Vantassel, J. P., and Manuel, L. (2020). "A statistical approach to account for azimuthal variability in single-station HVSR measurements." *Geophysical Journal International*, https://doi.org/10.1093/gji/ggaa342

Chang, T., Hallal M.M., Vantassel, J.P., and Cox, B.R. (2021). "Estimating Unbiased Statistics for Fundamental Site Frequency Using Spatially Distributed HVSR Measurements and Voronoi Tessellation." *Journal of Geotechnical and Geoenvironmental Engineering*, 147(8): 04021068.

Cox, B.R., Chang, T., Vantassel, J.P., and Manuel, L. (2020). "A Statistical Representation and Frequency-Domain Window-Rejection Algorithm for Single-Station HVSR Measurements," *Geophysical Journal International*, 221(3), 2170-2183. (https://doi.org/10.1093/gji/ggaa119).

Cox, B. R., and Teague, D. P. (2016). "Layering ratios: a systematic approach to the inversion of surface wave data in the absence of a priori information." *Geophysical Journal International*, 207(1), 422–438.

Cox, B. R., and Wood, C. M. (2011). "Surface Wave Benchmarking Exercise: Methodologies, Results, and Uncertainties." *GeoRisk 2011*, American Society of Civil Engineers, Atlanta, Georgia, United States, 845–852.

Darendeli, M. B. (2001). "Development of a New Family of Normalized Modulus Reduction and Material Damping Curves." Ph. D., The University of Texas at Austin, Austin, Texas.

Dunkin, J. (1965). "Computation of modal solution in layered, elastic media at high frequencies." *Bulletin of the Seismological Society of America*, 55(2), 335–358.

Foti, S., Comina, C., Boiero, D., and Socco, L. V. (2009). "Non-uniqueness in surface-wave inversion and consequences on seismic site response analyses." *Soil Dynamics and Earthquake Engineering*, 29(6), 982–993.

Foti, S., Lai, C. G., Rix, G. J., and Strobbia, C. (2015). *Surface Wave Methods for Near-Surface Site Characterization*. CRC Press, Boca Raton, FL.

Garofalo, F., Foti, S., Hollender, F., Bard, P. Y., Cornou, C., Cox, B. R., Dechamp, A., Ohrnberger, M., Perron, V., Sicilia, D., Teague, D., and Vergniault, C. (2016). "InterPACIFIC project: Comparison of invasive and non-invasive methods for seismic site characterization. Part II: Inter-comparison between surface-wave and borehole methods." *Soil Dynamics and Earthquake Engineering*, 82, 241–254.

Goulet, C.A., Kishida, T.K., Ancheta, T.D., Cramer, C.H., Darragh, R.B., Silva, W.J., Hashash, Y.M., Harmon, J., Parker, G.A., Stewart, J.P., and Youngs, R.R. (2021). "PEER NGA-East Database." *Earthquake Spectra*, Vol 37(SI), 1331-1353.

Griffiths, S. C., Cox, B. R., Rathje, E. M., and Teague, D. P. (2016a). "Surface-Wave Dispersion Approach for Evaluating Statistical Models That Account for Shear-Wave Velocity Uncertainty." *Journal of Geotechnical and Geoenvironmental Engineering*, 142(11), 04016061.

Griffiths, S. C., Cox, B. R., Rathje, E. M., and Teague, D. P. (2016b). “Mapping Dispersion Misfit and Uncertainty in Vs Profiles to Variability in Site Response Estimates.” *Journal of Geotechnical and Geoenvironmental Engineering*, 142(11), 04016062.

Hallal, M.M., Cox, B.R., and Vantassel, J.P. (2022). “Comparison of State-of-the-Art Approaches Used to Account for Spatial Variability in 1D Ground Response Analyses.” *ASCE Journal of Geotechnical and Geoenvironmental Engineering*, 148(5): 04022019. (https://doi.org/10.1061/(ASCE)GT.1943-5606.0002774).

Hallal M.M., and Cox B.R. (2021a). “An H/V Geostatistical Approach for Building Pseudo-3D Vs Models to Account for Spatial Variability in Ground Response Analyses, Part I: Model Development.” *Earthquake Spectra*. 2021;37(3):2013-2040. (doi:10.1177/8755293020981989).

Hallal M.M., and Cox BR. (2021b). “An H/V Geostatistical Approach for Building Pseudo-3D Vs Models to Account for Spatial Variability in Ground Response Analyses Part II: Application to 1D Analyses at Two Downhole Array Sites.” *Earthquake Spectra*. 2021;37(3):1931-1954. (doi:10.1177/8755293020981982)

Hallal, M.M., and Cox, B.R. (2023). “What Spatial Area Influences Seismic Site Response: Insights Gained from Multi-Azimuthal 2D Ground Response Analyses at the Treasure Island Downhole Array,” *ASCE Journal of Geotechnical and Geoenvironmental Engineering*, 149 (1): 04022124. (https://doi.org/10.1061/JGGEFK.GTENG-11023).

Hashash, Y.M.A., Musgrove, M.I., Harmon, J.A., Ilhan, O., Xing, G., Numanoglu, O., Groholski, D.R., Phillips, C.A., and Park, D. (2020) “DEEPSOIL 7.0, User Manual.” Urbana, IL, Board of Trustees of University of Illinois at Urbana-Champaign.

Haskell, N.A. (1953). “The dispersion of surface waves on multilayered media,” 86–103, in *Vincit Veritas: A Portrait of the Life and Work of Norman Abraham Haskell*, 1905–1970, Vol. 30, pp. 86–103, ed. Ben-Menahem, A., American Geophysical Union. (doi:10.1029/SP030p0086).

Haskell, N. A. (1953). “The dispersion of surface waves on multilayered media.” (A. Ben-Menahem, ed.), 86–103.

Knopoff, L. (1964). “A matrix method for elastic wave problems.” *Bulletin of the Seismological Society of America*, 54(1), 431–439.

Kusanovic, D., E. Seylabi, and D. Asimaki. (2022). “Seismo-VLAB.” Accessed July 2023. https://seismovlab.com/.

Lachet, C., and Bard, P.-Y. (1994). “Numerical and Theoretical Investigations on the Possibilities and Limitations of Nakamura’s Technique.” *Journal of Physics of the Earth*, 42(5), 377–397.

Lermo, J., and Chávez-García, F. J. (1993). “Site effect evaluation using spectral ratios with only one station.” *Bulletin of the Seismological Society of America*, 83(5), 1574–1594.

Malischewsky, P. G., and Scherbaum, F. (2004). “Love’s formula and H/V-ratio (ellipticity) of Rayleigh waves.” *Wave Motion*, 40(1), 57–67.

Mayne, P. (2001). “Stress-strain-strength-flow parameters from enhanced in-situ tests.” Proceedings, International Conference on In-Situ Measurement of Soil Properties & Case Histories [In-Situ 2001], Bali, Indonesia, May 21-24, 2001, pp. 27-48.

Perron, V., Bergamo, P., and Fäh, D. (2022). “Site Amplification at High Spatial Resolution from Combined Ambient Noise and Earthquake Recordings in Sion, Switzerland.” *Seismological Research Letters*, 93(4): 2281–2298. (https://doi.org/10.1785/022021028).

Poggi, V., and Fah, D. (2010). “Estimating Rayleigh wave particle motion from three-component array analysis of ambient vibrations.” *Geophysical Journal International*, 180(1), 251–267.

Sambridge, M. (1999). “Geophysical inversion with a neighbourhood algorithm-I. Searching a parameter space.” *Geophysical Journal International*, 138(2), 479–494.

SESAME. (2004). *Guidelines for the Implementation of the H/V Spectral Ratio Technique on Ambient Vibrations Measurements*, Processing, and Interpretation. European Commission - Research General Directorate, 62.

Stevens, R. (2018). innolitics/natural-neighbor-interpolation: Latest (Concept). Github. https://github.com/innolitics/natural-neighbor-interpolation.

Teague, D. P., and Cox, B. R. (2016). “Site response implications associated with using non-unique Vs profiles from surface wave inversion in comparison with other commonly used methods of accounting for Vs uncertainty.” *Soil Dynamics and Earthquake Engineering*, 91, 87–103.

Teague, D. P., Cox, B. R., and Rathje, E. M. (2018b). “Measured vs. predicted site response at the Garner Valley Downhole Array considering shear wave velocity uncertainty from borehole and surface wave methods.” *Soil Dynamics and Earthquake Engineering*, 113, 339–355.

Teague, D.P., Cox, B.R., Bradley, B., and Wotherspoon, L. (2018a). “Development of Deep Shear Wave Velocity Profiles with Estimates of Uncertainty in the Complex Inter-Bedded Geology of Christchurch, New Zealand,” *Earthquake Spectra*, 34(2), 639-672. (https://doi.org/10.1193/041117EQS069M).

Thompson, E. M., L. G. Baise, Y. Tanaka, and R. E. Kayen. (2012). “A taxonomy of site response complexity.” *Soil Dyn. Earthquake. Eng*. 41: 32–43. https://doi.org/10.1016/j.soildyn.2012.04.005.

Thomson, W. T. (1950). “Transmission of Elastic Waves through a Stratified Solid Medium.” *Journal of Applied Physics*, 21(2), 89–93.

U.S. Geological Survey. (2023). “Earthquake Hazards Program: Search Earthquake Catalog” https://earthquake.usgs.gov/earthquakes/search/. (Accessed May 15, 2023).

Vantassel, J.P., and Cox, B.R. (2021). “SWinvert: a workflow for performing rigorous surface wave inversions,” *Geophysical Journal International*, 224(2), 1141-1156. (https://doi.org/10.1093/gji/ggaa426).

Vantassel, J.P., and Cox, B.R. (2022). “SWprocess: a workflow for developing robust estimates of surface wave dispersion uncertainty,” *Journal of Seismology*. (https://doi.org/10.1007/s10950-021-10035-y)

Vantassel, J. P. (2020). jpvantassel/hvsrpy: Latest (Concept). Zenodo. http://doi.org/10.5281/zenodo.3666956

Wathelet, M., Guillier, B., Roux, P., Cornou, C., and Ohrnberger, M. (2018). “Rayleigh wave three-component beamforming: signed ellipticity assessment from high-resolution frequency-wavenumber processing of ambient vibration arrays.” *Geophysical Journal International*, 215(1), 507–523.

Wathelet, M., Jongmans, D., and Ohrnberger, M. (2004). “Surface-wave inversion using a direct search algorithm and its application to ambient vibration measurements.” *Near Surface Geophysics*, 2(4), 211–221.

Wathelet, M., Jongmans, D., Ohrnberger, M., and Bonnefoy-Claudet, S. (2008). “Array performances for ambient vibrations on a shallow structure and consequences over Vs inversion.” *Journal of Seismology*, 12(1), 1–19.

Youd, T. L., and Briggs, D. H. (2003). Downhole Seismic Array at The Intersection Of I-15, I-80 And SR-201, Salt Lake City, Utah. UDOT Report UT-13.18.

Zywicki, D.J. (1999). “Advanced signal processing methods applied to engineering analysis of seismic surface waves.” Ph.D. Dissertation, School of Civil and Environmental Engineering, Georgia Institute of Technology, Atlanta, GA, 357 p.

APPENDIX A: TABULATED GROUND MOTION INFORMATION

Table A.1 Small-strain ground motion events used to calculate the LM_{ETF}.

Station	Component	USGS Event ID	UTC Event Time	Mag.	Mag. Type	PGA (g's)
40	NS	uu60364822	2020-03-18T19:07:30.25	3.41	M_L	0.00459
40	EW	uu60364822	2020-03-18T19:07:30.25	3.41	M_L	0.00360
F0	NS	uu60364822	2020-03-18T19:07:30.25	3.41	M_L	0.01579
F0	EW	uu60364822	2020-03-18T19:07:30.25	3.41	M_L	0.01197
40	NS	uu60365152	2020-03-18T21:11:10.74	2.88	M_L	0.00327
40	EW	uu60365152	2020-03-18T21:11:10.74	2.88	M_L	0.00181
F0	NS	uu60365152	2020-03-18T21:11:10.74	2.88	M_L	0.00866
F0	EW	uu60365152	2020-03-18T21:11:10.74	2.88	M_L	0.00549
40	NS	uu60366502	2020-03-19T12:44:47.70	3.2	M_L	0.00260
40	EW	uu60366502	2020-03-19T12:44:47.70	3.2	M_L	0.00605
F0	NS	uu60366502	2020-03-19T12:44:47.70	3.2	M_L	0.01202
F0	EW	uu60366502	2020-03-19T12:44:47.70	3.2	M_L	0.01187
40	NS	uu60368447	2020-03-21T16:59:31.93	3.37	M_L	0.00364
40	EW	uu60368447	2020-03-21T16:59:31.93	3.37	M_L	0.00188
F0	NS	uu60368447	2020-03-21T16:59:31.93	3.37	M_L	0.00903
F0	EW	uu60368447	2020-03-21T16:59:31.93	3.37	M_L	0.00866
40	NS	uu60369062	2020-03-23T01:17:15.31	3.94	M_L	0.00701
40	EW	uu60369062	2020-03-23T01:17:15.31	3.94	M_L	0.00994
F0	NS	uu60369062	2020-03-23T01:17:15.31	3.94	M_L	0.02438
F0	EW	uu60369062	2020-03-23T01:17:15.31	3.94	M_L	0.03213
40	NS	uu60370427	2020-03-26T16:12:42.89	3.25	M_L	0.00361
40	EW	uu60370427	2020-03-26T16:12:42.89	3.25	M_L	0.00291
F0	NS	uu60370427	2020-03-26T16:12:42.89	3.25	M_L	0.00936
F0	EW	uu60370427	2020-03-26T16:12:42.89	3.25	M_L	0.01040
40	NS	uu60370437	2020-03-26T16:21:56.75	2.95	M_L	0.00116
40	EW	uu60370437	2020-03-26T16:21:56.75	2.95	M_L	0.00151
F0	NS	uu60370437	2020-03-26T16:21:56.75	2.95	M_L	0.00359
F0	EW	uu60370437	2020-03-26T16:21:56.75	2.95	M_L	0.00354

APPENDIX B: MAM STATIONS COORDINATES AND H/V VALUES

Table B.1 MAM station coordinates and $f_{0,mc}$ values for the I15DA site. For stations where the H/V curves were not of sufficient quality to determine $f_{0,mc}$, no values are reported, as indicated by the dash (-) symbol.

Position	Station	Latitude (deg)	Longitude (deg)	$f_{0,mc}$ (Hz)
C60-01	US.STN01	40.72063196	-111.900932	0.842
C60-02	US.STN02	40.72090297	-111.9009352	0.842
C60-03	US.STN03	40.7208407	-111.9007069	0.827
C60-04	US.STN04	40.72068033	-111.9005841	0.827
C60-05	US.STN05	40.72049905	-111.9006228	0.827
C60-L300-06	US.STN06	40.7203775	-111.9008095	0.827
C60-07	US.STN07	40.72037626	-111.901052	0.827
C60-08	US.STN08	40.72049491	-111.9012395	0.827
C60-09	US.STN09	40.72067742	-111.9012826	0.842
C60-L300-10	US.STN10	40.7208378	-111.9011615	0.842
L300-L1000-01	US.STN01	40.72224227	-111.9023914	0.889
L300-02	US.STN02	40.72105742	-111.9023085	0.842
L300-L1000-03	US.STN03	40.72023782	-111.902312	0.889
L300-04	US.STN04	40.71967488	-111.9022785	-
L300-L1000-05	US.STN05	40.71929132	-111.9021943	0.821
L300-07	US.STN07	40.71922327	-111.9017115	0.946
L300-08	US.STN08	40.71920408	-111.9010873	0.889
L300-L1000-09	US.STN09	40.71922757	-111.899869	-
L1000-02	US.STN02	40.7251863	-111.9018305	0.873
L1000-04	US.STN04	40.71918594	-111.8967664	0.873
L1000-06	US.STN06	40.72154893	-111.8941137	0.905
L1000-07	US.STN07	40.71920612	-111.8941262	0.905
L1000-09	US.STN09	40.71909761	-111.8889985	0.922
L1000-10	US.STN10	40.72339335	-111.8999056	0.889

Table B.2 Individual H/V station coordinates and $f_{0,mc}$ values for the I15DA site. For stations where the H/V curves were not of sufficient quality to determine $f_{0,mc}$, no values are reported, as indicated by the dash (-) symbol.

Position	Station	Latitude (deg)	Longitude (deg)	$f_{0,mc}$ (Hz)
001	US.STN10	40.73327109	-111.9188823	0.933
002	US.STN05	40.73340824	-111.91711	0.922
003	US.STN07	40.73336963	-111.9134516	0.922
004	US.STN07	40.73338437	-111.9117895	0.956
005	US.STN10	40.73332731	-111.9087456	0.918
006	US.STN05	40.73336201	-111.906505	0.89
007	US.STN06	40.73338397	-111.90399	-
008	US.STN08	40.73340601	-111.901154	0.803
009	US.STN06	40.73342102	-111.898785	0.801
010	US.STN08	40.73338699	-111.896751	0.905
011	US.STN06	40.73332001	-111.894056	-
013	US.STN10	40.73121234	-111.9167171	0.991
014	US.STN07	40.73080357	-111.9140141	0.828
015	US.STN05	40.73138993	-111.9110573	0.889
016	US.STN05	40.73159785	-111.9081113	0.905
017	US.STN07	40.7310755	-111.9056101	-
018	US.STN05	40.73140416	-111.903643	0.922
019	US.STN07	40.73173271	-111.9016581	0.833
020	US.STN08	40.731837	-111.898955	0.895
021	US.STN06	40.73145898	-111.896457	0.756
022	US.STN08	40.73135898	-111.894042	-
023	US.STN07	40.7287783	-111.9187111	0.827
024	US.STN05	40.72944067	-111.9166864	-
025	US.STN07	40.73017218	-111.913871	-
026	US.STN10	40.72957805	-111.9112746	0.973
028	US.STN10	40.72979457	-111.9057435	-
029	US.STN06	40.72927902	-111.903666	0.991
030	US.STN08	40.72933903	-111.901811	0.842
031	US.STN06	40.72941396	-111.898881	0.854
032	US.STN08	40.72924297	-111.896709	0.858
033	US.STN06	40.72923803	-111.893911	0.956
034	US.STN10	40.72718699	-111.9198117	0.871
035	US.STN10	40.7269702	-111.9165676	-
036	US.STN05	40.72718902	-111.9140086	0.866
037	US.STN10	40.72785865	-111.9110393	1.009
041	US.STN06	40.72767799	-111.901485	0.813
042	US.STN08	40.72728203	-111.89839	0.813
043	US.STN06	40.72731597	-111.896545	0.923
044	US.STN08	40.727104	-111.894074	-

Table B.2 H/V station coordinates and data continued.

Position	Station	Latitude (deg)	Longitude (deg)	$f_{0,mc}$ (Hz)
045	US.STN05	40.72602192	-111.9195329	-
046	US.STN07	40.72588632	-111.9165556	0.913
047	US.STN05	40.72574711	-111.914178	0.905
048	US.STN07	40.72596084	-111.9115984	1.028
049	US.STN02	40.72521698	-111.9093	0.858
053	US.STN09	40.72528202	-111.898918	0.922
054	US.STN02	40.72526299	-111.89627	0.873
055	US.STN03	40.72507599	-111.894447	0.889
056	US.STN09	40.72322099	-111.917641	-
058	US.STN02	40.72315101	-111.913639	0.866
059	US.STN03	40.72279897	-111.911545	0.981
060	US.STN03	40.72351302	-111.90978	0.923
061	US.STN02	40.72288002	-111.907113	0.889
065	US.STN04	40.72272101	-111.896744	0.981
066	US.STN01	40.72278497	-111.89423	0.93
067	US.STN02	40.72090801	-111.919114	0.88
068	US.STN03	40.72077197	-111.91728	-
069	US.STN03	40.72059997	-111.913636	0.943
070	US.STN02	40.72104204	-111.911114	0.922
072	US.STN03	40.72137798	-111.90665	-
075	US.STN01	40.721165	-111.898996	-
076	US.STN04	40.72100499	-111.896797	1.003
078	US.STN09	40.71872897	-111.91793	-
079	US.STN09	40.71925996	-111.917071	-
080	US.STN02	40.71881002	-111.914077	0.851
081	US.STN03	40.71897497	-111.911307	0.9
083	US.STN02	40.71918997	-111.907103	0.991
089	US.STN09	40.716909	-111.919409	0.858
090	US.STN09	40.71687296	-111.917645	0.939
091	US.STN03	40.71688998	-111.913424	0.939
092	US.STN02	40.71684698	-111.91156	1.006
094	US.STN03	40.71694898	-111.907091	1.009
096	US.STN01	40.71667003	-111.901537	-
097	US.STN04	40.71686299	-111.899425	0.949
098	US.STN01	40.71694898	-111.896734	0.986
099	US.STN04	40.71704504	-111.894379	0.915
100	US.STN09	40.71487203	-111.919031	0.905
101	US.STN09	40.71512802	-111.916526	0.967
102	US.STN09	40.71486801	-111.914024	0.986
103	US.STN03	40.71486298	-111.91163	1.065
105	US.STN02	40.71470104	-111.90707	1.028
106	US.STN04	40.71482803	-111.903441	0.835

Table B.2 H/V station coordinates and data continued.

Position	Station	Latitude (deg)	Longitude (deg)	$f_{0,mc}$ (Hz)
107	US.STN01	40.71471898	-111.901294	0.798
108	US.STN01	40.71517001	-111.899399	-
109	US.STN01	40.71509901	-111.896799	0.939
110	US.STN04	40.71500103	-111.894105	-
111	US.STN09	40.71257003	-111.919293	0.851
112	US.STN09	40.71273297	-111.916834	1.046
114	US.STN02	40.71271403	-111.9116	1.037
116	US.STN03	40.71232804	-111.906774	1.008
117	US.STN01	40.71292098	-111.903462	0.951
118	US.STN04	40.71300304	-111.901261	0.978
119	US.STN04	40.71277496	-111.89899	1.008
120	US.STN01	40.71228404	-111.8956	-
121	US.STN04	40.71247799	-111.894315	0.851
400	US.STN02	40.72314439	-111.9069675	0.922
401	US.STN01	40.72335482	-111.907482	0.915

APPENDIX C: TABULATED DISPERSION DATA AND VS PROFILES

Table C.1 Tabulated experimental dispersion data for the I15DA site in terms of mean phase velocity (Vel.) and standard deviation (σ) as a function of frequency.

Fundamental Mode Rayleigh (R_0 Targeted)					
Frequency (Hz)	Velocity (m/s)	σ (m/s)	Frequency (Hz)	Velocity (m/s)	σ (m/s)
0.42	1829.8	92.0	2.52	256.1	12.8
0.45	1673.9	84.7	2.73	239.9	12.0
0.47	1525.6	76.3	2.96	225.2	11.3
0.49	1373.4	68.7	3.26	214.4	10.7
0.51	1247.3	62.4	3.54	201.6	10.1
0.55	1148.9	57.4	3.91	192.7	9.6
0.59	1077.2	53.9	4.26	181.9	9.1
0.64	1008.6	50.4	4.78	176.6	8.8
0.69	938.4	46.9	5.37	171.6	8.6
0.74	879.3	44.0	6.06	167.6	8.4
0.80	818.2	40.9	6.90	165.1	8.3
0.87	772.0	38.6	7.83	162.3	8.1
0.94	722.1	36.1	9.03	162.0	8.1
1.02	674.4	33.7	10.22	158.8	7.9
1.11	634.8	31.7	11.79	158.5	7.9
1.19	593.0	29.7	13.49	157.0	7.8
1.28	550.3	27.5	15.30	154.1	7.7
1.36	506.7	25.3	17.50	152.6	7.6
1.48	475.9	23.8	19.97	150.7	7.5
1.56	433.5	21.7	22.79	148.9	7.4
1.63	392.7	19.6	26.07	147.4	7.4
1.76	368.4	18.4	29.65	145.1	7.3
1.89	340.9	17.0	35.07	148.6	7.4
2.02	316.3	15.8	41.33	151.5	7.6
2.16	292.3	14.6	47.90	152.0	7.6
2.33	273.6	13.7	55.33	152.0	7.6
0.42	1829.8	92.0	64.45	153.2	7.7

Table C.2 Tabulated median inversion-derived Vs profiles to a depth of 1,500 m at the I15DA site for layering inversion parameterizations of LR = 1.5, 2.0, 3.0, and 5.0. Note that d_{res} = 785 m. At depths greater than d_{res}, the Vs profiles are constrained by less reliable dispersion data and should be used with caution. Vs profiles at depths greater than d_{res} are reported herein because, while less certain, they provide guiding information about the deep Vs structure that is more reliable than simply guessing. The dark-gray shaded rows represent the depths where the Vs profiles can be truncated, if desired, to stay within the array resolution limits.

LR = 1.5		LR = 2.0		LR = 3.0		LR = 5.0	
Depth (m)	Vs (m/s)	Depth (m)	Vs (m/s)	Depth (m)	Vs (m/s)	Depth (m)	Vs (m/s)
0.00	150	0.00	149	0.00	152	0.00	155
1.00	150	0.89	149	0.96	152	1.06	155
1.00	159	0.89	162	0.96	161	1.06	163
1.95	159	2.07	162	3.43	161	5.76	163
1.95	165	2.07	171	3.43	167	5.76	181
4.17	165	7.09	171	13.45	167	27.61	181
4.17	172	7.09	182	13.45	210	27.61	329
7.76	172	14.60	182	38.41	210	100.68	329
7.76	183	14.60	196	38.41	377	100.68	791
12.57	183	28.47	196	114.15	377	233.17	791
12.57	192	28.47	316	114.15	866	233.17	1085
19.91	192	56.82	316	350.50	866	785.00	1085
19.91	220	56.82	386	350.50	1151	1000.47	1085
32.32	220	112.07	386	785.00	1151	1000.47	2397
32.32	287	112.07	856	964.08	1151	1500.00	2397
46.44	287	232.77	856	964.08	2398	-	-
46.44	348	232.77	1089	1500.00	2398	-	-
75.85	348	381.13	1089	-	-	-	-
75.85	425	381.13	1200	-	-	-	-
103.36	425	785.00	1200	-	-	-	-
103.36	598	1019.22	1200	-	-	-	-
161.97	598	1019.22	2022	-	-	-	-
161.97	869	1336.81	2022	-	-	-	-
256.85	869	1336.81	2566	-	-	-	-
256.85	1026	1500.00	2566	-	-	-	-
366.17	1026	-	-	-	-	-	-
366.17	1117	-	-	-	-	-	-
584.56	1117	-	-	-	-	-	-
584.56	1234	-	-	-	-	-	-
785.00	1234	-	-	-	-	-	-
874.00	1234	-	-	-	-	-	-
874.00	1532	-	-	-	-	-	-
1136.15	1532	-	-	-	-	-	-
1136.15	2287	-	-	-	-	-	-
1500.00	2287	-	-	-	-	-	-

Table C.3 Tabulated nine-layer simplified PS-Logging profile to a depth of 120 m at the I15DA. The PS-logging was performed in the boring for the 120-m downhole sensor by GEOVision Geophysical Services in August of 2003 and April of 2003.

Depth (m)	Vs (m/s)
0	137.50
9.5	137.50
9.5	172.20
19	172.20
19	178.06
27	178.06
27	252.13
46	252.13
46	359.38
74	359.38
74	444.26
97	444.26
97	615.53
106	615.53
106	652.47
115	652.47
115	652.47
120	652.47

APPENDIX D: TABULATED LM_{ETF} AND TTFS

Table D.1 Tabulated $\boldsymbol{LM_{ETF}}$ and $\boldsymbol{\sigma_{ln,ETF}}$ sampled from 0.5 Hz to 10 Hz with 2,048 points.

Freq. (Hz)	$\boldsymbol{LM_{ETF}}$	$\boldsymbol{\sigma_{ln,ETF}}$	**Freq.** (Hz)	$\boldsymbol{LM_{ETF}}$	$\boldsymbol{\sigma_{ln,ETF}}$	**Freq.** (Hz)	$\boldsymbol{LM_{ETF}}$	$\boldsymbol{\sigma_{ln,ETF}}$	**Freq.** (Hz)	$\boldsymbol{LM_{ETF}}$	$\boldsymbol{\sigma_{ln,ETF}}$
0.5000	1.92	0.179	0.5255	2.21	0.177	0.5523	2.43	0.191	0.5805	2.67	0.156
0.5007	1.93	0.179	0.5263	2.21	0.177	0.5531	2.44	0.191	0.5813	2.68	0.154
0.5015	1.94	0.178	0.5270	2.22	0.177	0.5539	2.44	0.191	0.5822	2.69	0.152
0.5022	1.95	0.178	0.5278	2.23	0.178	0.5547	2.45	0.191	0.5830	2.70	0.150
0.5029	1.96	0.178	0.5286	2.23	0.178	0.5556	2.46	0.191	0.5839	2.71	0.147
0.5037	1.97	0.177	0.5294	2.24	0.179	0.5564	2.46	0.191	0.5848	2.72	0.145
0.5044	1.97	0.177	0.5301	2.25	0.179	0.5572	2.47	0.190	0.5856	2.73	0.143
0.5051	1.98	0.177	0.5309	2.26	0.180	0.5580	2.48	0.190	0.5865	2.74	0.141
0.5059	1.99	0.176	0.5317	2.26	0.181	0.5588	2.48	0.189	0.5873	2.74	0.139
0.5066	2.00	0.176	0.5325	2.27	0.181	0.5596	2.49	0.188	0.5882	2.75	0.137
0.5074	2.01	0.176	0.5333	2.28	0.182	0.5605	2.50	0.188	0.5891	2.76	0.135
0.5081	2.02	0.175	0.5340	2.28	0.182	0.5613	2.50	0.187	0.5899	2.77	0.133
0.5089	2.03	0.175	0.5348	2.29	0.183	0.5621	2.51	0.187	0.5908	2.78	0.131
0.5096	2.04	0.175	0.5356	2.30	0.183	0.5629	2.52	0.186	0.5916	2.79	0.128
0.5103	2.04	0.175	0.5364	2.30	0.184	0.5638	2.52	0.186	0.5925	2.80	0.126
0.5111	2.05	0.174	0.5372	2.31	0.184	0.5646	2.53	0.185	0.5934	2.81	0.124
0.5118	2.06	0.174	0.5380	2.32	0.185	0.5654	2.54	0.183	0.5942	2.82	0.122
0.5126	2.07	0.174	0.5387	2.32	0.186	0.5662	2.54	0.182	0.5951	2.83	0.120
0.5133	2.08	0.174	0.5395	2.33	0.186	0.5671	2.55	0.181	0.5960	2.84	0.118
0.5141	2.09	0.174	0.5403	2.34	0.187	0.5679	2.56	0.180	0.5969	2.85	0.116
0.5149	2.09	0.174	0.5411	2.34	0.187	0.5687	2.57	0.179	0.5977	2.87	0.114
0.5156	2.10	0.174	0.5419	2.35	0.188	0.5696	2.57	0.177	0.5986	2.88	0.112
0.5164	2.11	0.174	0.5427	2.35	0.188	0.5704	2.58	0.176	0.5995	2.89	0.110
0.5171	2.12	0.174	0.5435	2.36	0.189	0.5712	2.59	0.175	0.6004	2.90	0.108
0.5179	2.13	0.174	0.5443	2.37	0.189	0.5721	2.60	0.174	0.6012	2.91	0.106
0.5186	2.14	0.174	0.5451	2.37	0.189	0.5729	2.60	0.172	0.6021	2.92	0.104
0.5194	2.14	0.174	0.5459	2.38	0.190	0.5737	2.61	0.170	0.6030	2.93	0.102
0.5202	2.15	0.174	0.5467	2.39	0.190	0.5746	2.62	0.168	0.6039	2.94	0.101
0.5209	2.16	0.175	0.5475	2.39	0.190	0.5754	2.63	0.167	0.6048	2.96	0.099
0.5217	2.17	0.175	0.5483	2.40	0.191	0.5763	2.63	0.165	0.6057	2.97	0.097
0.5224	2.18	0.175	0.5491	2.41	0.191	0.5771	2.64	0.163	0.6065	2.98	0.095
0.5232	2.18	0.176	0.5499	2.41	0.191	0.5780	2.65	0.161	0.6074	3.00	0.094
0.5240	2.19	0.176	0.5507	2.42	0.191	0.5788	2.66	0.160	0.6083	3.01	0.092
0.5247	2.20	0.176	0.5515	2.42	0.191	0.5796	2.67	0.158	0.6092	3.02	0.091

Freq. (Hz)	LM_{ETF}	$\sigma_{ln,ETF}$	**Freq.** (Hz)	LM_{ETF}	$\sigma_{ln,ETF}$	**Freq.** (Hz)	LM_{ETF}	$\sigma_{ln,ETF}$	**Freq.** (Hz)	LM_{ETF}	$\sigma_{ln,ETF}$
0.6101	3.03	0.089	0.6459	3.59	0.100	0.6839	3.97	0.174	0.7241	4.46	0.248
0.6110	3.05	0.088	0.6469	3.60	0.102	0.6849	3.97	0.175	0.7251	4.48	0.251
0.6119	3.06	0.087	0.6478	3.62	0.104	0.6859	3.98	0.176	0.7262	4.49	0.254
0.6128	3.07	0.085	0.6488	3.63	0.106	0.6869	3.99	0.177	0.7272	4.51	0.258
0.6137	3.09	0.084	0.6497	3.64	0.108	0.6879	4.00	0.178	0.7283	4.53	0.261
0.6146	3.10	0.083	0.6507	3.65	0.111	0.6889	4.01	0.180	0.7294	4.54	0.264
0.6155	3.12	0.082	0.6516	3.67	0.113	0.6899	4.02	0.181	0.7304	4.56	0.267
0.6164	3.13	0.081	0.6526	3.68	0.115	0.6909	4.03	0.183	0.7315	4.59	0.270
0.6173	3.14	0.080	0.6536	3.69	0.118	0.6919	4.04	0.184	0.7326	4.61	0.273
0.6182	3.16	0.079	0.6545	3.70	0.120	0.6930	4.05	0.185	0.7337	4.63	0.276
0.6191	3.17	0.078	0.6555	3.71	0.123	0.6940	4.06	0.186	0.7347	4.65	0.279
0.6200	3.19	0.078	0.6564	3.72	0.124	0.6950	4.07	0.187	0.7358	4.67	0.282
0.6209	3.20	0.077	0.6574	3.73	0.126	0.6960	4.08	0.188	0.7369	4.68	0.286
0.6218	3.22	0.076	0.6584	3.74	0.129	0.6970	4.09	0.190	0.7380	4.70	0.289
0.6227	3.23	0.076	0.6593	3.75	0.131	0.6980	4.10	0.191	0.7390	4.72	0.292
0.6237	3.25	0.075	0.6603	3.76	0.133	0.6991	4.11	0.193	0.7401	4.74	0.295
0.6246	3.26	0.075	0.6612	3.77	0.135	0.7001	4.12	0.195	0.7412	4.77	0.298
0.6255	3.27	0.075	0.6622	3.78	0.138	0.7011	4.13	0.196	0.7423	4.79	0.300
0.6264	3.29	0.075	0.6632	3.79	0.140	0.7021	4.14	0.198	0.7434	4.81	0.303
0.6273	3.30	0.075	0.6642	3.80	0.142	0.7032	4.16	0.199	0.7445	4.83	0.305
0.6282	3.32	0.075	0.6651	3.81	0.144	0.7042	4.17	0.201	0.7456	4.85	0.308
0.6292	3.33	0.075	0.6661	3.82	0.145	0.7052	4.18	0.203	0.7467	4.87	0.311
0.6301	3.35	0.076	0.6671	3.83	0.147	0.7063	4.20	0.205	0.7477	4.89	0.314
0.6310	3.36	0.076	0.6681	3.83	0.149	0.7073	4.21	0.207	0.7488	4.91	0.316
0.6319	3.38	0.077	0.6690	3.84	0.151	0.7083	4.22	0.209	0.7499	4.94	0.319
0.6328	3.39	0.078	0.6700	3.85	0.153	0.7094	4.23	0.211	0.7510	4.96	0.320
0.6338	3.41	0.079	0.6710	3.86	0.155	0.7104	4.25	0.214	0.7521	4.98	0.322
0.6347	3.42	0.080	0.6720	3.87	0.157	0.7115	4.26	0.216	0.7532	5.00	0.323
0.6356	3.44	0.081	0.6730	3.88	0.159	0.7125	4.28	0.218	0.7543	5.03	0.325
0.6366	3.45	0.082	0.6740	3.88	0.160	0.7135	4.29	0.220	0.7554	5.05	0.327
0.6375	3.47	0.083	0.6749	3.89	0.161	0.7146	4.31	0.223	0.7566	5.07	0.328
0.6384	3.48	0.085	0.6759	3.90	0.162	0.7156	4.33	0.225	0.7577	5.09	0.330
0.6394	3.50	0.086	0.6769	3.91	0.164	0.7167	4.34	0.228	0.7588	5.11	0.332
0.6403	3.51	0.088	0.6779	3.92	0.165	0.7177	4.36	0.231	0.7599	5.13	0.333
0.6412	3.52	0.090	0.6789	3.92	0.167	0.7188	4.37	0.234	0.7610	5.16	0.333
0.6422	3.54	0.092	0.6799	3.93	0.168	0.7198	4.38	0.237	0.7621	5.18	0.333
0.6431	3.55	0.094	0.6809	3.94	0.170	0.7209	4.40	0.239	0.7632	5.20	0.334
0.6441	3.57	0.096	0.6819	3.95	0.172	0.7219	4.42	0.242	0.7643	5.22	0.334
0.6450	3.58	0.098	0.6829	3.96	0.173	0.7230	4.44	0.245	0.7655	5.24	0.334

Freq. (Hz)	LM_{ETF}	$\sigma_{ln,ETF}$	**Freq.** (Hz)	LM_{ETF}	$\sigma_{ln,ETF}$	**Freq.** (Hz)	LM_{ETF}	$\sigma_{ln,ETF}$	**Freq.** (Hz)	LM_{ETF}	$\sigma_{ln,ETF}$
00.7666	5.26	0.334	0.8116	5.65	0.232	0.8593	5.20	0.161	0.9097	4.72	0.161
0.7677	5.28	0.335	0.8128	5.64	0.229	0.8605	5.19	0.160	0.9111	4.70	0.161
0.7688	5.30	0.335	0.8140	5.64	0.225	0.8618	5.17	0.160	0.9124	4.69	0.161
0.7700	5.32	0.335	0.8152	5.63	0.222	0.8631	5.16	0.160	0.9138	4.68	0.161
0.7711	5.34	0.334	0.8164	5.62	0.219	0.8643	5.15	0.160	0.9151	4.67	0.162
0.7722	5.36	0.332	0.8176	5.61	0.215	0.8656	5.13	0.160	0.9164	4.65	0.162
0.7733	5.38	0.331	0.8188	5.61	0.212	0.8669	5.12	0.160	0.9178	4.64	0.162
0.7745	5.40	0.329	0.8200	5.60	0.209	0.8681	5.11	0.160	0.9191	4.63	0.162
0.7756	5.42	0.328	0.8212	5.59	0.206	0.8694	5.09	0.160	0.9205	4.61	0.162
0.7767	5.44	0.327	0.8224	5.58	0.203	0.8707	5.08	0.160	0.9218	4.60	0.162
0.7779	5.45	0.325	0.8236	5.57	0.200	0.8719	5.07	0.160	0.9232	4.59	0.162
0.7790	5.47	0.324	0.8248	5.56	0.197	0.8732	5.06	0.160	0.9245	4.57	0.162
0.7802	5.49	0.322	0.8260	5.55	0.194	0.8745	5.04	0.160	0.9259	4.56	0.162
0.7813	5.50	0.320	0.8272	5.54	0.192	0.8758	5.03	0.160	0.9272	4.54	0.162
0.7825	5.52	0.317	0.8284	5.53	0.189	0.8771	5.02	0.160	0.9286	4.53	0.162
0.7836	5.53	0.314	0.8296	5.52	0.187	0.8784	5.01	0.160	0.9299	4.52	0.163
0.7847	5.54	0.312	0.8308	5.50	0.185	0.8796	4.99	0.160	0.9313	4.50	0.162
0.7859	5.56	0.309	0.8321	5.49	0.182	0.8809	4.98	0.160	0.9327	4.49	0.162
0.7870	5.57	0.306	0.8333	5.48	0.180	0.8822	4.97	0.160	0.9340	4.47	0.162
0.7882	5.58	0.303	0.8345	5.47	0.178	0.8835	4.96	0.160	0.9354	4.46	0.162
0.7894	5.59	0.301	0.8357	5.46	0.177	0.8848	4.95	0.160	0.9368	4.44	0.162
0.7905	5.61	0.298	0.8369	5.44	0.175	0.8861	4.93	0.160	0.9381	4.43	0.162
0.7917	5.62	0.295	0.8382	5.43	0.174	0.8874	4.92	0.160	0.9395	4.41	0.162
0.7928	5.62	0.291	0.8394	5.42	0.172	0.8887	4.91	0.160	0.9409	4.40	0.162
0.7940	5.63	0.287	0.8406	5.40	0.171	0.8900	4.90	0.160	0.9423	4.38	0.162
0.7951	5.63	0.284	0.8419	5.39	0.170	0.8913	4.89	0.160	0.9437	4.37	0.162
0.7963	5.64	0.280	0.8431	5.38	0.168	0.8926	4.87	0.160	0.9450	4.35	0.162
0.7975	5.65	0.277	0.8443	5.36	0.167	0.8939	4.86	0.160	0.9464	4.34	0.162
0.7986	5.65	0.273	0.8456	5.35	0.166	0.8952	4.85	0.160	0.9478	4.32	0.162
0.7998	5.66	0.270	0.8468	5.33	0.165	0.8965	4.84	0.160	0.9492	4.30	0.161
0.8010	5.66	0.266	0.8480	5.32	0.165	0.8978	4.83	0.160	0.9506	4.29	0.161
0.8022	5.66	0.263	0.8493	5.31	0.164	0.8992	4.81	0.160	0.9520	4.27	0.161
0.8033	5.66	0.259	0.8505	5.29	0.163	0.9005	4.80	0.160	0.9534	4.26	0.161
0.8045	5.66	0.255	0.8518	5.28	0.163	0.9018	4.79	0.161	0.9548	4.24	0.161
0.8057	5.66	0.251	0.8530	5.27	0.162	0.9031	4.78	0.161	0.9562	4.22	0.161
0.8069	5.66	0.247	0.8543	5.25	0.162	0.9044	4.77	0.161	0.9576	4.21	0.160
0.8081	5.65	0.243	0.8555	5.24	0.162	0.9058	4.75	0.161	0.9590	4.19	0.160
0.8092	5.65	0.240	0.8568	5.23	0.161	0.9071	4.74	0.161	0.9604	4.17	0.159
0.8104	5.65	0.236	0.8580	5.21	0.161	0.9084	4.73	0.161	0.9618	4.16	0.159

Freq. (Hz)	LM_{ETF}	$\sigma_{ln,ETF}$	**Freq.** (Hz)	LM_{ETF}	$\sigma_{ln,ETF}$	**Freq.** (Hz)	LM_{ETF}	$\sigma_{ln,ETF}$	**Freq.** (Hz)	LM_{ETF}	$\sigma_{ln,ETF}$
0.9632	4.14	0.159	1.0198	3.54	0.139	1.0797	2.98	0.168	1.1431	2.54	0.225
0.9646	4.12	0.158	1.0213	3.52	0.139	1.0812	2.96	0.170	1.1447	2.54	0.225
0.9660	4.11	0.158	1.0227	3.51	0.139	1.0828	2.95	0.172	1.1464	2.53	0.225
0.9674	4.09	0.158	1.0242	3.49	0.139	1.0844	2.94	0.174	1.1481	2.53	0.225
0.9688	4.07	0.157	1.0257	3.48	0.139	1.0860	2.92	0.176	1.1498	2.52	0.225
0.9703	4.06	0.157	1.0272	3.47	0.139	1.0876	2.91	0.178	1.1515	2.52	0.224
0.9717	4.04	0.156	1.0288	3.45	0.139	1.0892	2.89	0.180	1.1531	2.51	0.224
0.9731	4.02	0.156	1.0303	3.44	0.139	1.0908	2.88	0.182	1.1548	2.51	0.224
0.9745	4.01	0.155	1.0318	3.42	0.139	1.0924	2.86	0.184	1.1565	2.50	0.223
0.9760	3.99	0.154	1.0333	3.41	0.139	1.0940	2.85	0.186	1.1582	2.50	0.223
0.9774	3.98	0.154	1.0348	3.40	0.139	1.0956	2.84	0.188	1.1599	2.50	0.222
0.9788	3.96	0.153	1.0363	3.38	0.139	1.0972	2.82	0.190	1.1616	2.50	0.221
0.9802	3.94	0.153	1.0378	3.37	0.139	1.0988	2.81	0.192	1.1633	2.49	0.220
0.9817	3.93	0.152	1.0393	3.35	0.140	1.1004	2.80	0.194	1.1650	2.49	0.219
0.9831	3.91	0.152	1.0409	3.34	0.140	1.1020	2.78	0.196	1.1667	2.49	0.219
0.9846	3.89	0.151	1.0424	3.33	0.141	1.1036	2.77	0.198	1.1684	2.48	0.218
0.9860	3.88	0.150	1.0439	3.31	0.141	1.1052	2.76	0.200	1.1701	2.48	0.217
0.9874	3.86	0.150	1.0454	3.30	0.142	1.1069	2.75	0.202	1.1719	2.48	0.216
0.9889	3.85	0.149	1.0470	3.28	0.142	1.1085	2.73	0.204	1.1736	2.48	0.215
0.9903	3.83	0.149	1.0485	3.27	0.143	1.1101	2.72	0.206	1.1753	2.48	0.214
0.9918	3.82	0.148	1.0500	3.26	0.143	1.1117	2.71	0.207	1.1770	2.48	0.212
0.9932	3.80	0.147	1.0516	3.24	0.144	1.1133	2.70	0.209	1.1787	2.47	0.211
0.9947	3.78	0.147	1.0531	3.23	0.145	1.1150	2.69	0.210	1.1805	2.47	0.210
0.9962	3.77	0.146	1.0547	3.21	0.146	1.1166	2.68	0.212	1.1822	2.47	0.209
0.9976	3.75	0.146	1.0562	3.20	0.147	1.1182	2.67	0.213	1.1839	2.47	0.208
0.9991	3.74	0.145	1.0578	3.18	0.148	1.1199	2.66	0.215	1.1857	2.47	0.207
1.0005	3.72	0.145	1.0593	3.17	0.149	1.1215	2.65	0.216	1.1874	2.47	0.205
1.0020	3.71	0.144	1.0609	3.15	0.150	1.1232	2.63	0.218	1.1891	2.47	0.204
1.0035	3.69	0.144	1.0624	3.14	0.151	1.1248	2.62	0.219	1.1909	2.47	0.203
1.0049	3.68	0.143	1.0640	3.13	0.152	1.1265	2.62	0.220	1.1926	2.46	0.201
1.0064	3.66	0.143	1.0655	3.11	0.153	1.1281	2.61	0.221	1.1944	2.46	0.200
1.0079	3.65	0.142	1.0671	3.10	0.155	1.1298	2.60	0.221	1.1961	2.46	0.199
1.0094	3.63	0.142	1.0686	3.08	0.156	1.1314	2.59	0.222	1.1979	2.46	0.198
1.0108	3.62	0.141	1.0702	3.07	0.158	1.1331	2.59	0.223	1.1996	2.46	0.196
1.0123	3.61	0.141	1.0718	3.05	0.159	1.1347	2.58	0.223	1.2014	2.46	0.195
1.0138	3.59	0.141	1.0734	3.04	0.161	1.1364	2.57	0.224	1.2031	2.46	0.194
1.0153	3.58	0.140	1.0749	3.02	0.163	1.1381	2.56	0.225	1.2049	2.46	0.193
1.0168	3.56	0.140	1.0765	3.01	0.164	1.1397	2.55	0.225	1.2067	2.46	0.191
1.0183	3.55	0.140	1.0781	2.99	0.166	1.1414	2.55	0.225	1.2084	2.46	0.190

Freq. (Hz)	LM_{ETF}	$\sigma_{ln,ETF}$	**Freq.** (Hz)	LM_{ETF}	$\sigma_{ln,ETF}$	**Freq.** (Hz)	LM_{ETF}	$\sigma_{ln,ETF}$	**Freq.** (Hz)	LM_{ETF}	$\sigma_{ln,ETF}$
1.2102	2.46	0.189	1.2813	2.40	0.143	1.3565	2.38	0.116	1.4362	2.55	0.131
1.2120	2.46	0.188	1.2832	2.40	0.142	1.3585	2.38	0.116	1.4383	2.56	0.132
1.2138	2.46	0.186	1.2850	2.40	0.140	1.3605	2.38	0.117	1.4404	2.57	0.133
1.2155	2.46	0.185	1.2869	2.40	0.139	1.3625	2.38	0.118	1.4425	2.58	0.133
1.2173	2.45	0.184	1.2888	2.39	0.138	1.3645	2.38	0.118	1.4447	2.59	0.134
1.2191	2.45	0.183	1.2907	2.39	0.136	1.3665	2.39	0.119	1.4468	2.60	0.135
1.2209	2.45	0.182	1.2926	2.39	0.135	1.3685	2.39	0.119	1.4489	2.61	0.137
1.2227	2.45	0.181	1.2945	2.39	0.133	1.3705	2.39	0.120	1.4510	2.62	0.138
1.2245	2.45	0.179	1.2964	2.39	0.132	1.3725	2.39	0.120	1.4531	2.63	0.139
1.2263	2.45	0.178	1.2983	2.39	0.130	1.3745	2.39	0.121	1.4553	2.65	0.141
1.2280	2.45	0.177	1.3002	2.39	0.129	1.3765	2.39	0.122	1.4574	2.66	0.142
1.2298	2.45	0.176	1.3021	2.38	0.128	1.3786	2.40	0.122	1.4595	2.67	0.143
1.2316	2.45	0.175	1.3040	2.38	0.126	1.3806	2.40	0.123	1.4617	2.68	0.145
1.2335	2.45	0.174	1.3059	2.38	0.125	1.3826	2.40	0.123	1.4638	2.70	0.146
1.2353	2.45	0.173	1.3078	2.38	0.124	1.3846	2.41	0.123	1.4660	2.71	0.148
1.2371	2.44	0.172	1.3097	2.38	0.123	1.3867	2.41	0.124	1.4681	2.72	0.150
1.2389	2.44	0.171	1.3116	2.38	0.122	1.3887	2.41	0.124	1.4703	2.73	0.152
1.2407	2.44	0.170	1.3136	2.38	0.121	1.3907	2.42	0.125	1.4724	2.75	0.154
1.2425	2.44	0.168	1.3155	2.38	0.120	1.3928	2.42	0.125	1.4746	2.76	0.156
1.2443	2.44	0.167	1.3174	2.38	0.119	1.3948	2.42	0.126	1.4767	2.77	0.158
1.2462	2.44	0.166	1.3193	2.37	0.118	1.3968	2.43	0.126	1.4789	2.79	0.160
1.2480	2.44	0.165	1.3213	2.37	0.117	1.3989	2.43	0.126	1.4810	2.80	0.162
1.2498	2.43	0.164	1.3232	2.37	0.116	1.4009	2.44	0.126	1.4832	2.82	0.164
1.2516	2.43	0.163	1.3252	2.37	0.116	1.4030	2.44	0.126	1.4854	2.83	0.167
1.2535	2.43	0.162	1.3271	2.37	0.115	1.4050	2.45	0.126	1.4876	2.85	0.169
1.2553	2.43	0.161	1.3290	2.37	0.115	1.4071	2.45	0.126	1.4897	2.86	0.171
1.2571	2.43	0.160	1.3310	2.37	0.114	1.4092	2.46	0.127	1.4919	2.88	0.174
1.2590	2.43	0.158	1.3329	2.37	0.114	1.4112	2.46	0.127	1.4941	2.89	0.176
1.2608	2.42	0.157	1.3349	2.37	0.114	1.4133	2.47	0.127	1.4963	2.91	0.178
1.2627	2.42	0.156	1.3368	2.37	0.113	1.4154	2.47	0.128	1.4985	2.92	0.180
1.2645	2.42	0.155	1.3388	2.37	0.113	1.4174	2.48	0.128	1.5007	2.94	0.183
1.2664	2.42	0.154	1.3408	2.37	0.113	1.4195	2.49	0.128	1.5029	2.96	0.185
1.2682	2.42	0.153	1.3427	2.37	0.113	1.4216	2.50	0.128	1.5051	2.97	0.187
1.2701	2.41	0.152	1.3447	2.37	0.114	1.4237	2.51	0.128	1.5073	2.99	0.190
1.2719	2.41	0.150	1.3467	2.37	0.114	1.4258	2.51	0.129	1.5095	3.00	0.192
1.2738	2.41	0.149	1.3486	2.38	0.114	1.4278	2.52	0.129	1.5117	3.02	0.194
1.2757	2.41	0.147	1.3506	2.38	0.115	1.4299	2.53	0.130	1.5139	3.03	0.197
1.2775	2.41	0.146	1.3526	2.38	0.115	1.4320	2.54	0.130	1.5161	3.05	0.199
1.2794	2.40	0.144	1.3546	2.38	0.115	1.4341	2.54	0.131	1.5184	3.07	0.201

Freq. (Hz)	LM_{ETF}	$\sigma_{ln,ETF}$	**Freq.** (Hz)	LM_{ETF}	$\sigma_{ln,ETF}$	**Freq.** (Hz)	LM_{ETF}	$\sigma_{ln,ETF}$	**Freq.** (Hz)	LM_{ETF}	$\sigma_{ln,ETF}$
1.5206	3.09	0.203	1.6099	3.78	0.224	1.7045	4.60	0.195	1.8046	5.74	0.196
1.5228	3.10	0.204	1.6123	3.80	0.223	1.7069	4.62	0.195	1.8072	5.76	0.196
1.5250	3.12	0.206	1.6146	3.82	0.222	1.7094	4.65	0.195	1.8099	5.78	0.196
1.5273	3.14	0.208	1.6170	3.84	0.221	1.7120	4.67	0.195	1.8125	5.81	0.195
1.5295	3.16	0.210	1.6193	3.86	0.221	1.7145	4.70	0.195	1.8152	5.83	0.195
1.5317	3.17	0.212	1.6217	3.87	0.219	1.7170	4.73	0.195	1.8178	5.85	0.195
1.5340	3.19	0.214	1.6241	3.89	0.218	1.7195	4.76	0.195	1.8205	5.87	0.194
1.5362	3.21	0.216	1.6265	3.91	0.217	1.7220	4.79	0.195	1.8231	5.89	0.194
1.5385	3.22	0.217	1.6289	3.93	0.216	1.7245	4.82	0.195	1.8258	5.91	0.194
1.5407	3.24	0.218	1.6312	3.95	0.215	1.7271	4.84	0.195	1.8285	5.93	0.194
1.5430	3.26	0.220	1.6336	3.97	0.214	1.7296	4.87	0.195	1.8312	5.94	0.193
1.5453	3.28	0.221	1.6360	3.99	0.213	1.7321	4.90	0.195	1.8339	5.95	0.192
1.5475	3.30	0.222	1.6384	4.01	0.212	1.7347	4.93	0.195	1.8365	5.96	0.192
1.5498	3.31	0.224	1.6408	4.02	0.211	1.7372	4.96	0.195	1.8392	5.97	0.191
1.5521	3.33	0.225	1.6432	4.04	0.210	1.7397	4.99	0.195	1.8419	5.98	0.191
1.5543	3.35	0.226	1.6456	4.06	0.209	1.7423	5.02	0.195	1.8446	5.99	0.190
1.5566	3.37	0.227	1.6480	4.08	0.208	1.7448	5.05	0.195	1.8473	6.00	0.189
1.5589	3.38	0.227	1.6505	4.10	0.207	1.7474	5.08	0.196	1.8500	6.01	0.189
1.5612	3.40	0.228	1.6529	4.12	0.206	1.7499	5.11	0.196	1.8527	6.02	0.189
1.5635	3.42	0.228	1.6553	4.14	0.205	1.7525	5.15	0.196	1.8554	6.02	0.188
1.5657	3.44	0.229	1.6577	4.16	0.204	1.7551	5.18	0.196	1.8582	6.02	0.187
1.5680	3.46	0.229	1.6601	4.18	0.204	1.7576	5.21	0.196	1.8609	6.01	0.186
1.5703	3.47	0.230	1.6626	4.20	0.203	1.7602	5.24	0.196	1.8636	6.01	0.185
1.5726	3.49	0.230	1.6650	4.22	0.202	1.7628	5.27	0.196	1.8663	6.00	0.184
1.5749	3.51	0.231	1.6674	4.25	0.201	1.7654	5.30	0.196	1.8691	6.00	0.183
1.5772	3.53	0.231	1.6699	4.27	0.200	1.7680	5.33	0.196	1.8718	5.99	0.182
1.5796	3.55	0.230	1.6723	4.29	0.200	1.7706	5.36	0.196	1.8746	5.99	0.181
1.5819	3.56	0.230	1.6748	4.31	0.199	1.7732	5.39	0.197	1.8773	5.98	0.180
1.5842	3.58	0.230	1.6772	4.33	0.199	1.7757	5.43	0.197	1.8800	5.97	0.180
1.5865	3.60	0.229	1.6797	4.36	0.198	1.7783	5.46	0.197	1.8828	5.95	0.178
1.5888	3.62	0.229	1.6822	4.38	0.197	1.7810	5.49	0.197	1.8856	5.93	0.177
1.5912	3.64	0.229	1.6846	4.40	0.197	1.7836	5.52	0.197	1.8883	5.91	0.176
1.5935	3.65	0.229	1.6871	4.42	0.197	1.7862	5.54	0.197	1.8911	5.89	0.175
1.5958	3.67	0.228	1.6896	4.45	0.196	1.7888	5.57	0.196	1.8939	5.87	0.174
1.5982	3.69	0.228	1.6920	4.47	0.196	1.7914	5.60	0.196	1.8966	5.85	0.172
1.6005	3.71	0.227	1.6945	4.50	0.196	1.7940	5.63	0.196	1.8994	5.83	0.171
1.6028	3.73	0.226	1.6970	4.52	0.195	1.7967	5.66	0.196	1.9022	5.81	0.170
1.6052	3.75	0.225	1.6995	4.55	0.195	1.7993	5.69	0.196	1.9050	5.79	0.170
1.6075	3.76	0.224	1.7020	4.57	0.195	1.8019	5.71	0.196	1.9078	5.76	0.168

Freq. (Hz)	LM_{ETF}	$\sigma_{ln,ETF}$	**Freq.** (Hz)	LM_{ETF}	$\sigma_{ln,ETF}$	**Freq.** (Hz)	LM_{ETF}	$\sigma_{ln,ETF}$	**Freq.** (Hz)	LM_{ETF}	$\sigma_{ln,ETF}$
1.9106	5.72	0.167	2.0228	4.07	0.144	2.1416	2.94	0.182	2.2674	2.54	0.196
1.9134	5.69	0.166	2.0257	4.02	0.144	2.1447	2.92	0.183	2.2707	2.54	0.196
1.9162	5.66	0.165	2.0287	3.98	0.145	2.1479	2.90	0.184	2.2740	2.53	0.196
1.9190	5.63	0.163	2.0317	3.94	0.145	2.1510	2.89	0.186	2.2773	2.52	0.195
1.9218	5.59	0.162	2.0347	3.90	0.145	2.1542	2.87	0.186	2.2807	2.52	0.195
1.9246	5.56	0.161	2.0376	3.85	0.146	2.1573	2.86	0.187	2.2840	2.51	0.194
1.9274	5.53	0.160	2.0406	3.82	0.146	2.1605	2.85	0.188	2.2874	2.50	0.194
1.9302	5.49	0.160	2.0436	3.78	0.147	2.1636	2.83	0.189	2.2907	2.50	0.193
1.9331	5.45	0.158	2.0466	3.75	0.148	2.1668	2.82	0.190	2.2941	2.49	0.193
1.9359	5.41	0.157	2.0496	3.71	0.148	2.1700	2.81	0.191	2.2974	2.49	0.192
1.9387	5.37	0.156	2.0526	3.67	0.149	2.1732	2.80	0.192	2.3008	2.48	0.192
1.9416	5.33	0.155	2.0556	3.64	0.150	2.1763	2.78	0.193	2.3042	2.47	0.191
1.9444	5.28	0.154	2.0586	3.60	0.151	2.1795	2.77	0.194	2.3075	2.47	0.191
1.9473	5.24	0.153	2.0616	3.56	0.152	2.1827	2.76	0.194	2.3109	2.46	0.190
1.9501	5.20	0.153	2.0646	3.53	0.152	2.1859	2.75	0.195	2.3143	2.46	0.189
1.9530	5.16	0.152	2.0677	3.50	0.153	2.1891	2.74	0.195	2.3177	2.45	0.189
1.9558	5.11	0.151	2.0707	3.47	0.154	2.1923	2.73	0.196	2.3211	2.45	0.188
1.9587	5.07	0.150	2.0737	3.44	0.155	2.1955	2.72	0.196	2.3245	2.44	0.188
1.9616	5.02	0.150	2.0768	3.41	0.156	2.1987	2.71	0.197	2.3279	2.44	0.187
1.9644	4.98	0.149	2.0798	3.38	0.158	2.2020	2.70	0.197	2.3313	2.43	0.187
1.9673	4.93	0.148	2.0829	3.35	0.159	2.2052	2.69	0.198	2.3347	2.43	0.186
1.9702	4.89	0.147	2.0859	3.32	0.160	2.2084	2.68	0.198	2.3381	2.42	0.186
1.9731	4.84	0.147	2.0890	3.29	0.161	2.2117	2.67	0.198	2.3416	2.42	0.185
1.9760	4.79	0.146	2.0920	3.26	0.162	2.2149	2.66	0.198	2.3450	2.41	0.185
1.9789	4.74	0.146	2.0951	3.24	0.163	2.2181	2.66	0.198	2.3484	2.41	0.184
1.9818	4.70	0.145	2.0982	3.21	0.165	2.2214	2.65	0.198	2.3519	2.40	0.184
1.9847	4.65	0.145	2.1012	3.19	0.166	2.2246	2.64	0.198	2.3553	2.40	0.183
1.9876	4.61	0.145	2.1043	3.17	0.167	2.2279	2.63	0.199	2.3588	2.40	0.183
1.9905	4.56	0.144	2.1074	3.15	0.168	2.2312	2.62	0.199	2.3622	2.39	0.182
1.9934	4.51	0.144	2.1105	3.13	0.169	2.2344	2.62	0.199	2.3657	2.39	0.182
1.9963	4.47	0.144	2.1136	3.10	0.171	2.2377	2.61	0.199	2.3691	2.38	0.181
1.9992	4.42	0.143	2.1167	3.08	0.172	2.2410	2.60	0.199	2.3726	2.38	0.181
2.0022	4.37	0.143	2.1198	3.06	0.173	2.2443	2.59	0.198	2.3761	2.38	0.180
2.0051	4.33	0.143	2.1229	3.04	0.175	2.2476	2.58	0.198	2.3796	2.38	0.180
2.0080	4.28	0.143	2.1260	3.02	0.176	2.2508	2.58	0.198	2.3830	2.37	0.179
2.0110	4.23	0.143	2.1291	3.00	0.177	2.2541	2.57	0.197	2.3865	2.37	0.179
2.0139	4.19	0.143	2.1322	2.99	0.178	2.2574	2.56	0.197	2.3900	2.37	0.178
2.0169	4.15	0.144	2.1353	2.97	0.179	2.2607	2.56	0.197	2.3935	2.36	0.178
2.0198	4.11	0.144	2.1385	2.95	0.180	2.2641	2.55	0.197	2.3970	2.36	0.177

Freq. (Hz)	LM_{ETF}	$\sigma_{ln,ETF}$
2.4005	2.36	0.177
2.4041	2.36	0.176
2.4076	2.36	0.176
2.4111	2.36	0.175
2.4146	2.36	0.175
2.4182	2.35	0.175
2.4217	2.35	0.174
2.4253	2.35	0.174
2.4288	2.35	0.173
2.4324	2.35	0.173
2.4359	2.35	0.172
2.4395	2.35	0.172
2.4431	2.36	0.172
2.4467	2.36	0.171
2.4502	2.36	0.171
2.4538	2.36	0.170
2.4574	2.36	0.170
2.4610	2.36	0.170
2.4646	2.36	0.169
2.4682	2.37	0.169
2.4719	2.37	0.169
2.4755	2.38	0.168
2.4791	2.38	0.168
2.4827	2.38	0.168
2.4864	2.39	0.168
2.4900	2.39	0.167
2.4937	2.40	0.167
2.4973	2.40	0.167
2.5010	2.41	0.167
2.5046	2.42	0.167
2.5083	2.42	0.167
2.5120	2.43	0.167
2.5156	2.44	0.167
2.5193	2.45	0.167
2.5230	2.45	0.167
2.5267	2.46	0.167
2.5304	2.47	0.167
2.5341	2.48	0.167
2.5378	2.49	0.167
2.5415	2.50	0.168
2.5453	2.52	0.168
2.5490	2.53	0.168
2.5527	2.54	0.169
2.5565	2.55	0.169
2.5602	2.56	0.169
2.5640	2.57	0.170
2.5677	2.59	0.170
2.5715	2.60	0.171
2.5752	2.62	0.172
2.5790	2.64	0.173
2.5828	2.65	0.173
2.5866	2.67	0.174
2.5904	2.69	0.175
2.5942	2.70	0.176
2.5980	2.72	0.176
2.6018	2.74	0.177
2.6056	2.76	0.179
2.6094	2.78	0.180
2.6132	2.80	0.181
2.6170	2.82	0.182
2.6209	2.84	0.183
2.6247	2.86	0.184
2.6286	2.88	0.185
2.6324	2.91	0.187
2.6363	2.93	0.188
2.6401	2.95	0.189
2.6440	2.98	0.191
2.6479	3.01	0.192
2.6517	3.03	0.193
2.6556	3.06	0.195
2.6595	3.08	0.196
2.6634	3.11	0.197
2.6673	3.14	0.199
2.6712	3.16	0.200
2.6751	3.19	0.201
2.6790	3.22	0.203
2.6830	3.25	0.204
2.6869	3.28	0.206
2.6908	3.31	0.207
2.6948	3.34	0.208
2.6987	3.37	0.210
2.7027	3.40	0.211
2.7066	3.44	0.212
2.7106	3.47	0.213
2.7146	3.50	0.214
2.7185	3.53	0.216
2.7225	3.57	0.217
2.7265	3.60	0.218
2.7305	3.63	0.219
2.7345	3.67	0.220
2.7385	3.70	0.221
2.7425	3.73	0.222
2.7465	3.77	0.223
2.7505	3.80	0.223
2.7546	3.83	0.224
2.7586	3.87	0.225
2.7627	3.90	0.225
2.7667	3.93	0.226
2.7707	3.97	0.226
2.7748	4.00	0.227
2.7789	4.03	0.228
2.7829	4.06	0.228
2.7870	4.09	0.228
2.7911	4.12	0.228
2.7952	4.15	0.228
2.7993	4.18	0.227
2.8034	4.22	0.227
2.8075	4.25	0.227
2.8116	4.28	0.227
2.8157	4.31	0.227
2.8198	4.33	0.227
2.8240	4.36	0.227
2.8281	4.38	0.226
2.8322	4.40	0.225
2.8364	4.42	0.224
2.8405	4.45	0.224
2.8447	4.47	0.223
2.8489	4.49	0.223
2.8530	4.51	0.222
2.8572	4.54	0.222
2.8614	4.55	0.221
2.8656	4.56	0.219
2.8698	4.57	0.218
2.8740	4.58	0.217
2.8782	4.59	0.216
2.8824	4.60	0.216
2.8866	4.61	0.215
2.8909	4.62	0.214
2.8951	4.63	0.214
2.8993	4.63	0.213
2.9036	4.63	0.212
2.9078	4.62	0.211
2.9121	4.62	0.210
2.9164	4.62	0.209
2.9206	4.61	0.208
2.9249	4.61	0.208
2.9292	4.60	0.207
2.9335	4.60	0.207
2.9378	4.59	0.206
2.9421	4.57	0.206
2.9464	4.55	0.205
2.9507	4.53	0.205
2.9550	4.51	0.205
2.9594	4.49	0.205
2.9637	4.47	0.205
2.9680	4.45	0.205
2.9724	4.43	0.205
2.9767	4.40	0.205
2.9811	4.37	0.205
2.9855	4.34	0.205
2.9898	4.31	0.205
2.9942	4.27	0.206
2.9986	4.24	0.206
3.0030	4.21	0.207
3.0074	4.17	0.207
3.0118	4.14	0.208

Freq. (Hz)	LM_{ETF}	$\sigma_{ln,ETF}$	**Freq.** (Hz)	LM_{ETF}	$\sigma_{ln,ETF}$	**Freq.** (Hz)	LM_{ETF}	$\sigma_{ln,ETF}$	**Freq.** (Hz)	LM_{ETF}	$\sigma_{ln,ETF}$
3.0162	4.11	0.209	3.1934	2.60	0.239	3.3809	2.03	0.226	3.5795	2.03	0.191
3.0206	4.07	0.210	3.1980	2.58	0.239	3.3859	2.03	0.225	3.5848	2.03	0.190
3.0250	4.03	0.210	3.2027	2.55	0.239	3.3908	2.02	0.224	3.5900	2.03	0.190
3.0295	3.99	0.211	3.2074	2.52	0.239	3.3958	2.02	0.223	3.5953	2.03	0.189
3.0339	3.95	0.212	3.2121	2.50	0.240	3.4008	2.02	0.222	3.6005	2.04	0.188
3.0384	3.91	0.212	3.2168	2.47	0.240	3.4058	2.01	0.221	3.6058	2.04	0.188
3.0428	3.87	0.213	3.2215	2.44	0.241	3.4107	2.01	0.220	3.6111	2.04	0.187
3.0473	3.82	0.214	3.2262	2.41	0.241	3.4157	2.01	0.219	3.6164	2.05	0.187
3.0517	3.78	0.215	3.2310	2.39	0.241	3.4207	2.01	0.218	3.6217	2.05	0.186
3.0562	3.74	0.217	3.2357	2.38	0.241	3.4258	2.01	0.217	3.6270	2.05	0.186
3.0607	3.70	0.217	3.2404	2.36	0.241	3.4308	2.01	0.216	3.6323	2.06	0.185
3.0652	3.66	0.218	3.2452	2.34	0.241	3.4358	2.00	0.215	3.6376	2.06	0.185
3.0696	3.62	0.219	3.2499	2.32	0.241	3.4408	2.00	0.214	3.6429	2.06	0.185
3.0741	3.57	0.220	3.2547	2.30	0.241	3.4459	2.00	0.213	3.6483	2.07	0.184
3.0786	3.53	0.221	3.2595	2.28	0.241	3.4509	2.00	0.212	3.6536	2.07	0.184
3.0831	3.49	0.221	3.2642	2.26	0.241	3.4560	2.00	0.211	3.6590	2.08	0.183
3.0877	3.44	0.223	3.2690	2.24	0.241	3.4610	2.00	0.210	3.6643	2.09	0.183
3.0922	3.40	0.224	3.2738	2.22	0.241	3.4661	2.00	0.209	3.6697	2.09	0.182
3.0967	3.36	0.225	3.2786	2.21	0.240	3.4712	2.00	0.208	3.6751	2.10	0.182
3.1013	3.32	0.226	3.2834	2.20	0.240	3.4763	2.00	0.207	3.6804	2.10	0.182
3.1058	3.28	0.226	3.2882	2.19	0.239	3.4813	2.00	0.206	3.6858	2.11	0.181
3.1103	3.24	0.227	3.2930	2.17	0.239	3.4864	2.00	0.205	3.6912	2.11	0.181
3.1149	3.20	0.228	3.2979	2.16	0.239	3.4916	2.00	0.204	3.6966	2.12	0.181
3.1195	3.16	0.228	3.3027	2.15	0.238	3.4967	2.00	0.203	3.7020	2.13	0.180
3.1240	3.12	0.229	3.3075	2.14	0.238	3.5018	2.01	0.202	3.7075	2.14	0.180
3.1286	3.08	0.230	3.3124	2.12	0.237	3.5069	2.01	0.201	3.7129	2.15	0.180
3.1332	3.04	0.231	3.3172	2.11	0.237	3.5121	2.01	0.200	3.7183	2.16	0.179
3.1378	3.00	0.232	3.3221	2.10	0.236	3.5172	2.01	0.200	3.7238	2.17	0.179
3.1424	2.96	0.233	3.3269	2.10	0.235	3.5223	2.01	0.199	3.7292	2.18	0.179
3.1470	2.93	0.233	3.3318	2.09	0.235	3.5275	2.01	0.198	3.7347	2.19	0.178
3.1516	2.89	0.234	3.3367	2.08	0.234	3.5327	2.01	0.197	3.7402	2.20	0.178
3.1562	2.86	0.234	3.3416	2.07	0.233	3.5378	2.01	0.196	3.7456	2.21	0.178
3.1608	2.82	0.235	3.3465	2.07	0.232	3.5430	2.01	0.195	3.7511	2.22	0.178
3.1654	2.79	0.235	3.3514	2.06	0.232	3.5482	2.02	0.195	3.7566	2.23	0.177
3.1701	2.76	0.236	3.3563	2.05	0.231	3.5534	2.02	0.194	3.7621	2.25	0.177
3.1747	2.72	0.237	3.3612	2.04	0.230	3.5586	2.02	0.193	3.7676	2.26	0.177
3.1794	2.69	0.237	3.3661	2.04	0.229	3.5638	2.02	0.193	3.7732	2.28	0.176
3.1840	2.65	0.238	3.3710	2.04	0.228	3.5690	2.02	0.192	3.7787	2.29	0.176
3.1887	2.63	0.238	3.3760	2.03	0.227	3.5743	2.03	0.191	3.7842	2.31	0.176

Freq. (Hz)	LM_{ETF}	$\sigma_{ln,ETF}$
3.7898	2.32	0.176
3.7953	2.33	0.176
3.8009	2.36	0.176
3.8064	2.38	0.176
3.8120	2.40	0.175
3.8176	2.42	0.175
3.8232	2.44	0.175
3.8288	2.46	0.175
3.8344	2.48	0.175
3.8400	2.50	0.176
3.8456	2.52	0.176
3.8513	2.54	0.176
3.8569	2.57	0.176
3.8625	2.59	0.176
3.8682	2.62	0.176
3.8739	2.65	0.177
3.8795	2.67	0.177
3.8852	2.70	0.177
3.8909	2.73	0.178
3.8966	2.75	0.178
3.9023	2.78	0.178
3.9080	2.81	0.179
3.9138	2.84	0.179
3.9195	2.87	0.180
3.9252	2.90	0.180
3.9310	2.93	0.181
3.9367	2.96	0.181
3.9425	3.00	0.182
3.9483	3.03	0.182
3.9541	3.06	0.183
3.9598	3.09	0.183
3.9656	3.12	0.184
3.9715	3.15	0.184
3.9773	3.18	0.185
3.9831	3.22	0.185
3.9889	3.25	0.186
3.9948	3.28	0.187
4.0006	3.31	0.187
4.0065	3.34	0.188
4.0123	3.37	0.188
4.0182	3.40	0.188
4.0241	3.42	0.189
4.0300	3.45	0.189
4.0359	3.48	0.189
4.0418	3.51	0.190
4.0477	3.53	0.190
4.0537	3.56	0.190
4.0596	3.59	0.191
4.0655	3.61	0.191
4.0715	3.62	0.191
4.0775	3.64	0.191
4.0834	3.66	0.191
4.0894	3.68	0.191
4.0954	3.69	0.191
4.1014	3.71	0.192
4.1074	3.73	0.192
4.1134	3.75	0.192
4.1194	3.75	0.192
4.1255	3.76	0.192
4.1315	3.76	0.192
4.1376	3.76	0.192
4.1436	3.77	0.192
4.1497	3.77	0.193
4.1558	3.77	0.193
4.1619	3.77	0.193
4.1680	3.78	0.194
4.1741	3.77	0.194
4.1802	3.76	0.194
4.1863	3.75	0.195
4.1924	3.74	0.195
4.1986	3.73	0.195
4.2047	3.71	0.196
4.2109	3.70	0.197
4.2170	3.69	0.197
4.2232	3.68	0.198
4.2294	3.66	0.199
4.2356	3.64	0.200
4.2418	3.61	0.200
4.2480	3.59	0.201
4.2542	3.57	0.202
4.2605	3.54	0.203
4.2667	3.52	0.203
4.2730	3.49	0.204
4.2792	3.47	0.206
4.2855	3.44	0.207
4.2918	3.41	0.208
4.2980	3.38	0.208
4.3043	3.35	0.209
4.3106	3.32	0.210
4.3170	3.29	0.211
4.3233	3.26	0.212
4.3296	3.22	0.213
4.3360	3.19	0.214
4.3423	3.16	0.216
4.3487	3.13	0.216
4.3550	3.10	0.217
4.3614	3.06	0.218
4.3678	3.03	0.218
4.3742	3.00	0.219
4.3806	2.97	0.220
4.3870	2.93	0.221
4.3934	2.90	0.222
4.3999	2.87	0.223
4.4063	2.83	0.223
4.4128	2.80	0.224
4.4192	2.77	0.224
4.4257	2.74	0.225
4.4322	2.71	0.225
4.4387	2.68	0.226
4.4452	2.65	0.226
4.4517	2.62	0.227
4.4582	2.59	0.227
4.4647	2.56	0.228
4.4713	2.53	0.228
4.4778	2.51	0.228
4.4844	2.48	0.228
4.4910	2.46	0.228
4.4975	2.43	0.228
4.5041	2.41	0.228
4.5107	2.38	0.228
4.5173	2.35	0.228
4.5239	2.33	0.229
4.5306	2.31	0.228
4.5372	2.29	0.228
4.5438	2.27	0.228
4.5505	2.25	0.228
4.5572	2.23	0.228
4.5638	2.21	0.227
4.5705	2.19	0.227
4.5772	2.17	0.227
4.5839	2.15	0.227
4.5906	2.14	0.226
4.5974	2.12	0.226
4.6041	2.11	0.225
4.6108	2.10	0.224
4.6176	2.08	0.224
4.6243	2.07	0.223
4.6311	2.06	0.223
4.6379	2.04	0.222
4.6447	2.03	0.221
4.6515	2.02	0.221
4.6583	2.01	0.220
4.6651	2.00	0.219
4.6720	2.00	0.218
4.6788	1.99	0.217
4.6857	1.98	0.216
4.6925	1.98	0.215
4.6994	1.97	0.214
4.7063	1.96	0.213
4.7132	1.95	0.211
4.7201	1.95	0.210
4.7270	1.95	0.209
4.7339	1.95	0.207
4.7408	1.95	0.206
4.7478	1.95	0.204
4.7547	1.95	0.203

Freq. (Hz)	LM_{ETF}	$\sigma_{ln,ETF}$	**Freq.** (Hz)	LM_{ETF}	$\sigma_{ln,ETF}$	**Freq.** (Hz)	LM_{ETF}	$\sigma_{ln,ETF}$	**Freq.** (Hz)	LM_{ETF}	$\sigma_{ln,ETF}$
4.7617	1.95	0.202	5.0414	2.39	0.146	5.3375	3.22	0.168	5.6510	3.04	0.147
4.7687	1.94	0.200	5.0488	2.41	0.145	5.3453	3.23	0.168	5.6593	3.02	0.145
4.7757	1.94	0.199	5.0562	2.43	0.145	5.3531	3.24	0.169	5.6676	3.00	0.143
4.7826	1.95	0.197	5.0636	2.46	0.144	5.3610	3.25	0.169	5.6759	2.98	0.141
4.7897	1.95	0.196	5.0710	2.48	0.144	5.3688	3.26	0.170	5.6842	2.96	0.139
4.7967	1.96	0.194	5.0784	2.50	0.144	5.3767	3.27	0.171	5.6925	2.94	0.138
4.8037	1.96	0.192	5.0858	2.52	0.143	5.3846	3.28	0.172	5.7008	2.92	0.136
4.8107	1.96	0.191	5.0933	2.55	0.143	5.3924	3.29	0.172	5.7092	2.90	0.134
4.8178	1.97	0.189	5.1007	2.57	0.143	5.4003	3.30	0.172	5.7175	2.88	0.132
4.8248	1.97	0.188	5.1082	2.59	0.143	5.4083	3.30	0.172	5.7259	2.86	0.129
4.8319	1.98	0.186	5.1157	2.62	0.144	5.4162	3.30	0.172	5.7343	2.84	0.127
4.8390	1.98	0.185	5.1232	2.64	0.144	5.4241	3.30	0.172	5.7427	2.82	0.125
4.8461	1.99	0.183	5.1307	2.67	0.144	5.4320	3.31	0.172	5.7511	2.80	0.123
4.8532	2.00	0.181	5.1382	2.69	0.144	5.4400	3.31	0.173	5.7595	2.78	0.121
4.8603	2.01	0.179	5.1457	2.71	0.145	5.4480	3.31	0.173	5.7680	2.76	0.119
4.8674	2.02	0.178	5.1533	2.74	0.146	5.4559	3.31	0.173	5.7764	2.74	0.118
4.8745	2.03	0.176	5.1608	2.76	0.146	5.4639	3.31	0.173	5.7849	2.73	0.116
4.8816	2.04	0.174	5.1684	2.79	0.147	5.4719	3.31	0.172	5.7933	2.71	0.114
4.8888	2.05	0.173	5.1759	2.81	0.148	5.4800	3.30	0.172	5.8018	2.69	0.112
4.8960	2.06	0.171	5.1835	2.83	0.148	5.4880	3.29	0.171	5.8103	2.67	0.110
4.9031	2.07	0.170	5.1911	2.86	0.149	5.4960	3.29	0.170	5.8188	2.65	0.108
4.9103	2.08	0.168	5.1987	2.88	0.150	5.5041	3.28	0.170	5.8274	2.63	0.107
4.9175	2.09	0.166	5.2063	2.90	0.151	5.5121	3.27	0.169	5.8359	2.61	0.105
4.9247	2.11	0.165	5.2140	2.93	0.152	5.5202	3.27	0.168	5.8444	2.60	0.104
4.9319	2.12	0.163	5.2216	2.95	0.153	5.5283	3.26	0.168	5.8530	2.58	0.102
4.9391	2.14	0.162	5.2292	2.97	0.154	5.5364	3.25	0.167	5.8616	2.57	0.101
4.9464	2.15	0.160	5.2369	2.99	0.155	5.5445	3.24	0.166	5.8702	2.55	0.099
4.9536	2.17	0.159	5.2446	3.02	0.156	5.5526	3.23	0.165	5.8787	2.54	0.098
4.9609	2.18	0.157	5.2522	3.04	0.157	5.5607	3.21	0.164	5.8874	2.52	0.097
4.9681	2.20	0.156	5.2599	3.06	0.158	5.5689	3.20	0.162	5.8960	2.51	0.096
4.9754	2.21	0.155	5.2676	3.07	0.159	5.5770	3.18	0.161	5.9046	2.49	0.095
4.9827	2.23	0.154	5.2754	3.09	0.160	5.5852	3.17	0.160	5.9133	2.48	0.094
4.9900	2.25	0.152	5.2831	3.11	0.161	5.5934	3.16	0.158	5.9219	2.46	0.094
4.9973	2.27	0.151	5.2908	3.13	0.162	5.6016	3.14	0.157	5.9306	2.45	0.093
5.0046	2.29	0.150	5.2986	3.15	0.163	5.6098	3.13	0.156	5.9393	2.44	0.092
5.0120	2.31	0.149	5.3063	3.16	0.164	5.6180	3.11	0.154	5.9480	2.43	0.092
5.0193	2.33	0.148	5.3141	3.18	0.165	5.6262	3.09	0.152	5.9567	2.43	0.091
5.0266	2.35	0.147	5.3219	3.20	0.167	5.6345	3.07	0.151	5.9654	2.42	0.091
5.0340	2.37	0.147	5.3297	3.21	0.167	5.6427	3.06	0.149	5.9742	2.41	0.091

Freq. (Hz)	LM_{ETF}	$\sigma_{ln,ETF}$
5.9829	2.40	0.091
5.9917	2.39	0.091
6.0004	2.38	0.091
6.0092	2.37	0.091
6.0180	2.37	0.091
6.0268	2.37	0.091
6.0357	2.37	0.092
6.0445	2.36	0.092
6.0534	2.36	0.092
6.0622	2.36	0.093
6.0711	2.36	0.093
6.0800	2.36	0.094
6.0889	2.35	0.094
6.0978	2.36	0.095
6.1067	2.36	0.095
6.1157	2.37	0.095
6.1246	2.37	0.096
6.1336	2.38	0.096
6.1426	2.38	0.097
6.1516	2.38	0.097
6.1606	2.39	0.098
6.1696	2.39	0.099
6.1787	2.40	0.099
6.1877	2.41	0.099
6.1968	2.42	0.100
6.2059	2.43	0.100
6.2149	2.44	0.101
6.2240	2.46	0.101
6.2332	2.47	0.102
6.2423	2.48	0.102
6.2514	2.49	0.103
6.2606	2.50	0.104
6.2698	2.51	0.104
6.2789	2.53	0.104
6.2881	2.55	0.105
6.2973	2.56	0.105
6.3066	2.58	0.106
6.3158	2.59	0.107
6.3250	2.61	0.107
6.3343	2.62	0.108
6.3436	2.64	0.109
6.3529	2.65	0.110
6.3622	2.67	0.110
6.3715	2.69	0.111
6.3808	2.70	0.112
6.3902	2.72	0.113
6.3995	2.74	0.113
6.4089	2.75	0.114
6.4183	2.77	0.115
6.4277	2.79	0.117
6.4371	2.80	0.117
6.4465	2.82	0.118
6.4560	2.83	0.119
6.4654	2.85	0.120
6.4749	2.86	0.121
6.4844	2.87	0.122
6.4939	2.89	0.124
6.5034	2.90	0.125
6.5129	2.92	0.126
6.5225	2.93	0.127
6.5320	2.94	0.128
6.5416	2.94	0.129
6.5512	2.95	0.130
6.5607	2.96	0.131
6.5704	2.97	0.132
6.5800	2.97	0.133
6.5896	2.98	0.135
6.5993	2.99	0.136
6.6089	2.99	0.137
6.6186	2.99	0.138
6.6283	2.99	0.138
6.6380	2.99	0.139
6.6477	2.98	0.140
6.6575	2.98	0.141
6.6672	2.98	0.142
6.6770	2.98	0.143
6.6868	2.97	0.144
6.6966	2.97	0.145
6.7064	2.96	0.145
6.7162	2.95	0.145
6.7260	2.94	0.145
6.7359	2.92	0.145
6.7457	2.91	0.146
6.7556	2.90	0.146
6.7655	2.89	0.146
6.7754	2.87	0.147
6.7853	2.86	0.147
6.7953	2.85	0.147
6.8052	2.83	0.146
6.8152	2.81	0.146
6.8252	2.79	0.145
6.8352	2.77	0.145
6.8452	2.75	0.144
6.8552	2.73	0.144
6.8652	2.71	0.143
6.8753	2.70	0.143
6.8854	2.68	0.142
6.8955	2.66	0.141
6.9056	2.63	0.139
6.9157	2.61	0.138
6.9258	2.59	0.137
6.9359	2.57	0.136
6.9461	2.55	0.135
6.9563	2.53	0.133
6.9665	2.51	0.132
6.9767	2.49	0.131
6.9869	2.47	0.129
6.9971	2.45	0.127
7.0074	2.43	0.126
7.0176	2.41	0.124
7.0279	2.39	0.122
7.0382	2.37	0.121
7.0485	2.36	0.119
7.0588	2.34	0.118
7.0692	2.32	0.117
7.0795	2.30	0.115
7.0899	2.29	0.113
7.1003	2.28	0.112
7.1107	2.26	0.110
7.1211	2.25	0.109
7.1315	2.23	0.108
7.1420	2.22	0.107
7.1524	2.20	0.107
7.1629	2.19	0.106
7.1734	2.18	0.105
7.1839	2.17	0.105
7.1944	2.17	0.105
7.2049	2.16	0.105
7.2155	2.15	0.105
7.2261	2.14	0.105
7.2366	2.14	0.106
7.2472	2.13	0.107
7.2579	2.12	0.108
7.2685	2.12	0.110
7.2791	2.12	0.111
7.2898	2.12	0.112
7.3005	2.11	0.114
7.3112	2.11	0.115
7.3219	2.11	0.117
7.3326	2.11	0.120
7.3433	2.11	0.122
7.3541	2.11	0.125
7.3649	2.11	0.127
7.3756	2.12	0.129
7.3864	2.12	0.131
7.3973	2.13	0.134
7.4081	2.13	0.136
7.4189	2.14	0.139
7.4298	2.14	0.141
7.4407	2.15	0.144
7.4516	2.15	0.147
7.4625	2.16	0.150
7.4734	2.17	0.151
7.4844	2.18	0.153
7.4953	2.19	0.155
7.5063	2.20	0.157

Freq. (Hz)	LM_{ETF}	$\sigma_{ln,ETF}$
7.5173	2.21	0.158
7.5283	2.22	0.160
7.5393	2.23	0.162
7.5504	2.23	0.164
7.5614	2.24	0.167
7.5725	2.26	0.167
7.5836	2.27	0.168
7.5947	2.28	0.168
7.6058	2.29	0.169
7.6170	2.30	0.170
7.6281	2.32	0.170
7.6393	2.33	0.171
7.6505	2.34	0.172
7.6617	2.35	0.173
7.6729	2.36	0.173
7.6841	2.37	0.172
7.6954	2.38	0.171
7.7067	2.39	0.170
7.7180	2.40	0.170
7.7293	2.42	0.169
7.7406	2.43	0.168
7.7519	2.44	0.168
7.7633	2.45	0.168
7.7746	2.46	0.167
7.7860	2.46	0.165
7.7974	2.47	0.163
7.8089	2.47	0.161
7.8203	2.48	0.160
7.8317	2.48	0.158
7.8432	2.49	0.156
7.8547	2.49	0.155
7.8662	2.50	0.154
7.8777	2.50	0.152
7.8893	2.50	0.150
7.9008	2.50	0.148
7.9124	2.50	0.146
7.9240	2.50	0.144
7.9356	2.50	0.142
7.9472	2.50	0.140
7.9588	2.49	0.139
7.9705	2.49	0.137
7.9822	2.49	0.136
7.9939	2.48	0.134
8.0056	2.47	0.133
8.0173	2.46	0.131
8.0290	2.45	0.130
8.0408	2.45	0.129
8.0526	2.44	0.128
8.0644	2.43	0.127
8.0762	2.42	0.126
8.0880	2.41	0.126
8.0998	2.40	0.125
8.1117	2.38	0.125
8.1236	2.37	0.125
8.1355	2.35	0.125
8.1474	2.34	0.125
8.1593	2.32	0.125
8.1713	2.31	0.125
8.1832	2.29	0.126
8.1952	2.28	0.126
8.2072	2.26	0.127
8.2193	2.25	0.128
8.2313	2.23	0.129
8.2433	2.21	0.130
8.2554	2.20	0.131
8.2675	2.18	0.132
8.2796	2.16	0.133
8.2917	2.14	0.135
8.3039	2.13	0.136
8.3160	2.11	0.138
8.3282	2.09	0.139
8.3404	2.08	0.140
8.3526	2.06	0.142
8.3649	2.05	0.143
8.3771	2.03	0.144
8.3894	2.01	0.146
8.4017	2.00	0.148
8.4140	1.98	0.150
8.4263	1.96	0.152
8.4386	1.95	0.153
8.4510	1.94	0.154
8.4634	1.92	0.155
8.4758	1.91	0.157
8.4882	1.90	0.158
8.5006	1.89	0.160
8.5131	1.87	0.161
8.5255	1.86	0.163
8.5380	1.85	0.165
8.5505	1.84	0.166
8.5631	1.83	0.167
8.5756	1.82	0.168
8.5882	1.81	0.169
8.6007	1.80	0.170
8.6133	1.79	0.172
8.6259	1.78	0.173
8.6386	1.78	0.174
8.6512	1.77	0.176
8.6639	1.76	0.176
8.6766	1.76	0.177
8.6893	1.75	0.178
8.7020	1.75	0.178
8.7148	1.75	0.179
8.7275	1.74	0.180
8.7403	1.74	0.180
8.7531	1.74	0.181
8.7659	1.73	0.182
8.7788	1.73	0.183
8.7916	1.73	0.183
8.8045	1.73	0.183
8.8174	1.74	0.183
8.8303	1.74	0.183
8.8432	1.74	0.183
8.8562	1.74	0.183
8.8692	1.74	0.183
8.8822	1.74	0.183
8.8952	1.74	0.183
8.9082	1.75	0.182
8.9212	1.76	0.182
8.9343	1.76	0.181
8.9474	1.77	0.180
8.9605	1.77	0.179
8.9736	1.78	0.179
8.9868	1.78	0.178
8.9999	1.79	0.177
9.0131	1.79	0.177
9.0263	1.80	0.175
9.0395	1.81	0.174
9.0528	1.82	0.172
9.0660	1.83	0.170
9.0793	1.83	0.169
9.0926	1.84	0.167
9.1059	1.85	0.166
9.1192	1.86	0.165
9.1326	1.87	0.163
9.1460	1.88	0.162
9.1594	1.88	0.159
9.1728	1.89	0.157
9.1862	1.90	0.155
9.1997	1.91	0.154
9.2131	1.92	0.152
9.2266	1.93	0.150
9.2401	1.94	0.149
9.2537	1.95	0.147
9.2672	1.95	0.145
9.2808	1.96	0.144
9.2944	1.97	0.142
9.3080	1.98	0.141
9.3216	1.99	0.139
9.3353	2.00	0.138
9.3490	2.00	0.137
9.3627	2.01	0.136
9.3764	2.02	0.135
9.3901	2.03	0.135
9.4038	2.03	0.134
9.4176	2.04	0.134
9.4314	2.05	0.134

Freq. (Hz)	LM_{ETF}	$\sigma_{ln,ETF}$	**Freq.** (Hz)	LM_{ETF}	$\sigma_{ln,ETF}$	**Freq.** (Hz)	LM_{ETF}	$\sigma_{ln,ETF}$	**Freq.** (Hz)	LM_{ETF}	$\sigma_{ln,ETF}$
9.4452	2.05	0.134	9.5845	2.12	0.145	9.7258	2.19	0.167	9.8692	2.26	0.194
9.4591	2.06	0.135	9.5985	2.13	0.147	9.7400	2.19	0.170	9.8836	2.27	0.197
9.4729	2.07	0.135	9.6126	2.13	0.149	9.7543	2.20	0.173	9.8981	2.28	0.199
9.4868	2.08	0.136	9.6266	2.14	0.151	9.7686	2.21	0.176	9.9126	2.29	0.202
9.5007	2.08	0.136	9.6407	2.14	0.153	9.7829	2.21	0.178	9.9271	2.30	0.204
9.5146	2.09	0.137	9.6549	2.15	0.155	9.7972	2.22	0.181	9.9416	2.31	0.206
9.5285	2.09	0.139	9.6690	2.16	0.157	9.8115	2.23	0.183	9.9562	2.32	0.209
9.5425	2.10	0.140	9.6832	2.17	0.160	9.8259	2.24	0.186	9.9708	2.33	0.211
9.5565	2.11	0.141	9.6973	2.17	0.162	9.8403	2.25	0.189	9.9854	2.34	0.213
9.5705	2.11	0.143	9.7115	2.18	0.165	9.8547	2.26	0.191	10.0000	2.35	0.216

Table D.2 Tabulated 1D and 2D Mean Azimuth TTFs from I15DA GRAs sampled from 0.5 to 10 Hz with 2048 points.

Frequency (Hz)	1D PS-Logging	1D LR = 1.5	1D LR = 2.0	1D LR = 3.0	1D LR = 5.0	2D Mean Azimuth
0.5000	1.79	1.82	1.91	2.02	2.01	1.98
0.5007	1.79	1.83	1.92	2.03	2.01	1.99
0.5015	1.79	1.83	1.92	2.03	2.02	1.99
0.5022	1.80	1.83	1.93	2.04	2.03	2.00
0.5029	1.80	1.84	1.93	2.04	2.03	2.00
0.5037	1.81	1.84	1.94	2.05	2.04	2.01
0.5044	1.81	1.85	1.94	2.05	2.04	2.01
0.5051	1.81	1.85	1.95	2.06	2.05	2.02
0.5059	1.82	1.85	1.95	2.06	2.05	2.02
0.5066	1.82	1.86	1.95	2.07	2.06	2.03
0.5074	1.82	1.86	1.96	2.08	2.06	2.03
0.5081	1.83	1.87	1.96	2.08	2.07	2.04
0.5089	1.83	1.87	1.97	2.09	2.07	2.04
0.5096	1.84	1.87	1.97	2.09	2.08	2.05
0.5103	1.84	1.88	1.98	2.10	2.09	2.06
0.5111	1.84	1.88	1.98	2.10	2.09	2.06
0.5118	1.85	1.89	1.99	2.11	2.10	2.07
0.5126	1.85	1.89	1.99	2.12	2.10	2.07
0.5133	1.86	1.90	2.00	2.12	2.11	2.08
0.5141	1.86	1.90	2.00	2.13	2.12	2.08
0.5149	1.86	1.90	2.01	2.13	2.12	2.09
0.5156	1.87	1.91	2.01	2.14	2.13	2.10
0.5164	1.87	1.91	2.02	2.15	2.13	2.10
0.5171	1.88	1.92	2.02	2.15	2.14	2.11
0.5179	1.88	1.92	2.03	2.16	2.15	2.11
0.5186	1.89	1.93	2.04	2.17	2.15	2.12
0.5194	1.89	1.93	2.04	2.17	2.16	2.12
0.5202	1.89	1.94	2.05	2.18	2.16	2.13
0.5209	1.90	1.94	2.05	2.18	2.17	2.14
0.5217	1.90	1.95	2.06	2.19	2.18	2.14
0.5224	1.91	1.95	2.06	2.20	2.18	2.15
0.5232	1.91	1.95	2.07	2.20	2.19	2.16
0.5240	1.92	1.96	2.07	2.21	2.20	2.16
0.5247	1.92	1.96	2.08	2.22	2.20	2.17
0.5255	1.92	1.97	2.09	2.22	2.21	2.17
0.5263	1.93	1.97	2.09	2.23	2.22	2.18
0.5270	1.93	1.98	2.10	2.24	2.22	2.19
0.5278	1.94	1.98	2.10	2.25	2.23	2.19
0.5286	1.94	1.99	2.11	2.25	2.24	2.20
0.5294	1.95	1.99	2.11	2.26	2.25	2.21
0.5301	1.95	2.00	2.12	2.27	2.25	2.21
0.5309	1.96	2.00	2.13	2.27	2.26	2.22
0.5317	1.96	2.01	2.13	2.28	2.27	2.23
0.5325	1.97	2.01	2.14	2.29	2.27	2.23
0.5333	1.97	2.02	2.14	2.30	2.28	2.24
0.5340	1.98	2.02	2.15	2.30	2.29	2.25
0.5348	1.98	2.03	2.16	2.31	2.30	2.25
0.5356	1.99	2.04	2.16	2.32	2.30	2.26
0.5364	1.99	2.04	2.17	2.33	2.31	2.27
0.5372	2.00	2.05	2.18	2.33	2.32	2.28

Frequency (Hz)	1D PS-Logging	1D LR = 1.5	1D LR = 2.0	1D LR = 3.0	1D LR = 5.0	2D Mean Azimuth
0.5380	2.00	2.05	2.18	2.34	2.33	2.28
0.5387	2.01	2.06	2.19	2.35	2.33	2.29
0.5395	2.01	2.06	2.20	2.36	2.34	2.30
0.5403	2.02	2.07	2.20	2.36	2.35	2.31
0.5411	2.02	2.07	2.21	2.37	2.36	2.31
0.5419	2.03	2.08	2.22	2.38	2.37	2.32
0.5427	2.03	2.09	2.22	2.39	2.37	2.33
0.5435	2.04	2.09	2.23	2.40	2.38	2.34
0.5443	2.04	2.10	2.24	2.40	2.39	2.34
0.5451	2.05	2.10	2.24	2.41	2.40	2.35
0.5459	2.05	2.11	2.25	2.42	2.41	2.36
0.5467	2.06	2.11	2.26	2.43	2.42	2.37
0.5475	2.06	2.12	2.26	2.44	2.42	2.38
0.5483	2.07	2.13	2.27	2.45	2.43	2.38
0.5491	2.07	2.13	2.28	2.46	2.44	2.39
0.5499	2.08	2.14	2.29	2.46	2.45	2.40
0.5507	2.09	2.14	2.29	2.47	2.46	2.41
0.5515	2.09	2.15	2.30	2.48	2.47	2.42
0.5523	2.10	2.16	2.31	2.49	2.48	2.43
0.5531	2.10	2.16	2.31	2.50	2.49	2.43
0.5539	2.11	2.17	2.32	2.51	2.49	2.44
0.5547	2.11	2.18	2.33	2.52	2.50	2.45
0.5556	2.12	2.18	2.34	2.53	2.51	2.46
0.5564	2.13	2.19	2.35	2.54	2.52	2.47
0.5572	2.13	2.20	2.35	2.55	2.53	2.48
0.5580	2.14	2.20	2.36	2.56	2.54	2.49
0.5588	2.14	2.21	2.37	2.57	2.55	2.50
0.5596	2.15	2.21	2.38	2.58	2.56	2.51
0.5605	2.16	2.22	2.39	2.59	2.57	2.51
0.5613	2.16	2.23	2.39	2.60	2.58	2.52
0.5621	2.17	2.24	2.40	2.61	2.59	2.53
0.5629	2.17	2.24	2.41	2.62	2.60	2.54
0.5638	2.18	2.25	2.42	2.63	2.61	2.55
0.5646	2.19	2.26	2.43	2.64	2.62	2.56
0.5654	2.19	2.26	2.44	2.65	2.63	2.57
0.5662	2.20	2.27	2.44	2.66	2.64	2.58
0.5671	2.21	2.28	2.45	2.67	2.65	2.59
0.5679	2.21	2.28	2.46	2.68	2.66	2.60
0.5687	2.22	2.29	2.47	2.69	2.68	2.61
0.5696	2.23	2.30	2.48	2.70	2.69	2.62
0.5704	2.23	2.31	2.49	2.71	2.70	2.63
0.5712	2.24	2.31	2.50	2.73	2.71	2.64
0.5721	2.25	2.32	2.51	2.74	2.72	2.65
0.5729	2.25	2.33	2.52	2.75	2.73	2.67
0.5737	2.26	2.34	2.53	2.76	2.74	2.68
0.5746	2.27	2.34	2.54	2.77	2.75	2.69
0.5754	2.28	2.35	2.54	2.78	2.77	2.70
0.5763	2.28	2.36	2.55	2.80	2.78	2.71
0.5771	2.29	2.37	2.56	2.81	2.79	2.72
0.5780	2.30	2.38	2.57	2.82	2.80	2.73
0.5788	2.30	2.38	2.58	2.83	2.82	2.74
0.5796	2.31	2.39	2.59	2.84	2.83	2.76
0.5805	2.32	2.40	2.60	2.86	2.84	2.77
0.5813	2.33	2.41	2.61	2.87	2.85	2.78

Frequency (Hz)	1D PS-Logging	1D LR = 1.5	1D LR = 2.0	1D LR = 3.0	1D LR = 5.0	2D Mean Azimuth
0.5822	2.33	2.42	2.62	2.88	2.87	2.79
0.5830	2.34	2.43	2.64	2.90	2.88	2.80
0.5839	2.35	2.43	2.65	2.91	2.89	2.82
0.5848	2.36	2.44	2.66	2.92	2.91	2.83
0.5856	2.36	2.45	2.67	2.94	2.92	2.84
0.5865	2.37	2.46	2.68	2.95	2.93	2.85
0.5873	2.38	2.47	2.69	2.96	2.95	2.87
0.5882	2.39	2.48	2.70	2.98	2.96	2.88
0.5891	2.40	2.49	2.71	2.99	2.97	2.89
0.5899	2.40	2.50	2.72	3.01	2.99	2.90
0.5908	2.41	2.51	2.73	3.02	3.00	2.92
0.5916	2.42	2.52	2.75	3.03	3.02	2.93
0.5925	2.43	2.52	2.76	3.05	3.03	2.94
0.5934	2.44	2.53	2.77	3.06	3.05	2.96
0.5942	2.45	2.54	2.78	3.08	3.06	2.97
0.5951	2.45	2.55	2.79	3.09	3.08	2.99
0.5960	2.46	2.56	2.80	3.11	3.09	3.00
0.5969	2.47	2.57	2.82	3.13	3.11	3.02
0.5977	2.48	2.58	2.83	3.14	3.12	3.03
0.5986	2.49	2.59	2.84	3.16	3.14	3.04
0.5995	2.50	2.60	2.85	3.17	3.16	3.06
0.6004	2.51	2.61	2.87	3.19	3.17	3.07
0.6012	2.52	2.62	2.88	3.21	3.19	3.09
0.6021	2.53	2.63	2.89	3.22	3.21	3.11
0.6030	2.54	2.64	2.91	3.24	3.22	3.12
0.6039	2.54	2.65	2.92	3.26	3.24	3.14
0.6048	2.55	2.66	2.93	3.27	3.26	3.15
0.6057	2.56	2.68	2.95	3.29	3.28	3.17
0.6065	2.57	2.69	2.96	3.31	3.29	3.19
0.6074	2.58	2.70	2.97	3.33	3.31	3.20
0.6083	2.59	2.71	2.99	3.35	3.33	3.22
0.6092	2.60	2.72	3.00	3.36	3.35	3.24
0.6101	2.61	2.73	3.02	3.38	3.37	3.25
0.6110	2.62	2.74	3.03	3.40	3.39	3.27
0.6119	2.63	2.75	3.05	3.42	3.40	3.29
0.6128	2.64	2.77	3.06	3.44	3.42	3.31
0.6137	2.65	2.78	3.08	3.46	3.44	3.32
0.6146	2.66	2.79	3.09	3.48	3.46	3.34
0.6155	2.67	2.80	3.11	3.50	3.48	3.36
0.6164	2.69	2.81	3.12	3.52	3.50	3.38
0.6173	2.70	2.83	3.14	3.54	3.53	3.40
0.6182	2.71	2.84	3.15	3.56	3.55	3.42
0.6191	2.72	2.85	3.17	3.58	3.57	3.44
0.6200	2.73	2.86	3.19	3.61	3.59	3.46
0.6209	2.74	2.88	3.20	3.63	3.61	3.48
0.6218	2.75	2.89	3.22	3.65	3.63	3.50
0.6227	2.76	2.90	3.24	3.67	3.66	3.52
0.6237	2.77	2.92	3.25	3.69	3.68	3.54
0.6246	2.79	2.93	3.27	3.72	3.70	3.56
0.6255	2.80	2.94	3.29	3.74	3.73	3.58
0.6264	2.81	2.96	3.31	3.77	3.75	3.60
0.6273	2.82	2.97	3.32	3.79	3.77	3.62
0.6282	2.83	2.98	3.34	3.81	3.80	3.65
0.6292	2.85	3.00	3.36	3.84	3.82	3.67

Frequency (Hz)	1D PS-Logging	1D LR = 1.5	1D LR = 2.0	1D LR = 3.0	1D LR = 5.0	2D Mean Azimuth
0.6301	2.86	3.01	3.38	3.86	3.85	3.69
0.6310	2.87	3.03	3.40	3.89	3.88	3.71
0.6319	2.88	3.04	3.42	3.92	3.90	3.74
0.6328	2.90	3.06	3.44	3.94	3.93	3.76
0.6338	2.91	3.07	3.46	3.97	3.96	3.79
0.6347	2.92	3.09	3.48	4.00	3.98	3.81
0.6356	2.94	3.10	3.50	4.02	4.01	3.84
0.6366	2.95	3.12	3.52	4.05	4.04	3.86
0.6375	2.96	3.13	3.54	4.08	4.07	3.89
0.6384	2.98	3.15	3.56	4.11	4.10	3.91
0.6394	2.99	3.17	3.58	4.14	4.13	3.94
0.6403	3.00	3.18	3.60	4.17	4.16	3.97
0.6412	3.02	3.20	3.63	4.20	4.19	3.99
0.6422	3.03	3.21	3.65	4.23	4.22	4.02
0.6431	3.05	3.23	3.67	4.26	4.25	4.05
0.6441	3.06	3.25	3.69	4.29	4.28	4.08
0.6450	3.08	3.27	3.72	4.32	4.31	4.11
0.6459	3.09	3.28	3.74	4.36	4.35	4.14
0.6469	3.11	3.30	3.76	4.39	4.38	4.17
0.6478	3.12	3.32	3.79	4.42	4.42	4.20
0.6488	3.14	3.34	3.81	4.46	4.45	4.23
0.6497	3.15	3.35	3.84	4.49	4.49	4.26
0.6507	3.17	3.37	3.86	4.53	4.52	4.29
0.6516	3.18	3.39	3.89	4.56	4.56	4.32
0.6526	3.20	3.41	3.91	4.60	4.60	4.35
0.6536	3.22	3.43	3.94	4.64	4.63	4.39
0.6545	3.23	3.45	3.97	4.68	4.67	4.42
0.6555	3.25	3.47	3.99	4.72	4.71	4.46
0.6564	3.27	3.49	4.02	4.76	4.75	4.49
0.6574	3.28	3.51	4.05	4.80	4.79	4.53
0.6584	3.30	3.53	4.08	4.84	4.84	4.56
0.6593	3.32	3.55	4.11	4.88	4.88	4.60
0.6603	3.33	3.57	4.14	4.92	4.92	4.64
0.6612	3.35	3.59	4.17	4.96	4.97	4.68
0.6622	3.37	3.62	4.20	5.01	5.01	4.72
0.6632	3.39	3.64	4.23	5.05	5.06	4.76
0.6642	3.41	3.66	4.26	5.10	5.10	4.80
0.6651	3.43	3.68	4.29	5.15	5.15	4.84
0.6661	3.45	3.71	4.32	5.19	5.20	4.88
0.6671	3.46	3.73	4.36	5.24	5.25	4.92
0.6681	3.48	3.75	4.39	5.29	5.30	4.97
0.6690	3.50	3.78	4.42	5.34	5.35	5.01
0.6700	3.52	3.80	4.46	5.40	5.41	5.06
0.6710	3.54	3.83	4.49	5.45	5.46	5.10
0.6720	3.57	3.85	4.53	5.50	5.51	5.15
0.6730	3.59	3.88	4.57	5.56	5.57	5.20
0.6740	3.61	3.90	4.60	5.61	5.63	5.25
0.6749	3.63	3.93	4.64	5.67	5.69	5.30
0.6759	3.65	3.95	4.68	5.73	5.75	5.35
0.6769	3.67	3.98	4.72	5.79	5.81	5.40
0.6779	3.69	4.01	4.76	5.85	5.87	5.45
0.6789	3.72	4.04	4.80	5.91	5.94	5.51
0.6799	3.74	4.06	4.84	5.98	6.00	5.56
0.6809	3.76	4.09	4.88	6.04	6.07	5.62

Frequency (Hz)	1D PS-Logging	1D LR = 1.5	1D LR = 2.0	1D LR = 3.0	1D LR = 5.0	2D Mean Azimuth
0.6819	3.79	4.12	4.92	6.11	6.14	5.68
0.6829	3.81	4.15	4.97	6.18	6.21	5.74
0.6839	3.83	4.18	5.01	6.25	6.28	5.80
0.6849	3.86	4.21	5.06	6.32	6.36	5.86
0.6859	3.88	4.24	5.10	6.40	6.44	5.92
0.6869	3.91	4.27	5.15	6.47	6.51	5.99
0.6879	3.93	4.31	5.20	6.55	6.59	6.05
0.6889	3.96	4.34	5.25	6.63	6.68	6.12
0.6899	3.99	4.37	5.30	6.71	6.76	6.19
0.6909	4.01	4.41	5.35	6.79	6.85	6.26
0.6919	4.04	4.44	5.40	6.88	6.94	6.34
0.6930	4.07	4.47	5.45	6.97	7.03	6.41
0.6940	4.10	4.51	5.51	7.06	7.12	6.49
0.6950	4.12	4.55	5.56	7.15	7.22	6.56
0.6960	4.15	4.58	5.62	7.25	7.32	6.65
0.6970	4.18	4.62	5.68	7.35	7.42	6.73
0.6980	4.21	4.66	5.74	7.45	7.53	6.81
0.6991	4.24	4.70	5.80	7.55	7.64	6.90
0.7001	4.27	4.73	5.86	7.66	7.75	6.99
0.7011	4.30	4.77	5.92	7.77	7.87	7.08
0.7021	4.33	4.81	5.99	7.88	7.99	7.17
0.7032	4.37	4.86	6.05	8.00	8.11	7.27
0.7042	4.40	4.90	6.12	8.12	8.24	7.37
0.7052	4.43	4.94	6.19	8.25	8.37	7.47
0.7063	4.47	4.98	6.26	8.38	8.50	7.58
0.7073	4.50	5.03	6.33	8.51	8.65	7.69
0.7083	4.53	5.07	6.41	8.65	8.79	7.80
0.7094	4.57	5.12	6.49	8.79	8.94	7.92
0.7104	4.61	5.17	6.56	8.94	9.10	8.03
0.7115	4.64	5.22	6.64	9.09	9.26	8.16
0.7125	4.68	5.27	6.73	9.24	9.43	8.28
0.7135	4.72	5.32	6.81	9.41	9.60	8.41
0.7146	4.75	5.37	6.90	9.58	9.78	8.55
0.7156	4.79	5.42	6.99	9.75	9.97	8.69
0.7167	4.83	5.47	7.08	9.93	10.16	8.83
0.7177	4.87	5.53	7.17	10.12	10.37	8.98
0.7188	4.92	5.58	7.27	10.32	10.58	9.14
0.7198	4.96	5.64	7.37	10.53	10.80	9.30
0.7209	5.00	5.70	7.47	10.74	11.03	9.46
0.7219	5.04	5.76	7.58	10.96	11.27	9.63
0.7230	5.09	5.82	7.69	11.19	11.52	9.81
0.7241	5.13	5.88	7.80	11.43	11.79	10.00
0.7251	5.18	5.94	7.91	11.69	12.06	10.19
0.7262	5.23	6.01	8.03	11.95	12.35	10.39
0.7272	5.27	6.07	8.16	12.23	12.66	10.60
0.7283	5.32	6.14	8.28	12.52	12.97	10.82
0.7294	5.37	6.21	8.41	12.82	13.31	11.05
0.7304	5.42	6.28	8.55	13.14	13.66	11.28
0.7315	5.47	6.36	8.69	13.47	14.04	11.53
0.7326	5.53	6.43	8.83	13.83	14.43	11.78
0.7337	5.58	6.51	8.98	14.20	14.85	12.06
0.7347	5.64	6.59	9.14	14.59	15.29	12.34
0.7358	5.69	6.67	9.30	15.01	15.76	12.64
0.7369	5.75	6.75	9.46	15.45	16.26	12.95

Frequency (Hz)	1D PS-Logging	1D LR = 1.5	1D LR = 2.0	1D LR = 3.0	1D LR = 5.0	2D Mean Azimuth
0.7380	5.81	6.83	9.63	15.92	16.80	13.28
0.7390	5.87	6.92	9.81	16.41	17.37	13.62
0.7401	5.93	7.01	10.00	16.94	17.98	13.98
0.7412	5.99	7.10	10.19	17.50	18.63	14.37
0.7423	6.05	7.20	10.39	18.10	19.33	14.77
0.7434	6.12	7.29	10.60	18.75	20.09	15.20
0.7445	6.19	7.39	10.82	19.44	20.91	15.65
0.7456	6.25	7.49	11.04	20.18	21.79	16.14
0.7467	6.32	7.60	11.28	20.99	22.76	16.65
0.7477	6.40	7.71	11.53	21.86	23.81	17.20
0.7488	6.47	7.82	11.79	22.80	24.96	17.78
0.7499	6.54	7.94	12.06	23.82	26.23	18.40
0.7510	6.62	8.06	12.34	24.95	27.63	19.07
0.7521	6.70	8.18	12.64	26.18	29.19	19.79
0.7532	6.78	8.30	12.95	27.53	30.92	20.56
0.7543	6.86	8.43	13.28	29.03	32.86	21.40
0.7554	6.95	8.57	13.62	30.69	35.05	22.29
0.7566	7.03	8.71	13.98	32.55	37.53	23.29
0.7577	7.12	8.85	14.37	34.64	40.36	24.35
0.7588	7.21	9.00	14.77	37.00	43.62	25.53
0.7599	7.31	9.16	15.20	39.68	47.38	26.80
0.7610	7.40	9.32	15.66	42.74	51.76	28.24
0.7621	7.50	9.48	16.14	46.28	56.89	29.79
0.7632	7.61	9.65	16.65	50.37	62.89	31.56
0.7643	7.71	9.83	17.20	55.15	69.89	33.49
0.7655	7.82	10.02	17.79	60.75	77.93	35.72
0.7666	7.93	10.21	18.41	67.31	86.81	38.19
0.7677	8.04	10.41	19.08	74.95	95.85	41.09
0.7688	8.16	10.62	19.80	83.65	103.64	44.39
0.7700	8.28	10.83	20.58	93.09	108.16	48.31
0.7711	8.41	11.06	21.42	102.35	107.82	52.99
0.7722	8.54	11.30	22.34	109.68	102.75	58.73
0.7733	8.67	11.54	23.33	112.92	94.66	66.21
0.7745	8.80	11.80	24.41	110.88	85.54	75.82
0.7756	8.95	12.07	25.60	104.33	76.71	82.61
0.7767	9.09	12.35	26.90	95.32	68.77	86.44
0.7779	9.24	12.65	28.34	85.78	61.87	86.33
0.7790	9.40	12.96	29.94	76.83	55.97	82.77
0.7802	9.56	13.28	31.72	68.92	50.93	79.50
0.7813	9.73	13.63	33.72	62.09	46.63	76.44
0.7825	9.90	13.99	35.98	56.26	42.92	71.87
0.7836	10.08	14.37	38.54	51.29	39.72	66.45
0.7847	10.27	14.77	41.46	47.04	36.93	61.46
0.7859	10.47	15.20	44.82	43.37	34.48	56.67
0.7870	10.67	15.65	48.71	40.20	32.32	52.80
0.7882	10.88	16.13	53.24	37.43	30.41	49.24
0.7894	11.10	16.64	58.54	34.99	28.69	46.46
0.7905	11.32	17.18	64.76	32.84	27.16	43.89
0.7917	11.56	17.76	72.03	30.93	25.77	41.97
0.7928	11.81	18.38	80.39	29.22	24.52	40.17
0.7940	12.06	19.04	89.65	27.68	23.38	38.92
0.7951	12.33	19.75	99.10	26.30	22.34	37.71
0.7963	12.62	20.52	107.24	25.04	21.38	36.72
0.7975	12.91	21.35	111.93	23.89	20.50	35.52

Frequency (Hz)	1D PS-Logging	1D LR = 1.5	1D LR = 2.0	1D LR = 3.0	1D LR = 5.0	2D Mean Azimuth
0.7986	13.22	22.25	111.51	22.84	19.69	34.15
0.7998	13.54	23.22	106.12	21.88	18.94	32.45
0.8010	13.89	24.28	97.62	20.99	18.24	30.67
0.8022	14.24	25.45	88.10	20.18	17.60	28.88
0.8033	14.62	26.72	78.92	19.42	16.99	27.22
0.8045	15.02	28.13	70.70	18.71	16.43	25.70
0.8057	15.44	29.69	63.58	18.06	15.90	24.33
0.8069	15.88	31.43	57.50	17.45	15.40	23.10
0.8081	16.35	33.37	52.31	16.87	14.93	21.99
0.8092	16.85	35.55	47.88	16.34	14.49	21.00
0.8104	17.38	38.02	44.07	15.83	14.08	20.09
0.8116	17.95	40.83	40.78	15.36	13.69	19.27
0.8128	18.55	44.04	37.92	14.91	13.32	18.50
0.8140	19.19	47.75	35.40	14.49	12.96	17.82
0.8152	19.88	52.04	33.19	14.09	12.63	17.17
0.8164	20.62	57.04	31.22	13.72	12.31	16.58
0.8176	21.42	62.86	29.47	13.36	12.01	16.02
0.8188	22.28	69.61	27.89	13.02	11.72	15.51
0.8200	23.21	77.33	26.47	12.70	11.45	15.03
0.8212	24.22	85.85	25.19	12.39	11.19	14.57
0.8224	25.31	94.61	24.02	12.10	10.94	14.15
0.8236	26.51	102.40	22.95	11.82	10.70	13.74
0.8248	27.83	107.44	21.97	11.55	10.47	13.37
0.8260	29.27	108.13	21.07	11.30	10.25	13.00
0.8272	30.87	104.22	20.24	11.05	10.04	12.67
0.8284	32.65	97.01	19.47	10.82	9.84	12.34
0.8296	34.63	88.36	18.75	10.59	9.64	12.04
0.8308	36.85	79.66	18.09	10.38	9.45	11.75
0.8321	39.35	71.65	17.47	10.17	9.28	11.47
0.8333	42.18	64.60	16.89	9.97	9.10	11.21
0.8345	45.41	58.50	16.35	9.78	8.94	10.95
0.8357	49.10	53.27	15.84	9.60	8.77	10.71
0.8369	53.35	48.77	15.36	9.42	8.62	10.48
0.8382	58.25	44.90	14.91	9.25	8.47	10.26
0.8394	63.91	41.54	14.48	9.09	8.32	10.04
0.8406	70.40	38.62	14.08	8.93	8.19	9.84
0.8419	77.72	36.05	13.70	8.78	8.05	9.65
0.8431	85.71	33.79	13.34	8.63	7.92	9.46
0.8443	93.86	31.78	13.00	8.49	7.79	9.28
0.8456	101.15	29.98	12.67	8.35	7.67	9.10
0.8468	106.13	28.37	12.36	8.21	7.55	8.93
0.8480	107.44	26.92	12.07	8.08	7.44	8.77
0.8493	104.64	25.61	11.79	7.96	7.32	8.62
0.8505	98.61	24.41	11.52	7.84	7.22	8.46
0.8518	90.85	23.32	11.26	7.72	7.11	8.32
0.8530	82.67	22.32	11.02	7.61	7.01	8.18
0.8543	74.89	21.40	10.78	7.49	6.91	8.04
0.8555	67.86	20.55	10.56	7.39	6.81	7.91
0.8568	61.69	19.76	10.34	7.28	6.72	7.78
0.8580	56.32	19.04	10.13	7.18	6.63	7.66
0.8593	51.67	18.36	9.93	7.08	6.54	7.54
0.8605	47.64	17.73	9.74	6.99	6.45	7.42
0.8618	44.13	17.14	9.56	6.89	6.37	7.31
0.8631	41.06	16.58	9.38	6.80	6.29	7.20

Frequency (Hz)	1D PS-Logging	1D LR = 1.5	1D LR = 2.0	1D LR = 3.0	1D LR = 5.0	2D Mean Azimuth
0.8643	38.36	16.07	9.21	6.71	6.21	7.09
0.8656	35.97	15.58	9.05	6.63	6.13	6.99
0.8669	33.84	15.12	8.89	6.54	6.05	6.89
0.8681	31.94	14.69	8.73	6.46	5.98	6.79
0.8694	30.24	14.28	8.58	6.38	5.91	6.69
0.8707	28.70	13.89	8.44	6.30	5.84	6.60
0.8719	27.30	13.52	8.30	6.23	5.77	6.51
0.8732	26.03	13.17	8.17	6.15	5.70	6.42
0.8745	24.87	12.84	8.04	6.08	5.63	6.34
0.8758	23.81	12.53	7.91	6.01	5.57	6.25
0.8771	22.83	12.23	7.79	5.94	5.51	6.17
0.8784	21.93	11.94	7.67	5.87	5.45	6.09
0.8796	21.09	11.67	7.56	5.81	5.39	6.01
0.8809	20.32	11.41	7.45	5.74	5.33	5.94
0.8822	19.60	11.16	7.34	5.68	5.27	5.86
0.8835	18.93	10.92	7.24	5.62	5.21	5.79
0.8848	18.30	10.69	7.13	5.56	5.16	5.72
0.8861	17.71	10.47	7.03	5.50	5.11	5.65
0.8874	17.16	10.26	6.94	5.45	5.05	5.59
0.8887	16.64	10.06	6.84	5.39	5.00	5.52
0.8900	16.15	9.87	6.75	5.33	4.95	5.46
0.8913	15.69	9.68	6.67	5.28	4.90	5.39
0.8926	15.26	9.50	6.58	5.23	4.85	5.33
0.8939	14.85	9.33	6.50	5.18	4.81	5.27
0.8952	14.46	9.16	6.41	5.13	4.76	5.21
0.8965	14.09	9.00	6.33	5.08	4.71	5.16
0.8978	13.74	8.84	6.26	5.03	4.67	5.10
0.8992	13.40	8.69	6.18	4.98	4.63	5.04
0.9005	13.08	8.55	6.11	4.93	4.58	4.99
0.9018	12.78	8.41	6.03	4.89	4.54	4.94
0.9031	12.49	8.27	5.96	4.84	4.50	4.89
0.9044	12.21	8.14	5.89	4.80	4.46	4.83
0.9058	11.95	8.01	5.83	4.76	4.42	4.78
0.9071	11.69	7.89	5.76	4.71	4.38	4.74
0.9084	11.45	7.77	5.70	4.67	4.34	4.69
0.9097	11.22	7.65	5.64	4.63	4.31	4.64
0.9111	11.00	7.54	5.57	4.59	4.27	4.59
0.9124	10.78	7.43	5.51	4.55	4.23	4.55
0.9138	10.57	7.32	5.46	4.51	4.20	4.51
0.9151	10.38	7.22	5.40	4.48	4.16	4.46
0.9164	10.18	7.12	5.34	4.44	4.13	4.42
0.9178	10.00	7.02	5.29	4.40	4.09	4.38
0.9191	9.82	6.93	5.23	4.37	4.06	4.34
0.9205	9.65	6.84	5.18	4.33	4.03	4.30
0.9218	9.49	6.75	5.13	4.30	4.00	4.26
0.9232	9.33	6.66	5.08	4.26	3.96	4.22
0.9245	9.17	6.57	5.03	4.23	3.93	4.18
0.9259	9.02	6.49	4.98	4.20	3.90	4.14
0.9272	8.88	6.41	4.93	4.17	3.87	4.10
0.9286	8.74	6.33	4.89	4.13	3.84	4.07
0.9299	8.61	6.25	4.84	4.10	3.81	4.03
0.9313	8.47	6.18	4.80	4.07	3.79	4.00
0.9327	8.35	6.11	4.75	4.04	3.76	3.96
0.9340	8.22	6.04	4.71	4.01	3.73	3.93

Frequency (Hz)	1D PS-Logging	1D LR = 1.5	1D LR = 2.0	1D LR = 3.0	1D LR = 5.0	2D Mean Azimuth
0.9354	8.11	5.97	4.67	3.98	3.70	3.90
0.9368	7.99	5.90	4.63	3.95	3.68	3.86
0.9381	7.88	5.83	4.59	3.93	3.65	3.83
0.9395	7.77	5.77	4.55	3.90	3.62	3.80
0.9409	7.66	5.70	4.51	3.87	3.60	3.77
0.9423	7.56	5.64	4.47	3.84	3.57	3.74
0.9437	7.46	5.58	4.43	3.82	3.55	3.71
0.9450	7.36	5.52	4.39	3.79	3.52	3.68
0.9464	7.27	5.46	4.36	3.77	3.50	3.65
0.9478	7.17	5.41	4.32	3.74	3.48	3.62
0.9492	7.08	5.35	4.29	3.72	3.45	3.60
0.9506	7.00	5.30	4.25	3.69	3.43	3.57
0.9520	6.91	5.24	4.22	3.67	3.41	3.54
0.9534	6.83	5.19	4.18	3.64	3.38	3.52
0.9548	6.75	5.14	4.15	3.62	3.36	3.49
0.9562	6.67	5.09	4.12	3.60	3.34	3.46
0.9576	6.59	5.04	4.09	3.57	3.32	3.44
0.9590	6.51	4.99	4.06	3.55	3.30	3.41
0.9604	6.44	4.95	4.03	3.53	3.28	3.39
0.9618	6.37	4.90	4.00	3.51	3.26	3.37
0.9632	6.30	4.85	3.97	3.49	3.24	3.34
0.9646	6.23	4.81	3.94	3.47	3.22	3.32
0.9660	6.16	4.77	3.91	3.44	3.20	3.30
0.9674	6.10	4.72	3.88	3.42	3.18	3.27
0.9688	6.03	4.68	3.85	3.40	3.16	3.25
0.9703	5.97	4.64	3.83	3.38	3.14	3.23
0.9717	5.91	4.60	3.80	3.36	3.12	3.21
0.9731	5.85	4.56	3.77	3.35	3.10	3.19
0.9745	5.79	4.52	3.75	3.33	3.09	3.17
0.9760	5.73	4.48	3.72	3.31	3.07	3.15
0.9774	5.68	4.45	3.70	3.29	3.05	3.13
0.9788	5.62	4.41	3.67	3.27	3.03	3.11
0.9802	5.57	4.37	3.65	3.25	3.02	3.09
0.9817	5.52	4.34	3.62	3.23	3.00	3.07
0.9831	5.46	4.30	3.60	3.22	2.98	3.05
0.9846	5.41	4.27	3.57	3.20	2.97	3.04
0.9860	5.36	4.24	3.55	3.18	2.95	3.02
0.9874	5.32	4.20	3.53	3.17	2.93	3.00
0.9889	5.27	4.17	3.51	3.15	2.92	2.98
0.9903	5.22	4.14	3.48	3.13	2.90	2.97
0.9918	5.18	4.11	3.46	3.12	2.89	2.95
0.9932	5.13	4.08	3.44	3.10	2.87	2.93
0.9947	5.09	4.05	3.42	3.08	2.86	2.92
0.9962	5.04	4.02	3.40	3.07	2.84	2.90
0.9976	5.00	3.99	3.38	3.05	2.83	2.89
0.9991	4.96	3.96	3.36	3.04	2.81	2.87
1.0005	4.92	3.93	3.34	3.02	2.80	2.86
1.0020	4.88	3.90	3.32	3.01	2.78	2.84
1.0035	4.84	3.87	3.30	2.99	2.77	2.83
1.0049	4.80	3.85	3.28	2.98	2.76	2.81
1.0064	4.76	3.82	3.26	2.97	2.74	2.80
1.0079	4.72	3.79	3.24	2.95	2.73	2.78
1.0094	4.69	3.77	3.22	2.94	2.72	2.77
1.0108	4.65	3.74	3.21	2.92	2.70	2.76

Frequency (Hz)	1D PS-Logging	1D LR = 1.5	1D LR = 2.0	1D LR = 3.0	1D LR = 5.0	2D Mean Azimuth
1.0123	4.62	3.72	3.19	2.91	2.69	2.74
1.0138	4.58	3.69	3.17	2.90	2.68	2.73
1.0153	4.55	3.67	3.15	2.88	2.67	2.72
1.0168	4.51	3.64	3.14	2.87	2.65	2.70
1.0183	4.48	3.62	3.12	2.86	2.64	2.69
1.0198	4.45	3.60	3.10	2.85	2.63	2.68
1.0213	4.42	3.57	3.09	2.83	2.62	2.67
1.0227	4.39	3.55	3.07	2.82	2.61	2.66
1.0242	4.35	3.53	3.05	2.81	2.59	2.64
1.0257	4.32	3.51	3.04	2.80	2.58	2.63
1.0272	4.29	3.48	3.02	2.78	2.57	2.62
1.0288	4.27	3.46	3.01	2.77	2.56	2.61
1.0303	4.24	3.44	2.99	2.76	2.55	2.60
1.0318	4.21	3.42	2.98	2.75	2.54	2.59
1.0333	4.18	3.40	2.96	2.74	2.53	2.58
1.0348	4.15	3.38	2.95	2.73	2.52	2.57
1.0363	4.13	3.36	2.93	2.72	2.51	2.56
1.0378	4.10	3.34	2.92	2.71	2.49	2.55
1.0393	4.07	3.32	2.91	2.70	2.48	2.54
1.0409	4.05	3.30	2.89	2.68	2.47	2.53
1.0424	4.02	3.28	2.88	2.67	2.46	2.52
1.0439	4.00	3.27	2.86	2.66	2.45	2.51
1.0454	3.97	3.25	2.85	2.65	2.44	2.50
1.0470	3.95	3.23	2.84	2.64	2.43	2.49
1.0485	3.92	3.21	2.82	2.63	2.42	2.48
1.0500	3.90	3.19	2.81	2.62	2.41	2.47
1.0516	3.88	3.18	2.80	2.61	2.41	2.46
1.0531	3.85	3.16	2.79	2.60	2.40	2.45
1.0547	3.83	3.14	2.77	2.60	2.39	2.44
1.0562	3.81	3.13	2.76	2.59	2.38	2.43
1.0578	3.79	3.11	2.75	2.58	2.37	2.42
1.0593	3.77	3.09	2.74	2.57	2.36	2.42
1.0609	3.74	3.08	2.73	2.56	2.35	2.41
1.0624	3.72	3.06	2.71	2.55	2.34	2.40
1.0640	3.70	3.05	2.70	2.54	2.33	2.39
1.0655	3.68	3.03	2.69	2.53	2.33	2.38
1.0671	3.66	3.02	2.68	2.52	2.32	2.37
1.0686	3.64	3.00	2.67	2.52	2.31	2.37
1.0702	3.62	2.99	2.66	2.51	2.30	2.36
1.0718	3.60	2.97	2.65	2.50	2.29	2.35
1.0734	3.59	2.96	2.64	2.49	2.28	2.34
1.0749	3.57	2.94	2.63	2.48	2.28	2.34
1.0765	3.55	2.93	2.62	2.47	2.27	2.33
1.0781	3.53	2.92	2.61	2.47	2.26	2.32
1.0797	3.51	2.90	2.60	2.46	2.25	2.31
1.0812	3.49	2.89	2.59	2.45	2.25	2.31
1.0828	3.48	2.88	2.58	2.44	2.24	2.30
1.0844	3.46	2.86	2.57	2.44	2.23	2.29
1.0860	3.44	2.85	2.56	2.43	2.22	2.28
1.0876	3.43	2.84	2.55	2.42	2.22	2.28
1.0892	3.41	2.82	2.54	2.41	2.21	2.27
1.0908	3.39	2.81	2.53	2.41	2.20	2.26
1.0924	3.38	2.80	2.52	2.40	2.20	2.26
1.0940	3.36	2.79	2.51	2.39	2.19	2.25

Frequency (Hz)	1D PS-Logging	1D LR = 1.5	1D LR = 2.0	1D LR = 3.0	1D LR = 5.0	2D Mean Azimuth
1.0956	3.35	2.78	2.50	2.39	2.18	2.24
1.0972	3.33	2.76	2.49	2.38	2.17	2.23
1.0988	3.32	2.75	2.48	2.37	2.17	2.23
1.1004	3.30	2.74	2.47	2.37	2.16	2.22
1.1020	3.29	2.73	2.47	2.36	2.16	2.21
1.1036	3.27	2.72	2.46	2.35	2.15	2.21
1.1052	3.26	2.71	2.45	2.35	2.14	2.20
1.1069	3.24	2.70	2.44	2.34	2.14	2.19
1.1085	3.23	2.68	2.43	2.34	2.13	2.19
1.1101	3.22	2.67	2.42	2.33	2.12	2.18
1.1117	3.20	2.66	2.42	2.32	2.12	2.18
1.1133	3.19	2.65	2.41	2.32	2.11	2.17
1.1150	3.18	2.64	2.40	2.31	2.11	2.16
1.1166	3.16	2.63	2.39	2.31	2.10	2.16
1.1182	3.15	2.62	2.39	2.30	2.09	2.15
1.1199	3.14	2.61	2.38	2.30	2.09	2.14
1.1215	3.13	2.60	2.37	2.29	2.08	2.14
1.1232	3.11	2.59	2.36	2.28	2.08	2.13
1.1248	3.10	2.58	2.36	2.28	2.07	2.13
1.1265	3.09	2.57	2.35	2.27	2.07	2.12
1.1281	3.08	2.56	2.34	2.27	2.06	2.11
1.1298	3.07	2.55	2.34	2.26	2.06	2.11
1.1314	3.05	2.54	2.33	2.26	2.05	2.10
1.1331	3.04	2.54	2.32	2.25	2.05	2.10
1.1347	3.03	2.53	2.32	2.25	2.04	2.09
1.1364	3.02	2.52	2.31	2.24	2.04	2.08
1.1381	3.01	2.51	2.30	2.24	2.03	2.08
1.1397	3.00	2.50	2.30	2.23	2.03	2.07
1.1414	2.99	2.49	2.29	2.23	2.02	2.07
1.1431	2.98	2.48	2.28	2.23	2.02	2.06
1.1447	2.97	2.48	2.28	2.22	2.01	2.06
1.1464	2.96	2.47	2.27	2.22	2.01	2.05
1.1481	2.95	2.46	2.26	2.21	2.00	2.05
1.1498	2.94	2.45	2.26	2.21	2.00	2.04
1.1515	2.93	2.44	2.25	2.20	1.99	2.04
1.1531	2.92	2.44	2.25	2.20	1.99	2.03
1.1548	2.91	2.43	2.24	2.20	1.99	2.03
1.1565	2.90	2.42	2.24	2.19	1.98	2.02
1.1582	2.89	2.41	2.23	2.19	1.98	2.01
1.1599	2.88	2.41	2.22	2.18	1.97	2.01
1.1616	2.87	2.40	2.22	2.18	1.97	2.00
1.1633	2.86	2.39	2.21	2.18	1.96	2.00
1.1650	2.85	2.38	2.21	2.17	1.96	2.00
1.1667	2.84	2.38	2.20	2.17	1.96	1.99
1.1684	2.84	2.37	2.20	2.17	1.95	1.99
1.1701	2.83	2.36	2.19	2.16	1.95	1.98
1.1719	2.82	2.36	2.19	2.16	1.95	1.98
1.1736	2.81	2.35	2.18	2.16	1.94	1.97
1.1753	2.80	2.34	2.18	2.15	1.94	1.97
1.1770	2.80	2.34	2.17	2.15	1.93	1.96
1.1787	2.79	2.33	2.17	2.15	1.93	1.96
1.1805	2.78	2.32	2.16	2.14	1.93	1.95
1.1822	2.77	2.32	2.16	2.14	1.92	1.95
1.1839	2.76	2.31	2.16	2.14	1.92	1.95

Frequency (Hz)	1D PS-Logging	1D LR = 1.5	1D LR = 2.0	1D LR = 3.0	1D LR = 5.0	2D Mean Azimuth
1.1857	2.76	2.30	2.15	2.14	1.92	1.94
1.1874	2.75	2.30	2.15	2.13	1.91	1.94
1.1891	2.74	2.29	2.14	2.13	1.91	1.93
1.1909	2.74	2.29	2.14	2.13	1.91	1.93
1.1926	2.73	2.28	2.13	2.12	1.90	1.93
1.1944	2.72	2.28	2.13	2.12	1.90	1.92
1.1961	2.72	2.27	2.13	2.12	1.90	1.92
1.1979	2.71	2.26	2.12	2.12	1.90	1.92
1.1996	2.70	2.26	2.12	2.12	1.89	1.91
1.2014	2.70	2.25	2.11	2.11	1.89	1.91
1.2031	2.69	2.25	2.11	2.11	1.89	1.91
1.2049	2.68	2.24	2.11	2.11	1.88	1.90
1.2067	2.68	2.24	2.10	2.11	1.88	1.90
1.2084	2.67	2.23	2.10	2.10	1.88	1.90
1.2102	2.66	2.23	2.10	2.10	1.88	1.89
1.2120	2.66	2.22	2.09	2.10	1.87	1.89
1.2138	2.65	2.22	2.09	2.10	1.87	1.89
1.2155	2.65	2.21	2.09	2.10	1.87	1.89
1.2173	2.64	2.21	2.08	2.10	1.87	1.88
1.2191	2.64	2.20	2.08	2.09	1.86	1.88
1.2209	2.63	2.20	2.08	2.09	1.86	1.88
1.2227	2.63	2.19	2.07	2.09	1.86	1.88
1.2245	2.62	2.19	2.07	2.09	1.86	1.87
1.2263	2.62	2.18	2.07	2.09	1.86	1.87
1.2280	2.61	2.18	2.06	2.09	1.85	1.87
1.2298	2.61	2.18	2.06	2.09	1.85	1.87
1.2316	2.60	2.17	2.06	2.08	1.85	1.86
1.2335	2.60	2.17	2.06	2.08	1.85	1.86
1.2353	2.59	2.16	2.05	2.08	1.85	1.86
1.2371	2.59	2.16	2.05	2.08	1.84	1.86
1.2389	2.58	2.16	2.05	2.08	1.84	1.86
1.2407	2.58	2.15	2.05	2.08	1.84	1.86
1.2425	2.57	2.15	2.04	2.08	1.84	1.86
1.2443	2.57	2.14	2.04	2.08	1.84	1.85
1.2462	2.56	2.14	2.04	2.08	1.84	1.85
1.2480	2.56	2.14	2.04	2.08	1.83	1.85
1.2498	2.56	2.13	2.03	2.08	1.83	1.85
1.2516	2.55	2.13	2.03	2.08	1.83	1.85
1.2535	2.55	2.13	2.03	2.08	1.83	1.85
1.2553	2.54	2.12	2.03	2.07	1.83	1.85
1.2571	2.54	2.12	2.03	2.07	1.83	1.85
1.2590	2.54	2.12	2.02	2.07	1.83	1.85
1.2608	2.53	2.11	2.02	2.07	1.82	1.85
1.2627	2.53	2.11	2.02	2.07	1.82	1.85
1.2645	2.53	2.11	2.02	2.07	1.82	1.84
1.2664	2.52	2.10	2.02	2.07	1.82	1.84
1.2682	2.52	2.10	2.02	2.07	1.82	1.84
1.2701	2.52	2.10	2.01	2.07	1.82	1.84
1.2719	2.51	2.09	2.01	2.07	1.82	1.84
1.2738	2.51	2.09	2.01	2.08	1.82	1.84
1.2757	2.51	2.09	2.01	2.08	1.82	1.84
1.2775	2.51	2.09	2.01	2.08	1.82	1.84
1.2794	2.50	2.08	2.01	2.08	1.82	1.84
1.2813	2.50	2.08	2.01	2.08	1.81	1.84

Frequency (Hz)	1D PS-Logging	1D LR = 1.5	1D LR = 2.0	1D LR = 3.0	1D LR = 5.0	2D Mean Azimuth
1.2832	2.50	2.08	2.00	2.08	1.81	1.84
1.2850	2.50	2.08	2.00	2.08	1.81	1.84
1.2869	2.49	2.07	2.00	2.08	1.81	1.84
1.2888	2.49	2.07	2.00	2.08	1.81	1.85
1.2907	2.49	2.07	2.00	2.08	1.81	1.85
1.2926	2.49	2.07	2.00	2.08	1.81	1.85
1.2945	2.48	2.06	2.00	2.08	1.81	1.85
1.2964	2.48	2.06	2.00	2.08	1.81	1.85
1.2983	2.48	2.06	2.00	2.09	1.81	1.85
1.3002	2.48	2.06	2.00	2.09	1.81	1.85
1.3021	2.48	2.06	2.00	2.09	1.81	1.85
1.3040	2.48	2.05	2.00	2.09	1.81	1.85
1.3059	2.47	2.05	1.99	2.09	1.81	1.85
1.3078	2.47	2.05	1.99	2.09	1.81	1.85
1.3097	2.47	2.05	1.99	2.09	1.81	1.85
1.3116	2.47	2.05	1.99	2.10	1.81	1.86
1.3136	2.47	2.05	1.99	2.10	1.81	1.86
1.3155	2.47	2.04	1.99	2.10	1.81	1.86
1.3174	2.47	2.04	1.99	2.10	1.81	1.86
1.3193	2.47	2.04	1.99	2.10	1.81	1.86
1.3213	2.46	2.04	1.99	2.11	1.81	1.86
1.3232	2.46	2.04	1.99	2.11	1.81	1.86
1.3252	2.46	2.04	1.99	2.11	1.81	1.86
1.3271	2.46	2.04	1.99	2.11	1.82	1.87
1.3290	2.46	2.04	1.99	2.11	1.82	1.87
1.3310	2.46	2.03	1.99	2.12	1.82	1.87
1.3329	2.46	2.03	1.99	2.12	1.82	1.87
1.3349	2.46	2.03	1.99	2.12	1.82	1.87
1.3368	2.46	2.03	2.00	2.13	1.82	1.87
1.3388	2.46	2.03	2.00	2.13	1.82	1.88
1.3408	2.46	2.03	2.00	2.13	1.82	1.88
1.3427	2.46	2.03	2.00	2.13	1.82	1.88
1.3447	2.46	2.03	2.00	2.14	1.82	1.88
1.3467	2.46	2.03	2.00	2.14	1.82	1.88
1.3486	2.46	2.03	2.00	2.14	1.83	1.89
1.3506	2.46	2.03	2.00	2.15	1.83	1.89
1.3526	2.46	2.03	2.00	2.15	1.83	1.89
1.3546	2.46	2.03	2.00	2.15	1.83	1.89
1.3565	2.46	2.03	2.00	2.16	1.83	1.89
1.3585	2.46	2.03	2.00	2.16	1.83	1.90
1.3605	2.46	2.03	2.01	2.17	1.83	1.90
1.3625	2.46	2.03	2.01	2.17	1.84	1.90
1.3645	2.46	2.03	2.01	2.17	1.84	1.90
1.3665	2.46	2.03	2.01	2.18	1.84	1.91
1.3685	2.47	2.03	2.01	2.18	1.84	1.91
1.3705	2.47	2.03	2.01	2.19	1.84	1.91
1.3725	2.47	2.03	2.02	2.19	1.85	1.91
1.3745	2.47	2.03	2.02	2.20	1.85	1.92
1.3765	2.47	2.03	2.02	2.20	1.85	1.92
1.3786	2.47	2.03	2.02	2.21	1.85	1.92
1.3806	2.47	2.03	2.02	2.21	1.85	1.92
1.3826	2.48	2.03	2.02	2.22	1.86	1.93
1.3846	2.48	2.03	2.03	2.22	1.86	1.93
1.3867	2.48	2.03	2.03	2.23	1.86	1.93

Frequency (Hz)	1D PS-Logging	1D LR = 1.5	1D LR = 2.0	1D LR = 3.0	1D LR = 5.0	2D Mean Azimuth
1.3887	2.48	2.03	2.03	2.23	1.86	1.93
1.3907	2.48	2.03	2.03	2.24	1.87	1.94
1.3928	2.48	2.03	2.04	2.24	1.87	1.94
1.3948	2.49	2.03	2.04	2.25	1.87	1.94
1.3968	2.49	2.03	2.04	2.25	1.88	1.95
1.3989	2.49	2.03	2.04	2.26	1.88	1.95
1.4009	2.49	2.04	2.05	2.27	1.88	1.95
1.4030	2.50	2.04	2.05	2.27	1.88	1.96
1.4050	2.50	2.04	2.05	2.28	1.89	1.96
1.4071	2.50	2.04	2.06	2.29	1.89	1.96
1.4092	2.50	2.04	2.06	2.29	1.89	1.97
1.4112	2.51	2.04	2.06	2.30	1.90	1.97
1.4133	2.51	2.04	2.06	2.31	1.90	1.97
1.4154	2.51	2.05	2.07	2.31	1.90	1.98
1.4174	2.52	2.05	2.07	2.32	1.91	1.98
1.4195	2.52	2.05	2.07	2.33	1.91	1.98
1.4216	2.52	2.05	2.08	2.34	1.92	1.99
1.4237	2.53	2.05	2.08	2.34	1.92	1.99
1.4258	2.53	2.05	2.09	2.35	1.92	2.00
1.4278	2.53	2.06	2.09	2.36	1.93	2.00
1.4299	2.54	2.06	2.09	2.37	1.93	2.00
1.4320	2.54	2.06	2.10	2.38	1.94	2.01
1.4341	2.55	2.06	2.10	2.38	1.94	2.01
1.4362	2.55	2.06	2.11	2.39	1.94	2.02
1.4383	2.56	2.07	2.11	2.40	1.95	2.02
1.4404	2.56	2.07	2.11	2.41	1.95	2.03
1.4425	2.56	2.07	2.12	2.42	1.96	2.03
1.4447	2.57	2.07	2.12	2.43	1.96	2.04
1.4468	2.57	2.08	2.13	2.44	1.97	2.04
1.4489	2.58	2.08	2.13	2.45	1.97	2.05
1.4510	2.58	2.08	2.14	2.46	1.98	2.05
1.4531	2.59	2.09	2.14	2.47	1.98	2.06
1.4553	2.59	2.09	2.15	2.48	1.99	2.06
1.4574	2.60	2.09	2.15	2.49	1.99	2.07
1.4595	2.61	2.09	2.16	2.50	2.00	2.07
1.4617	2.61	2.10	2.17	2.51	2.01	2.08
1.4638	2.62	2.10	2.17	2.52	2.01	2.08
1.4660	2.62	2.10	2.18	2.54	2.02	2.09
1.4681	2.63	2.11	2.18	2.55	2.02	2.10
1.4703	2.64	2.11	2.19	2.56	2.03	2.10
1.4724	2.64	2.12	2.19	2.57	2.04	2.11
1.4746	2.65	2.12	2.20	2.59	2.04	2.11
1.4767	2.65	2.12	2.21	2.60	2.05	2.12
1.4789	2.66	2.13	2.21	2.61	2.06	2.13
1.4810	2.67	2.13	2.22	2.62	2.06	2.13
1.4832	2.68	2.14	2.23	2.64	2.07	2.14
1.4854	2.68	2.14	2.23	2.65	2.08	2.15
1.4876	2.69	2.14	2.24	2.67	2.08	2.16
1.4897	2.70	2.15	2.25	2.68	2.09	2.16
1.4919	2.71	2.15	2.26	2.70	2.10	2.17
1.4941	2.71	2.16	2.26	2.71	2.11	2.18
1.4963	2.72	2.16	2.27	2.73	2.11	2.18
1.4985	2.73	2.17	2.28	2.74	2.12	2.19
1.5007	2.74	2.17	2.29	2.76	2.13	2.20

Frequency (Hz)	1D PS-Logging	1D LR = 1.5	1D LR = 2.0	1D LR = 3.0	1D LR = 5.0	2D Mean Azimuth
1.5029	2.75	2.18	2.29	2.77	2.14	2.21
1.5051	2.76	2.18	2.30	2.79	2.15	2.22
1.5073	2.76	2.19	2.31	2.81	2.16	2.22
1.5095	2.77	2.19	2.32	2.83	2.16	2.23
1.5117	2.78	2.20	2.33	2.84	2.17	2.24
1.5139	2.79	2.20	2.34	2.86	2.18	2.25
1.5161	2.80	2.21	2.35	2.88	2.19	2.26
1.5184	2.81	2.22	2.36	2.90	2.20	2.27
1.5206	2.82	2.22	2.36	2.92	2.21	2.28
1.5228	2.83	2.23	2.37	2.94	2.22	2.29
1.5250	2.84	2.23	2.38	2.96	2.23	2.30
1.5273	2.85	2.24	2.39	2.98	2.24	2.31
1.5295	2.86	2.25	2.40	3.00	2.25	2.32
1.5317	2.88	2.25	2.42	3.03	2.26	2.33
1.5340	2.89	2.26	2.43	3.05	2.27	2.34
1.5362	2.90	2.27	2.44	3.07	2.28	2.35
1.5385	2.91	2.27	2.45	3.09	2.29	2.36
1.5407	2.92	2.28	2.46	3.12	2.31	2.37
1.5430	2.93	2.29	2.47	3.14	2.32	2.39
1.5453	2.95	2.30	2.48	3.17	2.33	2.40
1.5475	2.96	2.30	2.49	3.19	2.34	2.41
1.5498	2.97	2.31	2.51	3.22	2.35	2.42
1.5521	2.99	2.32	2.52	3.25	2.37	2.44
1.5543	3.00	2.33	2.53	3.28	2.38	2.45
1.5566	3.01	2.33	2.54	3.30	2.39	2.46
1.5589	3.03	2.34	2.56	3.33	2.41	2.48
1.5612	3.04	2.35	2.57	3.36	2.42	2.49
1.5635	3.06	2.36	2.58	3.39	2.43	2.50
1.5657	3.07	2.37	2.60	3.43	2.45	2.52
1.5680	3.09	2.38	2.61	3.46	2.46	2.53
1.5703	3.10	2.39	2.63	3.49	2.48	2.55
1.5726	3.12	2.40	2.64	3.53	2.49	2.57
1.5749	3.13	2.41	2.66	3.56	2.51	2.58
1.5772	3.15	2.41	2.67	3.60	2.52	2.60
1.5796	3.17	2.42	2.69	3.63	2.54	2.61
1.5819	3.18	2.43	2.71	3.67	2.56	2.63
1.5842	3.20	2.45	2.72	3.71	2.57	2.65
1.5865	3.22	2.46	2.74	3.75	2.59	2.67
1.5888	3.24	2.47	2.76	3.79	2.61	2.69
1.5912	3.26	2.48	2.77	3.84	2.63	2.70
1.5935	3.28	2.49	2.79	3.88	2.64	2.72
1.5958	3.29	2.50	2.81	3.93	2.66	2.74
1.5982	3.31	2.51	2.83	3.97	2.68	2.76
1.6005	3.33	2.52	2.85	4.02	2.70	2.78
1.6028	3.36	2.53	2.87	4.07	2.72	2.80
1.6052	3.38	2.55	2.89	4.12	2.74	2.82
1.6075	3.40	2.56	2.91	4.18	2.76	2.85
1.6099	3.42	2.57	2.93	4.23	2.78	2.87
1.6123	3.44	2.58	2.95	4.29	2.81	2.89
1.6146	3.47	2.60	2.97	4.34	2.83	2.91
1.6170	3.49	2.61	2.99	4.41	2.85	2.94
1.6193	3.51	2.62	3.02	4.47	2.88	2.96
1.6217	3.54	2.64	3.04	4.53	2.90	2.99
1.6241	3.56	2.65	3.06	4.60	2.92	3.01

Frequency (Hz)	1D PS-Logging	1D LR = 1.5	1D LR = 2.0	1D LR = 3.0	1D LR = 5.0	2D Mean Azimuth
1.6265	3.59	2.67	3.09	4.67	2.95	3.04
1.6289	3.61	2.68	3.11	4.74	2.98	3.06
1.6312	3.64	2.70	3.14	4.81	3.00	3.09
1.6336	3.67	2.71	3.17	4.89	3.03	3.12
1.6360	3.70	2.73	3.19	4.97	3.06	3.15
1.6384	3.72	2.74	3.22	5.06	3.09	3.18
1.6408	3.75	2.76	3.25	5.14	3.12	3.21
1.6432	3.78	2.78	3.28	5.23	3.15	3.24
1.6456	3.81	2.79	3.31	5.33	3.18	3.27
1.6480	3.85	2.81	3.34	5.42	3.21	3.30
1.6505	3.88	2.83	3.37	5.53	3.24	3.33
1.6529	3.91	2.85	3.40	5.63	3.28	3.37
1.6553	3.95	2.87	3.43	5.74	3.31	3.40
1.6577	3.98	2.88	3.47	5.86	3.35	3.44
1.6601	4.02	2.90	3.50	5.98	3.38	3.47
1.6626	4.05	2.92	3.54	6.11	3.42	3.51
1.6650	4.09	2.94	3.58	6.24	3.46	3.55
1.6674	4.13	2.96	3.61	6.38	3.50	3.59
1.6699	4.17	2.99	3.65	6.53	3.54	3.63
1.6723	4.21	3.01	3.69	6.69	3.58	3.67
1.6748	4.25	3.03	3.73	6.85	3.62	3.71
1.6772	4.29	3.05	3.77	7.02	3.67	3.76
1.6797	4.33	3.07	3.82	7.21	3.72	3.80
1.6822	4.38	3.10	3.86	7.40	3.76	3.85
1.6846	4.42	3.12	3.91	7.60	3.81	3.90
1.6871	4.47	3.15	3.96	7.82	3.86	3.95
1.6896	4.52	3.17	4.00	8.05	3.91	4.00
1.6920	4.57	3.20	4.05	8.30	3.97	4.05
1.6945	4.62	3.22	4.11	8.56	4.02	4.10
1.6970	4.67	3.25	4.16	8.84	4.08	4.16
1.6995	4.73	3.28	4.22	9.14	4.14	4.22
1.7020	4.78	3.31	4.27	9.46	4.20	4.28
1.7045	4.84	3.34	4.33	9.81	4.27	4.34
1.7069	4.90	3.36	4.39	10.18	4.33	4.41
1.7094	4.96	3.40	4.45	10.58	4.40	4.47
1.7120	5.02	3.43	4.52	11.02	4.47	4.54
1.7145	5.09	3.46	4.59	11.50	4.55	4.62
1.7170	5.16	3.49	4.66	12.02	4.63	4.69
1.7195	5.22	3.52	4.73	12.59	4.71	4.77
1.7220	5.30	3.56	4.80	13.21	4.79	4.85
1.7245	5.37	3.59	4.88	13.91	4.88	4.93
1.7271	5.45	3.63	4.96	14.67	4.97	5.02
1.7296	5.52	3.67	5.05	15.52	5.06	5.11
1.7321	5.61	3.71	5.13	16.48	5.16	5.21
1.7347	5.69	3.74	5.23	17.55	5.26	5.30
1.7372	5.78	3.78	5.32	18.76	5.37	5.41
1.7397	5.87	3.83	5.42	20.13	5.48	5.51
1.7423	5.96	3.87	5.52	21.69	5.60	5.63
1.7448	6.06	3.91	5.63	23.47	5.72	5.74
1.7474	6.16	3.96	5.74	25.51	5.85	5.87
1.7499	6.26	4.00	5.86	27.82	5.99	6.00
1.7525	6.37	4.05	5.98	30.44	6.13	6.13
1.7551	6.49	4.10	6.11	33.32	6.28	6.27
1.7576	6.60	4.15	6.24	36.37	6.44	6.42

Frequency (Hz)	1D PS-Logging	1D LR = 1.5	1D LR = 2.0	1D LR = 3.0	1D LR = 5.0	2D Mean Azimuth
1.7602	6.73	4.20	6.38	39.37	6.61	6.58
1.7628	6.85	4.26	6.53	41.93	6.78	6.74
1.7654	6.99	4.31	6.68	43.54	6.97	6.92
1.7680	7.13	4.37	6.85	43.79	7.17	7.10
1.7706	7.27	4.43	7.02	42.61	7.38	7.30
1.7732	7.43	4.49	7.20	40.28	7.61	7.50
1.7757	7.59	4.55	7.40	37.32	7.84	7.72
1.7783	7.75	4.62	7.60	34.17	8.10	7.96
1.7810	7.93	4.69	7.82	31.14	8.37	8.20
1.7836	8.11	4.75	8.05	28.35	8.67	8.47
1.7862	8.31	4.83	8.29	25.87	8.98	8.75
1.7888	8.51	4.90	8.55	23.69	9.32	9.05
1.7914	8.72	4.98	8.83	21.78	9.69	9.38
1.7940	8.95	5.06	9.13	20.11	10.09	9.72
1.7967	9.19	5.14	9.44	18.64	10.52	10.10
1.7993	9.44	5.23	9.79	17.36	10.99	10.51
1.8019	9.71	5.32	10.16	16.22	11.51	10.95
1.8046	10.00	5.41	10.56	15.21	12.07	11.42
1.8072	10.30	5.51	10.99	14.31	12.69	11.94
1.8099	10.62	5.61	11.46	13.50	13.38	12.51
1.8125	10.97	5.71	11.97	12.77	14.15	13.13
1.8152	11.33	5.82	12.53	12.11	15.00	13.82
1.8178	11.73	5.94	13.14	11.52	15.95	14.58
1.8205	12.15	6.06	13.82	10.97	17.02	15.42
1.8231	12.61	6.18	14.57	10.48	18.23	16.34
1.8258	13.10	6.31	15.40	10.02	19.60	17.38
1.8285	13.63	6.45	16.32	9.60	21.15	18.55
1.8312	14.21	6.59	17.36	9.21	22.92	19.85
1.8339	14.84	6.75	18.53	8.85	24.91	21.29
1.8365	15.53	6.90	19.85	8.52	27.14	22.90
1.8392	16.28	7.07	21.35	8.21	29.59	24.69
1.8419	17.11	7.24	23.06	7.92	32.18	26.65
1.8446	18.02	7.43	25.01	7.65	34.72	28.72
1.8473	19.03	7.62	27.23	7.39	36.94	30.86
1.8500	20.16	7.83	29.73	7.16	38.45	32.93
1.8527	21.43	8.05	32.53	6.93	38.90	34.75
1.8554	22.84	8.28	35.53	6.72	38.18	36.13
1.8582	24.44	8.52	38.59	6.52	36.46	36.92
1.8609	26.26	8.79	41.37	6.34	34.10	36.99
1.8636	28.32	9.06	43.43	6.16	31.47	36.24
1.8663	30.66	9.36	44.29	5.99	28.85	34.81
1.8691	33.33	9.68	43.72	5.83	26.39	32.91
1.8718	36.35	10.02	41.85	5.68	24.16	30.74
1.8746	39.71	10.39	39.14	5.54	22.17	28.48
1.8773	43.37	10.78	36.05	5.40	20.42	26.30
1.8800	47.15	11.21	32.95	5.27	18.88	24.27
1.8828	50.72	11.67	30.05	5.14	17.52	22.41
1.8856	53.56	12.17	27.43	5.02	16.33	20.75
1.8883	55.09	12.72	25.10	4.91	15.27	19.27
1.8911	54.92	13.32	23.06	4.80	14.32	17.96
1.8939	53.09	13.98	21.27	4.70	13.48	16.79
1.8966	50.03	14.70	19.71	4.60	12.72	15.74
1.8994	46.34	15.50	18.33	4.50	12.04	14.81
1.9022	42.51	16.39	17.11	4.41	11.42	13.98

Frequency (Hz)	1D PS-Logging	1D LR = 1.5	1D LR = 2.0	1D LR = 3.0	1D LR = 5.0	2D Mean Azimuth
1.9050	38.84	17.39	16.03	4.32	10.86	13.22
1.9078	35.48	18.50	15.07	4.23	10.35	12.54
1.9106	32.49	19.75	14.21	4.15	9.88	11.92
1.9134	29.85	21.17	13.44	4.07	9.45	11.36
1.9162	27.53	22.79	12.74	4.00	9.06	10.84
1.9190	25.49	24.62	12.11	3.92	8.69	10.37
1.9218	23.70	26.72	11.53	3.85	8.36	9.94
1.9246	22.11	29.11	11.00	3.78	8.04	9.54
1.9274	20.71	31.82	10.52	3.72	7.75	9.17
1.9302	19.46	34.85	10.08	3.65	7.48	8.82
1.9331	18.34	38.11	9.67	3.59	7.23	8.50
1.9359	17.34	41.44	9.29	3.53	6.99	8.20
1.9387	16.44	44.49	8.94	3.48	6.76	7.92
1.9416	15.62	46.76	8.61	3.42	6.55	7.66
1.9444	14.87	47.72	8.31	3.37	6.36	7.42
1.9473	14.19	47.11	8.02	3.31	6.17	7.19
1.9501	13.57	45.09	7.76	3.26	5.99	6.97
1.9530	12.99	42.14	7.51	3.21	5.83	6.76
1.9558	12.46	38.79	7.27	3.17	5.67	6.57
1.9587	11.98	35.44	7.05	3.12	5.52	6.38
1.9616	11.52	32.30	6.85	3.07	5.38	6.21
1.9644	11.10	29.47	6.65	3.03	5.24	6.05
1.9673	10.71	26.97	6.46	2.99	5.11	5.89
1.9702	10.35	24.77	6.29	2.95	4.99	5.74
1.9731	10.00	22.85	6.12	2.91	4.87	5.60
1.9760	9.68	21.17	5.96	2.87	4.76	5.46
1.9789	9.38	19.69	5.81	2.83	4.65	5.33
1.9818	9.10	18.39	5.67	2.79	4.55	5.20
1.9847	8.83	17.23	5.53	2.76	4.45	5.09
1.9876	8.58	16.20	5.40	2.72	4.36	4.97
1.9905	8.34	15.28	5.28	2.69	4.27	4.86
1.9934	8.12	14.45	5.16	2.65	4.18	4.76
1.9963	7.90	13.70	5.05	2.62	4.10	4.66
1.9992	7.70	13.02	4.94	2.59	4.02	4.56
2.0022	7.51	12.41	4.84	2.56	3.94	4.47
2.0051	7.33	11.84	4.74	2.53	3.87	4.38
2.0080	7.15	11.33	4.64	2.50	3.80	4.30
2.0110	6.99	10.85	4.55	2.47	3.73	4.22
2.0139	6.83	10.41	4.46	2.44	3.66	4.14
2.0169	6.68	10.01	4.37	2.42	3.60	4.06
2.0198	6.53	9.63	4.29	2.39	3.54	3.99
2.0228	6.39	9.28	4.21	2.36	3.48	3.92
2.0257	6.26	8.96	4.14	2.34	3.42	3.85
2.0287	6.13	8.66	4.06	2.31	3.36	3.79
2.0317	6.01	8.37	3.99	2.29	3.31	3.73
2.0347	5.89	8.10	3.93	2.26	3.26	3.66
2.0376	5.78	7.85	3.86	2.24	3.21	3.61
2.0406	5.67	7.62	3.80	2.22	3.16	3.55
2.0436	5.57	7.40	3.74	2.20	3.11	3.49
2.0466	5.47	7.19	3.68	2.18	3.07	3.44
2.0496	5.37	6.99	3.62	2.15	3.02	3.39
2.0526	5.28	6.80	3.56	2.13	2.98	3.34
2.0556	5.19	6.62	3.51	2.11	2.94	3.29
2.0586	5.10	6.45	3.46	2.09	2.89	3.24

Frequency (Hz)	1D PS-Logging	1D LR = 1.5	1D LR = 2.0	1D LR = 3.0	1D LR = 5.0	2D Mean Azimuth
2.0616	5.02	6.29	3.40	2.07	2.86	3.20
2.0646	4.94	6.14	3.36	2.05	2.82	3.15
2.0677	4.86	6.00	3.31	2.04	2.78	3.11
2.0707	4.78	5.86	3.26	2.02	2.74	3.07
2.0737	4.71	5.72	3.22	2.00	2.71	3.03
2.0768	4.64	5.60	3.17	1.98	2.67	2.99
2.0798	4.57	5.48	3.13	1.96	2.64	2.95
2.0829	4.50	5.36	3.09	1.95	2.61	2.91
2.0859	4.44	5.25	3.05	1.93	2.57	2.88
2.0890	4.38	5.14	3.01	1.92	2.54	2.84
2.0920	4.32	5.04	2.97	1.90	2.51	2.81
2.0951	4.26	4.94	2.93	1.88	2.48	2.77
2.0982	4.20	4.85	2.90	1.87	2.45	2.74
2.1012	4.14	4.76	2.86	1.85	2.43	2.71
2.1043	4.09	4.67	2.83	1.84	2.40	2.68
2.1074	4.04	4.59	2.80	1.83	2.37	2.65
2.1105	3.99	4.51	2.76	1.81	2.35	2.62
2.1136	3.94	4.43	2.73	1.80	2.32	2.59
2.1167	3.89	4.35	2.70	1.78	2.30	2.56
2.1198	3.84	4.28	2.67	1.77	2.27	2.54
2.1229	3.80	4.21	2.64	1.76	2.25	2.51
2.1260	3.75	4.14	2.61	1.74	2.23	2.48
2.1291	3.71	4.08	2.59	1.73	2.20	2.46
2.1322	3.67	4.01	2.56	1.72	2.18	2.43
2.1353	3.63	3.95	2.53	1.71	2.16	2.41
2.1385	3.59	3.89	2.51	1.70	2.14	2.39
2.1416	3.55	3.83	2.48	1.68	2.12	2.36
2.1447	3.51	3.78	2.46	1.67	2.10	2.34
2.1479	3.48	3.72	2.43	1.66	2.08	2.32
2.1510	3.44	3.67	2.41	1.65	2.06	2.30
2.1542	3.40	3.62	2.39	1.64	2.04	2.28
2.1573	3.37	3.57	2.36	1.63	2.02	2.26
2.1605	3.34	3.52	2.34	1.62	2.00	2.24
2.1636	3.30	3.48	2.32	1.61	1.99	2.22
2.1668	3.27	3.43	2.30	1.60	1.97	2.20
2.1700	3.24	3.39	2.28	1.59	1.95	2.18
2.1732	3.21	3.34	2.26	1.58	1.94	2.16
2.1763	3.18	3.30	2.24	1.57	1.92	2.14
2.1795	3.15	3.26	2.22	1.56	1.90	2.12
2.1827	3.13	3.22	2.20	1.55	1.89	2.11
2.1859	3.10	3.19	2.18	1.54	1.87	2.09
2.1891	3.07	3.15	2.16	1.53	1.86	2.07
2.1923	3.05	3.11	2.15	1.53	1.84	2.06
2.1955	3.02	3.08	2.13	1.52	1.83	2.04
2.1987	2.99	3.04	2.11	1.51	1.81	2.03
2.2020	2.97	3.01	2.10	1.50	1.80	2.01
2.2052	2.95	2.98	2.08	1.49	1.79	2.00
2.2084	2.92	2.94	2.06	1.48	1.77	1.98
2.2117	2.90	2.91	2.05	1.48	1.76	1.97
2.2149	2.88	2.88	2.03	1.47	1.75	1.96
2.2181	2.86	2.85	2.02	1.46	1.74	1.94
2.2214	2.83	2.82	2.00	1.45	1.72	1.93
2.2246	2.81	2.80	1.99	1.45	1.71	1.92
2.2279	2.79	2.77	1.97	1.44	1.70	1.91

Frequency (Hz)	1D PS-Logging	1D LR = 1.5	1D LR = 2.0	1D LR = 3.0	1D LR = 5.0	2D Mean Azimuth
2.2312	2.77	2.74	1.96	1.43	1.69	1.89
2.2344	2.75	2.72	1.95	1.43	1.68	1.88
2.2377	2.73	2.69	1.93	1.42	1.67	1.87
2.2410	2.72	2.67	1.92	1.41	1.66	1.86
2.2443	2.70	2.64	1.91	1.41	1.65	1.85
2.2476	2.68	2.62	1.90	1.40	1.63	1.84
2.2508	2.66	2.59	1.88	1.40	1.62	1.83
2.2541	2.64	2.57	1.87	1.39	1.61	1.82
2.2574	2.63	2.55	1.86	1.38	1.60	1.81
2.2607	2.61	2.53	1.85	1.38	1.60	1.80
2.2641	2.60	2.51	1.84	1.37	1.59	1.79
2.2674	2.58	2.49	1.83	1.37	1.58	1.78
2.2707	2.56	2.47	1.82	1.36	1.57	1.77
2.2740	2.55	2.45	1.81	1.36	1.56	1.76
2.2773	2.53	2.43	1.80	1.35	1.55	1.75
2.2807	2.52	2.41	1.79	1.35	1.54	1.74
2.2840	2.51	2.39	1.78	1.34	1.53	1.73
2.2874	2.49	2.37	1.77	1.34	1.52	1.72
2.2907	2.48	2.35	1.76	1.33	1.52	1.72
2.2941	2.47	2.34	1.75	1.33	1.51	1.71
2.2974	2.45	2.32	1.74	1.32	1.50	1.70
2.3008	2.44	2.30	1.73	1.32	1.49	1.69
2.3042	2.43	2.29	1.72	1.31	1.49	1.68
2.3075	2.42	2.27	1.71	1.31	1.48	1.68
2.3109	2.40	2.25	1.70	1.30	1.47	1.67
2.3143	2.39	2.24	1.70	1.30	1.46	1.66
2.3177	2.38	2.22	1.69	1.30	1.46	1.65
2.3211	2.37	2.21	1.68	1.29	1.45	1.65
2.3245	2.36	2.20	1.67	1.29	1.44	1.64
2.3279	2.35	2.18	1.66	1.28	1.44	1.63
2.3313	2.34	2.17	1.66	1.28	1.43	1.63
2.3347	2.33	2.16	1.65	1.28	1.43	1.62
2.3381	2.32	2.14	1.64	1.27	1.42	1.61
2.3416	2.31	2.13	1.64	1.27	1.41	1.61
2.3450	2.30	2.12	1.63	1.27	1.41	1.60
2.3484	2.29	2.10	1.62	1.26	1.40	1.60
2.3519	2.28	2.09	1.62	1.26	1.40	1.59
2.3553	2.28	2.08	1.61	1.26	1.39	1.58
2.3588	2.27	2.07	1.60	1.26	1.39	1.58
2.3622	2.26	2.06	1.60	1.25	1.38	1.57
2.3657	2.25	2.05	1.59	1.25	1.38	1.57
2.3691	2.24	2.04	1.59	1.25	1.37	1.56
2.3726	2.24	2.03	1.58	1.24	1.37	1.56
2.3761	2.23	2.02	1.58	1.24	1.36	1.55
2.3796	2.22	2.01	1.57	1.24	1.36	1.55
2.3830	2.22	2.00	1.57	1.24	1.35	1.54
2.3865	2.21	1.99	1.56	1.23	1.35	1.54
2.3900	2.20	1.98	1.56	1.23	1.34	1.54
2.3935	2.20	1.97	1.55	1.23	1.34	1.53
2.3970	2.19	1.96	1.55	1.23	1.34	1.53
2.4005	2.18	1.95	1.54	1.23	1.33	1.52
2.4041	2.18	1.94	1.54	1.22	1.33	1.52
2.4076	2.17	1.93	1.53	1.22	1.32	1.52
2.4111	2.17	1.92	1.53	1.22	1.32	1.51

Frequency (Hz)	1D PS-Logging	1D LR = 1.5	1D LR = 2.0	1D LR = 3.0	1D LR = 5.0	2D Mean Azimuth
2.4146	2.16	1.92	1.53	1.22	1.32	1.51
2.4182	2.16	1.91	1.52	1.22	1.31	1.51
2.4217	2.15	1.90	1.52	1.22	1.31	1.50
2.4253	2.15	1.89	1.51	1.22	1.31	1.50
2.4288	2.14	1.89	1.51	1.21	1.30	1.50
2.4324	2.14	1.88	1.51	1.21	1.30	1.50
2.4359	2.14	1.87	1.50	1.21	1.30	1.49
2.4395	2.13	1.87	1.50	1.21	1.29	1.49
2.4431	2.13	1.86	1.50	1.21	1.29	1.49
2.4467	2.13	1.85	1.50	1.21	1.29	1.49
2.4502	2.12	1.85	1.49	1.21	1.29	1.49
2.4538	2.12	1.84	1.49	1.21	1.28	1.48
2.4574	2.12	1.84	1.49	1.21	1.28	1.48
2.4610	2.11	1.83	1.49	1.21	1.28	1.48
2.4646	2.11	1.82	1.48	1.21	1.28	1.48
2.4682	2.11	1.82	1.48	1.20	1.27	1.48
2.4719	2.11	1.81	1.48	1.20	1.27	1.48
2.4755	2.10	1.81	1.48	1.20	1.27	1.48
2.4791	2.10	1.80	1.47	1.20	1.27	1.48
2.4827	2.10	1.80	1.47	1.20	1.27	1.47
2.4864	2.10	1.79	1.47	1.20	1.27	1.47
2.4900	2.10	1.79	1.47	1.20	1.26	1.47
2.4937	2.10	1.79	1.47	1.20	1.26	1.47
2.4973	2.10	1.78	1.47	1.20	1.26	1.47
2.5010	2.10	1.78	1.47	1.20	1.26	1.47
2.5046	2.09	1.77	1.47	1.20	1.26	1.47
2.5083	2.09	1.77	1.46	1.21	1.26	1.47
2.5120	2.09	1.77	1.46	1.21	1.26	1.47
2.5156	2.09	1.76	1.46	1.21	1.26	1.47
2.5193	2.09	1.76	1.46	1.21	1.25	1.47
2.5230	2.09	1.76	1.46	1.21	1.25	1.47
2.5267	2.09	1.75	1.46	1.21	1.25	1.47
2.5304	2.10	1.75	1.46	1.21	1.25	1.47
2.5341	2.10	1.75	1.46	1.21	1.25	1.47
2.5378	2.10	1.75	1.46	1.21	1.25	1.47
2.5415	2.10	1.74	1.46	1.21	1.25	1.47
2.5453	2.10	1.74	1.46	1.21	1.25	1.47
2.5490	2.10	1.74	1.46	1.22	1.25	1.48
2.5527	2.10	1.74	1.46	1.22	1.25	1.48
2.5565	2.10	1.74	1.46	1.22	1.25	1.48
2.5602	2.11	1.73	1.46	1.22	1.25	1.48
2.5640	2.11	1.73	1.46	1.22	1.25	1.48
2.5677	2.11	1.73	1.47	1.22	1.25	1.48
2.5715	2.11	1.73	1.47	1.23	1.25	1.48
2.5752	2.12	1.73	1.47	1.23	1.25	1.49
2.5790	2.12	1.73	1.47	1.23	1.25	1.49
2.5828	2.12	1.73	1.47	1.23	1.25	1.49
2.5866	2.13	1.73	1.47	1.24	1.25	1.49
2.5904	2.13	1.73	1.47	1.24	1.26	1.50
2.5942	2.13	1.73	1.48	1.24	1.26	1.50
2.5980	2.14	1.72	1.48	1.24	1.26	1.50
2.6018	2.14	1.72	1.48	1.25	1.26	1.50
2.6056	2.15	1.72	1.48	1.25	1.26	1.51
2.6094	2.15	1.72	1.48	1.25	1.26	1.51

Frequency (Hz)	1D PS-Logging	1D LR = 1.5	1D LR = 2.0	1D LR = 3.0	1D LR = 5.0	2D Mean Azimuth
2.6132	2.16	1.73	1.49	1.26	1.26	1.52
2.6170	2.16	1.73	1.49	1.26	1.26	1.52
2.6209	2.17	1.73	1.49	1.26	1.27	1.52
2.6247	2.17	1.73	1.50	1.27	1.27	1.53
2.6286	2.18	1.73	1.50	1.27	1.27	1.53
2.6324	2.19	1.73	1.50	1.27	1.27	1.54
2.6363	2.19	1.73	1.51	1.28	1.27	1.54
2.6401	2.20	1.73	1.51	1.28	1.28	1.55
2.6440	2.21	1.73	1.51	1.29	1.28	1.55
2.6479	2.21	1.73	1.52	1.29	1.28	1.56
2.6517	2.22	1.74	1.52	1.29	1.28	1.56
2.6556	2.23	1.74	1.52	1.30	1.29	1.57
2.6595	2.24	1.74	1.53	1.30	1.29	1.57
2.6634	2.24	1.74	1.53	1.31	1.29	1.58
2.6673	2.25	1.75	1.54	1.31	1.30	1.59
2.6712	2.26	1.75	1.54	1.32	1.30	1.59
2.6751	2.27	1.75	1.55	1.32	1.30	1.60
2.6790	2.28	1.75	1.55	1.33	1.30	1.61
2.6830	2.29	1.76	1.56	1.33	1.31	1.61
2.6869	2.30	1.76	1.56	1.34	1.31	1.62
2.6908	2.31	1.76	1.57	1.35	1.32	1.63
2.6948	2.32	1.77	1.58	1.35	1.32	1.64
2.6987	2.33	1.77	1.58	1.36	1.32	1.64
2.7027	2.34	1.77	1.59	1.36	1.33	1.65
2.7066	2.36	1.78	1.60	1.37	1.33	1.66
2.7106	2.37	1.78	1.60	1.38	1.34	1.67
2.7146	2.38	1.79	1.61	1.38	1.34	1.68
2.7185	2.39	1.79	1.62	1.39	1.35	1.69
2.7225	2.41	1.80	1.62	1.40	1.35	1.70
2.7265	2.42	1.80	1.63	1.41	1.36	1.71
2.7305	2.43	1.81	1.64	1.41	1.36	1.72
2.7345	2.45	1.81	1.65	1.42	1.37	1.73
2.7385	2.46	1.82	1.66	1.43	1.37	1.74
2.7425	2.48	1.82	1.67	1.44	1.38	1.75
2.7465	2.49	1.83	1.68	1.45	1.39	1.76
2.7505	2.51	1.84	1.68	1.45	1.39	1.78
2.7546	2.53	1.84	1.69	1.46	1.40	1.79
2.7586	2.54	1.85	1.70	1.47	1.40	1.80
2.7627	2.56	1.86	1.71	1.48	1.41	1.81
2.7667	2.58	1.86	1.73	1.49	1.42	1.83
2.7707	2.60	1.87	1.74	1.50	1.43	1.84
2.7748	2.62	1.88	1.75	1.51	1.43	1.86
2.7789	2.64	1.89	1.76	1.52	1.44	1.87
2.7829	2.66	1.90	1.77	1.53	1.45	1.89
2.7870	2.68	1.90	1.78	1.54	1.46	1.90
2.7911	2.70	1.91	1.80	1.55	1.46	1.92
2.7952	2.72	1.92	1.81	1.57	1.47	1.94
2.7993	2.75	1.93	1.82	1.58	1.48	1.95
2.8034	2.77	1.94	1.84	1.59	1.49	1.97
2.8075	2.80	1.95	1.85	1.60	1.50	1.99
2.8116	2.82	1.96	1.86	1.62	1.51	2.01
2.8157	2.85	1.97	1.88	1.63	1.52	2.03
2.8198	2.88	1.98	1.89	1.64	1.53	2.05
2.8240	2.90	1.99	1.91	1.66	1.54	2.07

Frequency (Hz)	1D PS-Logging	1D LR = 1.5	1D LR = 2.0	1D LR = 3.0	1D LR = 5.0	2D Mean Azimuth
2.8281	2.93	2.01	1.93	1.67	1.55	2.09
2.8322	2.96	2.02	1.94	1.69	1.56	2.12
2.8364	2.99	2.03	1.96	1.70	1.57	2.14
2.8405	3.02	2.04	1.98	1.72	1.58	2.16
2.8447	3.06	2.05	2.00	1.73	1.60	2.19
2.8489	3.09	2.07	2.02	1.75	1.61	2.21
2.8530	3.12	2.08	2.04	1.77	1.62	2.24
2.8572	3.16	2.10	2.06	1.78	1.63	2.27
2.8614	3.20	2.11	2.08	1.80	1.65	2.30
2.8656	3.24	2.13	2.10	1.82	1.66	2.33
2.8698	3.28	2.14	2.12	1.84	1.68	2.36
2.8740	3.32	2.16	2.15	1.86	1.69	2.39
2.8782	3.36	2.17	2.17	1.88	1.71	2.42
2.8824	3.40	2.19	2.20	1.90	1.72	2.46
2.8866	3.45	2.21	2.22	1.92	1.74	2.49
2.8909	3.50	2.22	2.25	1.94	1.75	2.53
2.8951	3.54	2.24	2.28	1.97	1.77	2.57
2.8993	3.60	2.26	2.31	1.99	1.79	2.61
2.9036	3.65	2.28	2.34	2.01	1.81	2.65
2.9078	3.70	2.30	2.37	2.04	1.82	2.69
2.9121	3.76	2.32	2.40	2.07	1.84	2.74
2.9164	3.82	2.34	2.43	2.09	1.86	2.78
2.9206	3.88	2.37	2.47	2.12	1.88	2.83
2.9249	3.94	2.39	2.50	2.15	1.90	2.89
2.9292	4.01	2.41	2.54	2.18	1.93	2.94
2.9335	4.08	2.44	2.58	2.21	1.95	3.00
2.9378	4.15	2.46	2.62	2.24	1.97	3.05
2.9421	4.23	2.49	2.66	2.27	2.00	3.12
2.9464	4.30	2.51	2.71	2.31	2.02	3.18
2.9507	4.39	2.54	2.75	2.34	2.05	3.25
2.9550	4.47	2.57	2.80	2.38	2.07	3.32
2.9594	4.56	2.60	2.85	2.42	2.10	3.40
2.9637	4.66	2.63	2.90	2.45	2.13	3.47
2.9680	4.75	2.66	2.95	2.50	2.16	3.56
2.9724	4.86	2.69	3.01	2.54	2.19	3.64
2.9767	4.97	2.72	3.07	2.58	2.22	3.74
2.9811	5.08	2.76	3.13	2.63	2.25	3.83
2.9855	5.20	2.79	3.20	2.68	2.29	3.94
2.9898	5.33	2.83	3.26	2.72	2.32	4.05
2.9942	5.46	2.87	3.34	2.78	2.36	4.16
2.9986	5.60	2.91	3.41	2.83	2.40	4.29
3.0030	5.75	2.95	3.49	2.89	2.44	4.42
3.0074	5.91	2.99	3.58	2.95	2.48	4.56
3.0118	6.08	3.04	3.66	3.01	2.52	4.71
3.0162	6.25	3.08	3.76	3.07	2.57	4.87
3.0206	6.44	3.13	3.86	3.14	2.61	5.04
3.0250	6.64	3.18	3.96	3.21	2.66	5.22
3.0295	6.86	3.23	4.07	3.28	2.71	5.42
3.0339	7.09	3.29	4.19	3.36	2.77	5.63
3.0384	7.33	3.34	4.32	3.44	2.82	5.86
3.0428	7.60	3.40	4.45	3.53	2.88	6.11
3.0473	7.88	3.46	4.60	3.62	2.94	6.38
3.0517	8.19	3.53	4.75	3.71	3.01	6.67
3.0562	8.53	3.59	4.92	3.82	3.08	6.98

Frequency (Hz)	1D PS-Logging	1D LR = 1.5	1D LR = 2.0	1D LR = 3.0	1D LR = 5.0	2D Mean Azimuth
3.0607	8.89	3.66	5.09	3.92	3.15	7.33
3.0652	9.28	3.74	5.29	4.04	3.22	7.70
3.0696	9.71	3.81	5.50	4.16	3.30	8.11
3.0741	10.18	3.89	5.72	4.28	3.38	8.56
3.0786	10.69	3.97	5.97	4.42	3.47	9.05
3.0831	11.26	4.06	6.24	4.56	3.57	9.57
3.0877	11.89	4.15	6.53	4.72	3.67	10.14
3.0922	12.59	4.25	6.85	4.88	3.77	10.75
3.0967	13.38	4.35	7.21	5.06	3.88	11.38
3.1013	14.25	4.46	7.61	5.25	4.00	12.04
3.1058	15.24	4.58	8.05	5.46	4.13	12.70
3.1103	16.35	4.70	8.54	5.68	4.26	13.33
3.1149	17.60	4.82	9.10	5.92	4.41	13.89
3.1195	19.02	4.96	9.72	6.18	4.56	14.35
3.1240	20.62	5.10	10.43	6.47	4.73	14.66
3.1286	22.41	5.25	11.24	6.78	4.91	14.80
3.1332	24.38	5.42	12.17	7.12	5.11	14.75
3.1378	26.48	5.59	13.24	7.50	5.32	14.54
3.1424	28.62	5.77	14.45	7.92	5.55	14.19
3.1470	30.61	5.97	15.84	8.38	5.81	13.75
3.1516	32.16	6.18	17.39	8.90	6.08	13.25
3.1562	33.00	6.41	19.07	9.48	6.38	12.74
3.1608	32.93	6.66	20.77	10.13	6.72	12.23
3.1654	31.97	6.93	22.30	10.86	7.09	11.72
3.1701	30.34	7.22	23.38	11.69	7.50	11.22
3.1747	28.31	7.53	23.73	12.64	7.97	10.69
3.1794	26.17	7.88	23.25	13.73	8.49	10.15
3.1840	24.08	8.26	22.08	14.96	9.08	9.59
3.1887	22.13	8.67	20.48	16.36	9.74	9.03
3.1934	20.37	9.13	18.75	17.93	10.50	8.51
3.1980	18.80	9.64	17.06	19.64	11.38	8.01
3.2027	17.41	10.20	15.51	21.40	12.38	7.56
3.2074	16.17	10.83	14.12	23.07	13.54	7.15
3.2121	15.08	11.54	12.91	24.40	14.87	6.78
3.2168	14.12	12.34	11.85	25.12	16.37	6.44
3.2215	13.26	13.25	10.93	25.05	18.02	6.13
3.2262	12.49	14.28	10.13	24.22	19.75	5.85
3.2310	11.80	15.46	9.42	22.83	21.37	5.59
3.2357	11.18	16.81	8.80	21.16	22.61	5.35
3.2404	10.62	18.35	8.25	19.44	23.17	5.14
3.2452	10.11	20.09	7.76	17.79	22.89	4.94
3.2499	9.65	22.03	7.32	16.29	21.84	4.75
3.2547	9.22	24.11	6.93	14.95	20.30	4.58
3.2595	8.84	26.21	6.57	13.77	18.58	4.42
3.2642	8.48	28.08	6.25	12.73	16.88	4.27
3.2690	8.15	29.39	5.96	11.82	15.32	4.13
3.2738	7.85	29.83	5.69	11.02	13.93	4.00
3.2786	7.57	29.27	5.45	10.32	12.71	3.88
3.2834	7.31	27.87	5.22	9.69	11.65	3.77
3.2882	7.06	25.95	5.02	9.14	10.73	3.67
3.2930	6.84	23.84	4.82	8.64	9.93	3.57
3.2979	6.62	21.77	4.65	8.19	9.23	3.47
3.3027	6.42	19.85	4.48	7.79	8.62	3.38
3.3075	6.24	18.13	4.33	7.43	8.08	3.30

Frequency (Hz)	1D PS-Logging	1D LR = 1.5	1D LR = 2.0	1D LR = 3.0	1D LR = 5.0	2D Mean Azimuth
3.3124	6.06	16.62	4.19	7.10	7.59	3.22
3.3172	5.90	15.29	4.05	6.79	7.16	3.15
3.3221	5.74	14.13	3.93	6.52	6.78	3.07
3.3269	5.60	13.11	3.81	6.26	6.43	3.00
3.3318	5.46	12.22	3.70	6.03	6.12	2.94
3.3367	5.33	11.43	3.59	5.81	5.83	2.88
3.3416	5.20	10.73	3.49	5.61	5.57	2.82
3.3465	5.09	10.11	3.40	5.43	5.33	2.76
3.3514	4.97	9.55	3.31	5.26	5.11	2.70
3.3563	4.87	9.05	3.23	5.10	4.91	2.65
3.3612	4.77	8.60	3.15	4.95	4.73	2.60
3.3661	4.67	8.19	3.08	4.81	4.56	2.55
3.3710	4.58	7.82	3.00	4.68	4.40	2.50
3.3760	4.49	7.48	2.94	4.55	4.25	2.46
3.3809	4.41	7.17	2.87	4.44	4.11	2.41
3.3859	4.33	6.88	2.81	4.33	3.98	2.37
3.3908	4.25	6.62	2.75	4.23	3.86	2.33
3.3958	4.18	6.37	2.69	4.13	3.74	2.29
3.4008	4.11	6.14	2.64	4.04	3.64	2.25
3.4058	4.04	5.93	2.59	3.95	3.54	2.22
3.4107	3.98	5.74	2.54	3.87	3.44	2.18
3.4157	3.92	5.56	2.49	3.79	3.35	2.15
3.4207	3.86	5.38	2.45	3.72	3.27	2.12
3.4258	3.80	5.22	2.40	3.65	3.19	2.08
3.4308	3.75	5.07	2.36	3.58	3.11	2.05
3.4358	3.69	4.93	2.32	3.52	3.04	2.03
3.4408	3.64	4.80	2.28	3.46	2.97	2.00
3.4459	3.60	4.68	2.25	3.40	2.91	1.97
3.4509	3.55	4.56	2.21	3.35	2.84	1.94
3.4560	3.51	4.44	2.18	3.30	2.78	1.92
3.4610	3.46	4.34	2.15	3.25	2.73	1.90
3.4661	3.42	4.24	2.11	3.20	2.67	1.87
3.4712	3.38	4.14	2.08	3.16	2.62	1.85
3.4763	3.34	4.05	2.05	3.11	2.57	1.83
3.4813	3.31	3.97	2.03	3.07	2.53	1.81
3.4864	3.27	3.88	2.00	3.03	2.48	1.79
3.4916	3.24	3.81	1.97	2.99	2.44	1.77
3.4967	3.20	3.73	1.95	2.96	2.40	1.75
3.5018	3.17	3.66	1.92	2.93	2.36	1.73
3.5069	3.14	3.59	1.90	2.89	2.32	1.72
3.5121	3.11	3.53	1.87	2.86	2.28	1.70
3.5172	3.09	3.47	1.85	2.83	2.25	1.68
3.5223	3.06	3.41	1.83	2.80	2.21	1.67
3.5275	3.03	3.35	1.81	2.78	2.18	1.65
3.5327	3.01	3.30	1.79	2.75	2.15	1.64
3.5378	2.98	3.25	1.77	2.73	2.12	1.62
3.5430	2.96	3.20	1.75	2.70	2.09	1.61
3.5482	2.94	3.15	1.73	2.68	2.06	1.60
3.5534	2.92	3.10	1.72	2.66	2.04	1.59
3.5586	2.90	3.06	1.70	2.64	2.01	1.57
3.5638	2.88	3.02	1.68	2.62	1.99	1.56
3.5690	2.86	2.97	1.67	2.60	1.96	1.55
3.5743	2.84	2.94	1.65	2.59	1.94	1.54
3.5795	2.82	2.90	1.64	2.57	1.92	1.53

Frequency (Hz)	1D PS-Logging	1D LR = 1.5	1D LR = 2.0	1D LR = 3.0	1D LR = 5.0	2D Mean Azimuth
3.5848	2.81	2.86	1.62	2.55	1.90	1.52
3.5900	2.79	2.83	1.61	2.54	1.87	1.51
3.5953	2.78	2.79	1.59	2.53	1.85	1.50
3.6005	2.76	2.76	1.58	2.51	1.84	1.49
3.6058	2.75	2.73	1.57	2.50	1.82	1.48
3.6111	2.73	2.70	1.55	2.49	1.80	1.47
3.6164	2.72	2.67	1.54	2.48	1.78	1.46
3.6217	2.71	2.64	1.53	2.47	1.76	1.45
3.6270	2.70	2.62	1.52	2.46	1.75	1.45
3.6323	2.69	2.59	1.51	2.45	1.73	1.44
3.6376	2.68	2.57	1.50	2.45	1.72	1.43
3.6429	2.67	2.54	1.49	2.44	1.70	1.42
3.6483	2.66	2.52	1.48	2.43	1.69	1.42
3.6536	2.65	2.50	1.47	2.43	1.67	1.41
3.6590	2.64	2.48	1.46	2.43	1.66	1.40
3.6643	2.64	2.46	1.45	2.42	1.65	1.40
3.6697	2.63	2.44	1.44	2.42	1.64	1.39
3.6751	2.63	2.42	1.44	2.42	1.62	1.39
3.6804	2.62	2.40	1.43	2.42	1.61	1.38
3.6858	2.62	2.38	1.42	2.41	1.60	1.38
3.6912	2.61	2.37	1.41	2.42	1.59	1.37
3.6966	2.61	2.35	1.41	2.42	1.58	1.37
3.7020	2.60	2.34	1.40	2.42	1.57	1.36
3.7075	2.60	2.32	1.39	2.42	1.56	1.36
3.7129	2.60	2.31	1.39	2.42	1.55	1.35
3.7183	2.60	2.29	1.38	2.43	1.54	1.35
3.7238	2.60	2.28	1.37	2.43	1.54	1.35
3.7292	2.60	2.27	1.37	2.44	1.53	1.34
3.7347	2.60	2.26	1.36	2.44	1.52	1.34
3.7402	2.60	2.25	1.36	2.45	1.51	1.34
3.7456	2.60	2.24	1.35	2.46	1.51	1.34
3.7511	2.60	2.23	1.35	2.47	1.50	1.33
3.7566	2.60	2.22	1.35	2.47	1.49	1.33
3.7621	2.61	2.21	1.34	2.48	1.49	1.33
3.7676	2.61	2.20	1.34	2.50	1.48	1.33
3.7732	2.62	2.19	1.33	2.51	1.47	1.33
3.7787	2.62	2.18	1.33	2.52	1.47	1.33
3.7842	2.62	2.18	1.33	2.54	1.46	1.33
3.7898	2.63	2.17	1.33	2.55	1.46	1.33
3.7953	2.64	2.17	1.32	2.57	1.46	1.33
3.8009	2.64	2.16	1.32	2.58	1.45	1.33
3.8064	2.65	2.15	1.32	2.60	1.45	1.33
3.8120	2.66	2.15	1.32	2.62	1.44	1.33
3.8176	2.67	2.15	1.31	2.64	1.44	1.33
3.8232	2.68	2.14	1.31	2.66	1.44	1.33
3.8288	2.69	2.14	1.31	2.69	1.43	1.33
3.8344	2.70	2.14	1.31	2.71	1.43	1.33
3.8400	2.71	2.13	1.31	2.74	1.43	1.33
3.8456	2.72	2.13	1.31	2.76	1.43	1.33
3.8513	2.74	2.13	1.31	2.79	1.43	1.34
3.8569	2.75	2.13	1.31	2.82	1.42	1.34
3.8625	2.77	2.13	1.31	2.86	1.42	1.34
3.8682	2.78	2.13	1.31	2.89	1.42	1.34
3.8739	2.80	2.13	1.31	2.93	1.42	1.35

Frequency (Hz)	1D PS-Logging	1D LR = 1.5	1D LR = 2.0	1D LR = 3.0	1D LR = 5.0	2D Mean Azimuth
3.8795	2.82	2.13	1.31	2.97	1.42	1.35
3.8852	2.83	2.13	1.31	3.01	1.42	1.35
3.8909	2.85	2.13	1.31	3.05	1.42	1.36
3.8966	2.87	2.14	1.31	3.09	1.42	1.36
3.9023	2.89	2.14	1.31	3.14	1.42	1.37
3.9080	2.91	2.14	1.32	3.19	1.42	1.37
3.9138	2.94	2.15	1.32	3.25	1.42	1.38
3.9195	2.96	2.15	1.32	3.30	1.42	1.38
3.9252	2.99	2.16	1.32	3.36	1.42	1.39
3.9310	3.01	2.16	1.33	3.43	1.43	1.40
3.9367	3.04	2.17	1.33	3.49	1.43	1.40
3.9425	3.07	2.17	1.33	3.57	1.43	1.41
3.9483	3.10	2.18	1.34	3.64	1.43	1.42
3.9541	3.13	2.19	1.34	3.72	1.44	1.42
3.9598	3.16	2.20	1.34	3.81	1.44	1.43
3.9656	3.19	2.20	1.35	3.90	1.44	1.44
3.9715	3.23	2.21	1.35	4.00	1.45	1.45
3.9773	3.27	2.22	1.36	4.11	1.45	1.46
3.9831	3.30	2.23	1.36	4.22	1.45	1.47
3.9889	3.34	2.24	1.37	4.34	1.46	1.48
3.9948	3.39	2.26	1.37	4.48	1.46	1.49
4.0006	3.43	2.27	1.38	4.62	1.47	1.50
4.0065	3.48	2.28	1.38	4.77	1.47	1.51
4.0123	3.52	2.30	1.39	4.94	1.48	1.52
4.0182	3.57	2.31	1.40	5.12	1.48	1.53
4.0241	3.63	2.33	1.40	5.32	1.49	1.54
4.0300	3.68	2.34	1.41	5.53	1.50	1.55
4.0359	3.74	2.36	1.42	5.77	1.50	1.57
4.0418	3.80	2.38	1.43	6.03	1.51	1.58
4.0477	3.86	2.39	1.44	6.32	1.52	1.60
4.0537	3.93	2.41	1.44	6.64	1.53	1.61
4.0596	4.00	2.43	1.45	6.99	1.54	1.63
4.0655	4.07	2.46	1.46	7.39	1.55	1.64
4.0715	4.15	2.48	1.47	7.83	1.55	1.66
4.0775	4.23	2.50	1.48	8.33	1.56	1.68
4.0834	4.31	2.53	1.49	8.90	1.57	1.69
4.0894	4.40	2.55	1.51	9.54	1.58	1.71
4.0954	4.50	2.58	1.52	10.28	1.60	1.73
4.1014	4.60	2.61	1.53	11.11	1.61	1.75
4.1074	4.70	2.63	1.54	12.05	1.62	1.77
4.1134	4.82	2.67	1.56	13.10	1.63	1.80
4.1194	4.93	2.70	1.57	14.26	1.64	1.82
4.1255	5.06	2.73	1.58	15.48	1.66	1.84
4.1315	5.19	2.77	1.60	16.68	1.67	1.87
4.1376	5.33	2.80	1.61	17.71	1.69	1.89
4.1436	5.48	2.84	1.63	18.37	1.70	1.92
4.1497	5.64	2.88	1.65	18.52	1.72	1.95
4.1558	5.82	2.92	1.66	18.08	1.73	1.98
4.1619	6.00	2.97	1.68	17.17	1.75	2.01
4.1680	6.20	3.01	1.70	15.97	1.77	2.04
4.1741	6.41	3.06	1.72	14.67	1.79	2.08
4.1802	6.64	3.12	1.74	13.39	1.80	2.11
4.1863	6.88	3.17	1.76	12.20	1.82	2.15
4.1924	7.15	3.23	1.78	11.13	1.84	2.19

Frequency (Hz)	1D PS-Logging	1D LR = 1.5	1D LR = 2.0	1D LR = 3.0	1D LR = 5.0	2D Mean Azimuth
4.1986	7.43	3.29	1.81	10.19	1.87	2.23
4.2047	7.75	3.35	1.83	9.36	1.89	2.27
4.2109	8.09	3.42	1.85	8.63	1.91	2.32
4.2170	8.46	3.49	1.88	7.99	1.94	2.36
4.2232	8.87	3.56	1.91	7.43	1.96	2.41
4.2294	9.32	3.64	1.93	6.93	1.99	2.47
4.2356	9.81	3.72	1.96	6.49	2.01	2.52
4.2418	10.36	3.81	1.99	6.09	2.04	2.58
4.2480	10.98	3.90	2.03	5.74	2.07	2.64
4.2542	11.66	4.00	2.06	5.43	2.10	2.70
4.2605	12.42	4.11	2.09	5.14	2.14	2.77
4.2667	13.28	4.22	2.13	4.88	2.17	2.84
4.2730	14.24	4.34	2.17	4.64	2.20	2.92
4.2792	15.33	4.47	2.21	4.43	2.24	3.00
4.2855	16.55	4.61	2.25	4.23	2.28	3.08
4.2918	17.91	4.76	2.29	4.05	2.32	3.17
4.2980	19.41	4.92	2.34	3.88	2.36	3.27
4.3043	21.03	5.09	2.39	3.73	2.40	3.37
4.3106	22.70	5.27	2.44	3.58	2.45	3.48
4.3170	24.32	5.47	2.49	3.45	2.50	3.59
4.3233	25.72	5.69	2.54	3.33	2.55	3.72
4.3296	26.67	5.93	2.60	3.21	2.60	3.85
4.3360	27.01	6.19	2.67	3.10	2.66	3.99
4.3423	26.65	6.47	2.73	3.00	2.72	4.14
4.3487	25.68	6.79	2.80	2.91	2.78	4.30
4.3550	24.28	7.13	2.87	2.82	2.84	4.47
4.3614	22.66	7.52	2.95	2.74	2.91	4.65
4.3678	21.00	7.94	3.03	2.66	2.99	4.85
4.3742	19.39	8.42	3.12	2.58	3.06	5.06
4.3806	17.91	8.95	3.22	2.51	3.14	5.28
4.3870	16.56	9.55	3.31	2.44	3.23	5.52
4.3934	15.35	10.24	3.42	2.38	3.32	5.78
4.3999	14.27	11.01	3.54	2.32	3.42	6.05
4.4063	13.32	11.88	3.66	2.26	3.52	6.33
4.4128	12.47	12.88	3.79	2.21	3.64	6.62
4.4192	11.71	14.00	3.93	2.16	3.75	6.93
4.4257	11.04	15.26	4.08	2.11	3.88	7.24
4.4322	10.43	16.63	4.25	2.06	4.02	7.54
4.4387	9.89	18.05	4.43	2.02	4.16	7.84
4.4452	9.40	19.43	4.62	1.98	4.32	8.12
4.4517	8.95	20.58	4.84	1.94	4.49	8.36
4.4582	8.55	21.28	5.07	1.90	4.68	8.57
4.4647	8.18	21.37	5.33	1.86	4.88	8.73
4.4713	7.84	20.83	5.61	1.83	5.09	8.82
4.4778	7.53	19.78	5.92	1.79	5.33	8.85
4.4844	7.25	18.42	6.27	1.76	5.59	8.82
4.4910	6.99	16.96	6.66	1.73	5.88	8.73
4.4975	6.74	15.54	7.09	1.70	6.20	8.58
4.5041	6.52	14.22	7.58	1.67	6.55	8.39
4.5107	6.31	13.03	8.13	1.64	6.93	8.18
4.5173	6.12	11.97	8.76	1.62	7.37	7.95
4.5239	5.94	11.05	9.47	1.59	7.85	7.72
4.5306	5.77	10.23	10.27	1.57	8.40	7.49
4.5372	5.61	9.51	11.18	1.54	9.01	7.27

Frequency (Hz)	1D PS-Logging	1D LR = 1.5	1D LR = 2.0	1D LR = 3.0	1D LR = 5.0	2D Mean Azimuth
4.5438	5.47	8.87	12.19	1.52	9.70	7.07
4.5505	5.33	8.31	13.30	1.50	10.49	6.89
4.5572	5.20	7.81	14.46	1.48	11.37	6.73
4.5638	5.08	7.36	15.60	1.46	12.35	6.58
4.5705	4.96	6.96	16.59	1.44	13.44	6.44
4.5772	4.86	6.60	17.26	1.42	14.60	6.28
4.5839	4.75	6.28	17.47	1.40	15.79	6.10
4.5906	4.66	5.98	17.18	1.38	16.90	5.90
4.5974	4.57	5.71	16.46	1.37	17.80	5.67
4.6041	4.48	5.46	15.45	1.35	18.34	5.44
4.6108	4.40	5.24	14.33	1.34	18.40	5.21
4.6176	4.33	5.03	13.20	1.32	17.97	4.98
4.6243	4.26	4.84	12.14	1.31	17.15	4.77
4.6311	4.19	4.66	11.17	1.29	16.10	4.58
4.6379	4.12	4.50	10.31	1.28	14.96	4.40
4.6447	4.06	4.34	9.54	1.27	13.82	4.23
4.6515	4.00	4.20	8.87	1.25	12.76	4.08
4.6583	3.95	4.07	8.27	1.24	11.78	3.94
4.6651	3.90	3.94	7.74	1.23	10.91	3.82
4.6720	3.85	3.83	7.27	1.22	10.13	3.70
4.6788	3.80	3.72	6.86	1.21	9.44	3.59
4.6857	3.76	3.62	6.48	1.20	8.83	3.49
4.6925	3.72	3.52	6.15	1.19	8.28	3.40
4.6994	3.68	3.43	5.85	1.18	7.80	3.31
4.7063	3.64	3.34	5.58	1.17	7.37	3.23
4.7132	3.61	3.26	5.33	1.16	6.98	3.15
4.7201	3.58	3.19	5.11	1.15	6.63	3.08
4.7270	3.55	3.12	4.90	1.15	6.32	3.01
4.7339	3.52	3.05	4.71	1.14	6.03	2.95
4.7408	3.49	2.98	4.54	1.13	5.77	2.89
4.7478	3.47	2.92	4.38	1.12	5.54	2.84
4.7547	3.44	2.86	4.24	1.12	5.32	2.78
4.7617	3.42	2.81	4.10	1.11	5.12	2.73
4.7687	3.40	2.76	3.98	1.11	4.94	2.69
4.7757	3.38	2.71	3.86	1.10	4.77	2.64
4.7826	3.37	2.66	3.75	1.09	4.62	2.60
4.7897	3.35	2.61	3.65	1.09	4.47	2.57
4.7967	3.34	2.57	3.55	1.08	4.34	2.53
4.8037	3.33	2.53	3.47	1.08	4.22	2.49
4.8107	3.32	2.49	3.38	1.08	4.10	2.46
4.8178	3.31	2.45	3.31	1.07	3.99	2.43
4.8248	3.30	2.41	3.23	1.07	3.89	2.40
4.8319	3.30	2.38	3.17	1.06	3.80	2.38
4.8390	3.29	2.35	3.10	1.06	3.71	2.35
4.8461	3.29	2.32	3.04	1.06	3.63	2.33
4.8532	3.29	2.29	2.98	1.06	3.55	2.31
4.8603	3.29	2.26	2.93	1.05	3.48	2.29
4.8674	3.29	2.23	2.88	1.05	3.41	2.27
4.8745	3.29	2.20	2.83	1.05	3.35	2.25
4.8816	3.30	2.18	2.79	1.05	3.28	2.23
4.8888	3.30	2.16	2.75	1.05	3.23	2.22
4.8960	3.31	2.13	2.71	1.04	3.17	2.20
4.9031	3.32	2.11	2.67	1.04	3.12	2.19
4.9103	3.33	2.09	2.63	1.04	3.08	2.18

Frequency (Hz)	1D PS-Logging	1D LR = 1.5	1D LR = 2.0	1D LR = 3.0	1D LR = 5.0	2D Mean Azimuth
4.9175	3.35	2.07	2.60	1.04	3.03	2.17
4.9247	3.36	2.05	2.57	1.04	2.99	2.15
4.9319	3.38	2.03	2.54	1.04	2.95	2.15
4.9391	3.39	2.02	2.51	1.04	2.91	2.14
4.9464	3.41	2.00	2.49	1.04	2.88	2.13
4.9536	3.44	1.99	2.46	1.04	2.84	2.12
4.9609	3.46	1.97	2.44	1.04	2.81	2.12
4.9681	3.48	1.96	2.42	1.05	2.78	2.11
4.9754	3.51	1.94	2.40	1.05	2.75	2.11
4.9827	3.54	1.93	2.38	1.05	2.73	2.10
4.9900	3.58	1.92	2.36	1.05	2.70	2.10
4.9973	3.61	1.91	2.35	1.05	2.68	2.10
5.0046	3.65	1.90	2.33	1.06	2.66	2.10
5.0120	3.69	1.89	2.32	1.06	2.64	2.10
5.0193	3.73	1.88	2.31	1.06	2.62	2.10
5.0266	3.78	1.87	2.29	1.07	2.61	2.10
5.0340	3.83	1.86	2.28	1.07	2.59	2.11
5.0414	3.88	1.86	2.28	1.07	2.58	2.11
5.0488	3.94	1.85	2.27	1.08	2.56	2.12
5.0562	4.00	1.85	2.26	1.08	2.55	2.12
5.0636	4.06	1.84	2.26	1.09	2.54	2.13
5.0710	4.13	1.84	2.25	1.09	2.53	2.14
5.0784	4.21	1.83	2.25	1.10	2.52	2.15
5.0858	4.28	1.83	2.25	1.11	2.52	2.16
5.0933	4.37	1.83	2.25	1.11	2.51	2.18
5.1007	4.46	1.82	2.25	1.12	2.51	2.19
5.1082	4.56	1.82	2.25	1.13	2.51	2.20
5.1157	4.66	1.82	2.25	1.13	2.50	2.22
5.1232	4.77	1.82	2.25	1.14	2.50	2.24
5.1307	4.89	1.82	2.26	1.15	2.50	2.26
5.1382	5.02	1.82	2.26	1.16	2.51	2.28
5.1457	5.16	1.82	2.27	1.17	2.51	2.30
5.1533	5.32	1.82	2.28	1.18	2.51	2.32
5.1608	5.48	1.83	2.29	1.19	2.52	2.35
5.1684	5.66	1.83	2.30	1.20	2.52	2.37
5.1759	5.85	1.83	2.31	1.21	2.53	2.40
5.1835	6.06	1.84	2.32	1.22	2.54	2.43
5.1911	6.29	1.84	2.33	1.24	2.55	2.47
5.1987	6.54	1.85	2.35	1.25	2.56	2.50
5.2063	6.82	1.85	2.37	1.26	2.57	2.54
5.2140	7.12	1.86	2.39	1.28	2.59	2.58
5.2216	7.46	1.87	2.41	1.29	2.60	2.62
5.2292	7.84	1.87	2.43	1.31	2.62	2.66
5.2369	8.25	1.88	2.45	1.32	2.64	2.71
5.2446	8.72	1.89	2.48	1.34	2.66	2.76
5.2522	9.24	1.90	2.50	1.36	2.68	2.81
5.2599	9.82	1.91	2.53	1.38	2.71	2.87
5.2676	10.48	1.92	2.56	1.40	2.73	2.93
5.2754	11.22	1.94	2.60	1.42	2.76	3.00
5.2831	12.06	1.95	2.63	1.44	2.79	3.06
5.2908	12.99	1.97	2.67	1.46	2.82	3.14
5.2986	14.02	1.98	2.71	1.49	2.85	3.21
5.3063	15.14	2.00	2.76	1.51	2.89	3.29
5.3141	16.31	2.01	2.80	1.54	2.93	3.38

Frequency (Hz)	1D PS-Logging	1D LR = 1.5	1D LR = 2.0	1D LR = 3.0	1D LR = 5.0	2D Mean Azimuth
5.3219	17.45	2.03	2.85	1.57	2.97	3.47
5.3297	18.44	2.05	2.91	1.60	3.01	3.57
5.3375	19.13	2.07	2.97	1.63	3.06	3.68
5.3453	19.39	2.09	3.03	1.66	3.11	3.79
5.3531	19.13	2.11	3.09	1.70	3.16	3.90
5.3610	18.41	2.14	3.17	1.73	3.22	4.02
5.3688	17.35	2.16	3.24	1.77	3.28	4.15
5.3767	16.13	2.19	3.33	1.81	3.34	4.29
5.3846	14.87	2.22	3.42	1.86	3.41	4.43
5.3924	13.66	2.25	3.51	1.90	3.48	4.58
5.4003	12.54	2.28	3.62	1.95	3.56	4.73
5.4083	11.52	2.31	3.73	2.00	3.64	4.88
5.4162	10.62	2.35	3.85	2.06	3.73	5.04
5.4241	9.82	2.38	3.99	2.11	3.83	5.19
5.4320	9.11	2.42	4.13	2.18	3.93	5.33
5.4400	8.48	2.46	4.29	2.24	4.05	5.47
5.4480	7.93	2.51	4.47	2.32	4.17	5.59
5.4559	7.43	2.55	4.66	2.39	4.30	5.70
5.4639	6.98	2.60	4.88	2.47	4.44	5.79
5.4719	6.59	2.65	5.12	2.56	4.60	5.85
5.4800	6.23	2.71	5.38	2.66	4.76	5.88
5.4880	5.90	2.76	5.68	2.76	4.95	5.88
5.4960	5.61	2.82	6.01	2.87	5.15	5.86
5.5041	5.34	2.89	6.39	2.99	5.37	5.81
5.5121	5.10	2.96	6.81	3.13	5.61	5.74
5.5202	4.87	3.03	7.30	3.27	5.88	5.65
5.5283	4.67	3.11	7.85	3.43	6.18	5.55
5.5364	4.48	3.19	8.48	3.61	6.51	5.45
5.5445	4.30	3.28	9.20	3.80	6.88	5.34
5.5526	4.14	3.38	10.01	4.02	7.30	5.24
5.5607	3.99	3.48	10.92	4.26	7.77	5.15
5.5689	3.85	3.59	11.89	4.53	8.30	5.06
5.5770	3.72	3.71	12.87	4.83	8.90	4.97
5.5852	3.60	3.84	13.75	5.17	9.59	4.88
5.5934	3.49	3.98	14.38	5.56	10.37	4.78
5.6016	3.38	4.13	14.60	6.01	11.26	4.65
5.6098	3.28	4.30	14.36	6.51	12.26	4.50
5.6180	3.19	4.48	13.69	7.09	13.37	4.32
5.6262	3.10	4.67	12.76	7.76	14.54	4.12
5.6345	3.02	4.89	11.71	8.51	15.70	3.93
5.6427	2.94	5.12	10.67	9.34	16.72	3.74
5.6510	2.87	5.38	9.70	10.23	17.41	3.56
5.6593	2.80	5.67	8.83	11.12	17.61	3.40
5.6676	2.73	5.99	8.07	11.91	17.26	3.25
5.6759	2.67	6.35	7.40	12.45	16.44	3.11
5.6842	2.61	6.76	6.81	12.62	15.33	2.98
5.6925	2.55	7.21	6.30	12.38	14.11	2.87
5.7008	2.50	7.73	5.85	11.79	12.89	2.76
5.7092	2.45	8.31	5.45	11.00	11.77	2.66
5.7175	2.40	8.97	5.10	10.14	10.75	2.57
5.7259	2.36	9.72	4.79	9.29	9.85	2.48
5.7343	2.31	10.56	4.51	8.51	9.06	2.41
5.7427	2.27	11.50	4.26	7.80	8.37	2.33
5.7511	2.23	12.52	4.04	7.18	7.76	2.26

Frequency (Hz)	1D PS-Logging	1D LR = 1.5	1D LR = 2.0	1D LR = 3.0	1D LR = 5.0	2D Mean Azimuth
5.7595	2.20	13.57	3.83	6.64	7.23	2.20
5.7680	2.16	14.58	3.65	6.16	6.76	2.14
5.7764	2.13	15.43	3.48	5.74	6.34	2.08
5.7849	2.10	15.95	3.33	5.38	5.97	2.03
5.7933	2.06	16.03	3.18	5.05	5.63	1.98
5.8018	2.03	15.65	3.05	4.77	5.34	1.93
5.8103	2.01	14.90	2.94	4.51	5.07	1.88
5.8188	1.98	13.93	2.82	4.28	4.82	1.84
5.8274	1.95	12.87	2.72	4.08	4.60	1.80
5.8359	1.93	11.83	2.63	3.90	4.40	1.76
5.8444	1.91	10.86	2.54	3.73	4.21	1.73
5.8530	1.89	9.98	2.46	3.58	4.04	1.69
5.8616	1.86	9.19	2.38	3.44	3.89	1.66
5.8702	1.84	8.50	2.31	3.32	3.74	1.63
5.8787	1.83	7.89	2.24	3.20	3.61	1.60
5.8874	1.81	7.36	2.18	3.10	3.49	1.57
5.8960	1.79	6.88	2.12	3.00	3.37	1.55
5.9046	1.77	6.46	2.06	2.91	3.26	1.52
5.9133	1.76	6.08	2.01	2.83	3.17	1.50
5.9219	1.74	5.75	1.96	2.75	3.07	1.47
5.9306	1.73	5.45	1.91	2.68	2.99	1.45
5.9393	1.72	5.18	1.87	2.62	2.90	1.43
5.9480	1.71	4.93	1.82	2.56	2.83	1.41
5.9567	1.69	4.71	1.78	2.50	2.76	1.39
5.9654	1.68	4.51	1.75	2.45	2.69	1.38
5.9742	1.67	4.33	1.71	2.40	2.63	1.36
5.9829	1.66	4.16	1.68	2.35	2.57	1.34
5.9917	1.66	4.00	1.64	2.31	2.51	1.33
6.0004	1.65	3.86	1.61	2.27	2.46	1.31
6.0092	1.64	3.73	1.58	2.24	2.41	1.30
6.0180	1.63	3.61	1.56	2.20	2.36	1.29
6.0268	1.63	3.49	1.53	2.17	2.32	1.28
6.0357	1.62	3.39	1.50	2.14	2.27	1.26
6.0445	1.62	3.29	1.48	2.12	2.23	1.25
6.0534	1.61	3.20	1.46	2.09	2.20	1.24
6.0622	1.61	3.12	1.44	2.07	2.16	1.23
6.0711	1.60	3.04	1.42	2.05	2.13	1.22
6.0800	1.60	2.96	1.40	2.03	2.09	1.22
6.0889	1.60	2.89	1.38	2.01	2.06	1.21
6.0978	1.60	2.83	1.36	2.00	2.03	1.20
6.1067	1.60	2.77	1.34	1.98	2.01	1.19
6.1157	1.60	2.71	1.33	1.97	1.98	1.19
6.1246	1.60	2.66	1.31	1.96	1.96	1.18
6.1336	1.60	2.61	1.30	1.95	1.93	1.18
6.1426	1.60	2.56	1.28	1.94	1.91	1.17
6.1516	1.60	2.51	1.27	1.93	1.89	1.17
6.1606	1.61	2.47	1.26	1.93	1.87	1.16
6.1696	1.61	2.43	1.25	1.92	1.85	1.16
6.1787	1.61	2.40	1.23	1.92	1.83	1.16
6.1877	1.62	2.36	1.22	1.92	1.82	1.16
6.1968	1.62	2.33	1.21	1.92	1.80	1.15
6.2059	1.63	2.30	1.20	1.92	1.79	1.15
6.2149	1.64	2.27	1.20	1.92	1.77	1.15
6.2240	1.64	2.24	1.19	1.92	1.76	1.15

Frequency (Hz)	1D PS-Logging	1D LR = 1.5	1D LR = 2.0	1D LR = 3.0	1D LR = 5.0	2D Mean Azimuth
6.2332	1.65	2.21	1.18	1.93	1.75	1.15
6.2423	1.66	2.19	1.17	1.94	1.74	1.15
6.2514	1.67	2.17	1.16	1.94	1.73	1.15
6.2606	1.68	2.15	1.16	1.95	1.72	1.15
6.2698	1.69	2.13	1.15	1.97	1.71	1.16
6.2789	1.70	2.11	1.15	1.98	1.70	1.16
6.2881	1.72	2.09	1.14	1.99	1.70	1.16
6.2973	1.73	2.07	1.14	2.01	1.69	1.17
6.3066	1.74	2.06	1.13	2.03	1.68	1.17
6.3158	1.76	2.05	1.13	2.05	1.68	1.17
6.3250	1.77	2.03	1.13	2.07	1.68	1.18
6.3343	1.79	2.02	1.12	2.09	1.67	1.18
6.3436	1.81	2.01	1.12	2.12	1.67	1.19
6.3529	1.83	2.00	1.12	2.14	1.67	1.20
6.3622	1.85	2.00	1.12	2.18	1.67	1.20
6.3715	1.87	1.99	1.12	2.21	1.67	1.21
6.3808	1.90	1.98	1.12	2.24	1.67	1.22
6.3902	1.92	1.98	1.12	2.28	1.67	1.23
6.3995	1.95	1.97	1.12	2.33	1.67	1.24
6.4089	1.97	1.97	1.12	2.37	1.67	1.25
6.4183	2.00	1.97	1.12	2.42	1.67	1.26
6.4277	2.03	1.97	1.12	2.47	1.68	1.27
6.4371	2.06	1.97	1.12	2.53	1.68	1.29
6.4465	2.10	1.97	1.12	2.59	1.69	1.30
6.4560	2.13	1.97	1.13	2.66	1.69	1.31
6.4654	2.17	1.97	1.13	2.74	1.70	1.33
6.4749	2.21	1.98	1.13	2.82	1.71	1.34
6.4844	2.25	1.98	1.14	2.90	1.72	1.36
6.4939	2.30	1.99	1.14	3.00	1.73	1.38
6.5034	2.35	2.00	1.15	3.11	1.74	1.40
6.5129	2.40	2.00	1.16	3.22	1.75	1.42
6.5225	2.45	2.01	1.16	3.35	1.76	1.44
6.5320	2.51	2.02	1.17	3.49	1.77	1.46
6.5416	2.57	2.03	1.18	3.64	1.79	1.49
6.5512	2.63	2.05	1.18	3.82	1.80	1.51
6.5607	2.70	2.06	1.19	4.01	1.82	1.54
6.5704	2.77	2.08	1.20	4.22	1.83	1.57
6.5800	2.85	2.09	1.21	4.46	1.85	1.60
6.5896	2.94	2.11	1.22	4.73	1.87	1.63
6.5993	3.02	2.13	1.23	5.04	1.89	1.66
6.6089	3.12	2.15	1.25	5.39	1.91	1.70
6.6186	3.22	2.17	1.26	5.78	1.94	1.73
6.6283	3.33	2.20	1.27	6.23	1.96	1.77
6.6380	3.45	2.22	1.29	6.74	1.99	1.81
6.6477	3.58	2.25	1.30	7.31	2.01	1.86
6.6575	3.72	2.28	1.32	7.94	2.04	1.90
6.6672	3.87	2.31	1.33	8.60	2.07	1.95
6.6770	4.04	2.34	1.35	9.26	2.11	2.00
6.6868	4.21	2.38	1.37	9.84	2.14	2.06
6.6966	4.41	2.41	1.39	10.25	2.18	2.11
6.7064	4.63	2.45	1.41	10.39	2.22	2.17
6.7162	4.86	2.50	1.44	10.22	2.26	2.24
6.7260	5.12	2.54	1.46	9.78	2.30	2.30
6.7359	5.41	2.59	1.49	9.15	2.35	2.37

Frequency (Hz)	1D PS-Logging	1D LR = 1.5	1D LR = 2.0	1D LR = 3.0	1D LR = 5.0	2D Mean Azimuth
6.7457	5.74	2.64	1.51	8.45	2.40	2.44
6.7556	6.09	2.70	1.54	7.74	2.45	2.52
6.7655	6.50	2.75	1.57	7.07	2.50	2.59
6.7754	6.95	2.82	1.60	6.46	2.56	2.67
6.7853	7.46	2.88	1.64	5.92	2.63	2.75
6.7953	8.04	2.95	1.67	5.45	2.69	2.83
6.8052	8.69	3.03	1.71	5.03	2.76	2.92
6.8152	9.43	3.11	1.75	4.66	2.84	3.00
6.8252	10.26	3.20	1.80	4.34	2.92	3.08
6.8352	11.18	3.30	1.84	4.05	3.01	3.16
6.8452	12.18	3.40	1.89	3.80	3.10	3.24
6.8552	13.22	3.51	1.95	3.57	3.21	3.31
6.8652	14.24	3.63	2.00	3.37	3.31	3.37
6.8753	15.11	3.76	2.07	3.19	3.43	3.43
6.8854	15.72	3.90	2.13	3.03	3.56	3.47
6.8955	15.95	4.05	2.20	2.88	3.69	3.51
6.9056	15.75	4.21	2.28	2.75	3.84	3.53
6.9157	15.18	4.39	2.36	2.62	4.01	3.55
6.9258	14.37	4.59	2.45	2.51	4.18	3.55
6.9359	13.44	4.81	2.55	2.41	4.38	3.54
6.9461	12.49	5.05	2.65	2.32	4.59	3.52
6.9563	11.57	5.32	2.77	2.23	4.82	3.49
6.9665	10.73	5.62	2.89	2.15	5.08	3.46
6.9767	9.97	5.95	3.03	2.08	5.37	3.42
6.9869	9.29	6.32	3.19	2.01	5.69	3.37
6.9971	8.69	6.73	3.36	1.95	6.05	3.32
7.0074	8.16	7.20	3.54	1.89	6.45	3.27
7.0176	7.69	7.74	3.75	1.83	6.91	3.21
7.0279	7.27	8.34	3.99	1.78	7.42	3.16
7.0382	6.90	9.03	4.25	1.73	8.01	3.11
7.0485	6.57	9.80	4.55	1.69	8.68	3.07
7.0588	6.27	10.68	4.88	1.65	9.44	3.03
7.0692	6.01	11.64	5.27	1.61	10.32	2.99
7.0795	5.77	12.68	5.70	1.57	11.30	2.96
7.0899	5.55	13.75	6.20	1.54	12.40	2.93
7.1003	5.36	14.74	6.76	1.50	13.59	2.92
7.1107	5.18	15.53	7.39	1.47	14.79	2.91
7.1211	5.02	15.97	8.09	1.45	15.90	2.91
7.1315	4.88	15.96	8.82	1.42	16.75	2.92
7.1420	4.74	15.52	9.54	1.39	17.15	2.92
7.1524	4.62	14.74	10.17	1.37	17.03	2.92
7.1629	4.51	13.78	10.60	1.35	16.43	2.91
7.1734	4.42	12.77	10.74	1.33	15.50	2.88
7.1839	4.32	11.78	10.56	1.31	14.41	2.83
7.1944	4.24	10.86	10.10	1.29	13.30	2.76
7.2049	4.17	10.03	9.48	1.27	12.24	2.68
7.2155	4.10	9.29	8.79	1.25	11.28	2.59
7.2261	4.04	8.64	8.10	1.24	10.42	2.51
7.2366	3.98	8.06	7.45	1.22	9.67	2.43
7.2472	3.93	7.56	6.86	1.21	9.01	2.36
7.2579	3.89	7.11	6.34	1.20	8.43	2.30
7.2685	3.85	6.71	5.88	1.19	7.92	2.24
7.2791	3.82	6.36	5.48	1.17	7.46	2.19
7.2898	3.79	6.04	5.12	1.16	7.07	2.14

Frequency (Hz)	1D PS-Logging	1D LR = 1.5	1D LR = 2.0	1D LR = 3.0	1D LR = 5.0	2D Mean Azimuth
7.3005	3.77	5.76	4.81	1.15	6.71	2.10
7.3112	3.75	5.51	4.53	1.15	6.40	2.06
7.3219	3.73	5.28	4.29	1.14	6.12	2.03
7.3326	3.72	5.07	4.07	1.13	5.87	2.00
7.3433	3.71	4.89	3.87	1.12	5.64	1.97
7.3541	3.71	4.72	3.70	1.12	5.43	1.94
7.3649	3.71	4.56	3.54	1.11	5.25	1.92
7.3756	3.72	4.42	3.40	1.11	5.08	1.90
7.3864	3.73	4.29	3.27	1.10	4.93	1.89
7.3973	3.75	4.17	3.15	1.10	4.79	1.87
7.4081	3.77	4.07	3.05	1.10	4.67	1.86
7.4189	3.79	3.97	2.95	1.10	4.55	1.85
7.4298	3.82	3.88	2.86	1.09	4.45	1.84
7.4407	3.85	3.80	2.78	1.09	4.36	1.84
7.4516	3.89	3.72	2.70	1.09	4.27	1.83
7.4625	3.93	3.65	2.64	1.09	4.19	1.83
7.4734	3.99	3.59	2.57	1.10	4.12	1.83
7.4844	4.04	3.53	2.52	1.10	4.06	1.83
7.4953	4.10	3.48	2.46	1.10	4.00	1.83
7.5063	4.17	3.43	2.42	1.10	3.95	1.83
7.5173	4.25	3.39	2.37	1.11	3.90	1.84
7.5283	4.34	3.35	2.33	1.11	3.86	1.84
7.5393	4.43	3.31	2.29	1.11	3.82	1.85
7.5504	4.53	3.28	2.26	1.12	3.79	1.86
7.5614	4.65	3.26	2.23	1.13	3.77	1.87
7.5725	4.78	3.23	2.20	1.13	3.74	1.89
7.5836	4.91	3.21	2.18	1.14	3.73	1.90
7.5947	5.07	3.20	2.15	1.15	3.71	1.92
7.6058	5.24	3.18	2.13	1.16	3.70	1.94
7.6170	5.43	3.17	2.11	1.17	3.70	1.96
7.6281	5.64	3.17	2.10	1.18	3.70	1.98
7.6393	5.87	3.17	2.08	1.19	3.70	2.00
7.6505	6.13	3.17	2.07	1.20	3.71	2.03
7.6617	6.42	3.17	2.06	1.22	3.72	2.06
7.6729	6.75	3.18	2.05	1.23	3.73	2.09
7.6841	7.12	3.19	2.05	1.25	3.75	2.12
7.6954	7.54	3.20	2.04	1.26	3.77	2.15
7.7067	8.01	3.22	2.04	1.28	3.80	2.19
7.7180	8.55	3.24	2.04	1.30	3.83	2.23
7.7293	9.17	3.26	2.04	1.32	3.87	2.27
7.7406	9.87	3.29	2.05	1.34	3.91	2.31
7.7519	10.67	3.33	2.05	1.37	3.96	2.35
7.7633	11.58	3.36	2.06	1.39	4.01	2.40
7.7746	12.57	3.40	2.07	1.42	4.07	2.44
7.7860	13.64	3.45	2.08	1.45	4.14	2.49
7.7974	14.72	3.50	2.10	1.48	4.21	2.54
7.8089	15.69	3.56	2.11	1.51	4.29	2.59
7.8203	16.38	3.62	2.13	1.55	4.38	2.64
7.8317	16.65	3.69	2.15	1.59	4.47	2.69
7.8432	16.40	3.77	2.17	1.63	4.58	2.74
7.8547	15.68	3.85	2.20	1.67	4.69	2.78
7.8662	14.66	3.95	2.23	1.72	4.82	2.83
7.8777	13.50	4.05	2.26	1.77	4.95	2.87
7.8893	12.34	4.16	2.29	1.82	5.11	2.91

Frequency (Hz)	1D PS-Logging	1D LR = 1.5	1D LR = 2.0	1D LR = 3.0	1D LR = 5.0	2D Mean Azimuth
7.9008	11.25	4.28	2.33	1.88	5.27	2.94
7.9124	10.27	4.42	2.37	1.94	5.45	2.97
7.9240	9.40	4.57	2.42	2.01	5.66	2.99
7.9356	8.63	4.73	2.47	2.08	5.88	3.01
7.9472	7.96	4.92	2.52	2.16	6.12	3.02
7.9588	7.38	5.12	2.58	2.25	6.40	3.02
7.9705	6.87	5.35	2.64	2.35	6.70	3.01
7.9822	6.41	5.60	2.71	2.45	7.04	3.00
7.9939	6.02	5.88	2.79	2.57	7.42	2.98
8.0056	5.66	6.20	2.87	2.69	7.84	2.96
8.0173	5.35	6.56	2.96	2.83	8.32	2.93
8.0290	5.06	6.97	3.06	2.99	8.86	2.89
8.0408	4.81	7.43	3.17	3.16	9.46	2.86
8.0526	4.58	7.96	3.29	3.35	10.14	2.82
8.0644	4.38	8.56	3.42	3.57	10.90	2.78
8.0762	4.19	9.23	3.57	3.81	11.75	2.73
8.0880	4.02	9.99	3.73	4.09	12.67	2.69
8.0998	3.86	10.83	3.91	4.40	13.64	2.65
8.1117	3.72	11.73	4.11	4.76	14.62	2.61
8.1236	3.59	12.64	4.33	5.16	15.52	2.58
8.1355	3.47	13.47	4.58	5.63	16.23	2.54
8.1474	3.36	14.09	4.87	6.15	16.63	2.51
8.1593	3.26	14.37	5.18	6.74	16.64	2.49
8.1713	3.16	14.23	5.54	7.39	16.25	2.47
8.1832	3.08	13.69	5.95	8.06	15.54	2.45
8.1952	3.00	12.88	6.41	8.70	14.62	2.44
8.2072	2.92	11.93	6.92	9.25	13.62	2.44
8.2193	2.85	10.95	7.48	9.59	12.61	2.44
8.2313	2.79	10.01	8.09	9.65	11.66	2.45
8.2433	2.73	9.16	8.71	9.44	10.78	2.46
8.2554	2.68	8.39	9.30	9.01	9.99	2.47
8.2675	2.63	7.72	9.79	8.45	9.29	2.47
8.2796	2.58	7.13	10.10	7.84	8.66	2.47
8.2917	2.54	6.61	10.16	7.25	8.10	2.44
8.3039	2.50	6.15	9.96	6.70	7.61	2.40
8.3160	2.46	5.75	9.55	6.20	7.17	2.34
8.3282	2.43	5.39	8.98	5.76	6.78	2.27
8.3404	2.39	5.08	8.36	5.37	6.43	2.20
8.3526	2.37	4.79	7.72	5.03	6.11	2.13
8.3649	2.34	4.54	7.12	4.73	5.83	2.07
8.3771	2.32	4.31	6.57	4.47	5.58	2.00
8.3894	2.30	4.11	6.08	4.24	5.35	1.95
8.4017	2.28	3.92	5.64	4.03	5.14	1.90
8.4140	2.26	3.76	5.24	3.85	4.95	1.86
8.4263	2.25	3.60	4.90	3.69	4.78	1.82
8.4386	2.23	3.46	4.59	3.54	4.62	1.78
8.4510	2.22	3.34	4.32	3.41	4.47	1.75
8.4634	2.21	3.22	4.08	3.30	4.34	1.72
8.4758	2.21	3.11	3.86	3.20	4.22	1.70
8.4882	2.20	3.01	3.67	3.10	4.11	1.68
8.5006	2.20	2.92	3.50	3.02	4.01	1.66
8.5131	2.20	2.84	3.34	2.95	3.92	1.64
8.5255	2.20	2.76	3.20	2.88	3.83	1.63
8.5380	2.21	2.69	3.07	2.82	3.76	1.62

Frequency (Hz)	1D PS-Logging	1D LR = 1.5	1D LR = 2.0	1D LR = 3.0	1D LR = 5.0	2D Mean Azimuth
8.5505	2.21	2.62	2.96	2.77	3.69	1.61
8.5631	2.22	2.56	2.85	2.73	3.62	1.60
8.5756	2.23	2.50	2.75	2.68	3.56	1.59
8.5882	2.24	2.45	2.67	2.65	3.51	1.59
8.6007	2.25	2.40	2.58	2.62	3.46	1.58
8.6133	2.27	2.36	2.51	2.59	3.42	1.58
8.6259	2.29	2.31	2.44	2.57	3.38	1.58
8.6386	2.31	2.28	2.38	2.56	3.34	1.59
8.6512	2.33	2.24	2.32	2.54	3.31	1.59
8.6639	2.36	2.21	2.27	2.53	3.29	1.59
8.6766	2.39	2.18	2.22	2.53	3.26	1.60
8.6893	2.42	2.15	2.18	2.53	3.25	1.61
8.7020	2.46	2.12	2.14	2.53	3.23	1.62
8.7148	2.50	2.10	2.10	2.54	3.22	1.63
8.7275	2.54	2.08	2.07	2.55	3.21	1.64
8.7403	2.59	2.06	2.04	2.57	3.21	1.65
8.7531	2.64	2.04	2.01	2.59	3.21	1.67
8.7659	2.69	2.03	1.99	2.61	3.21	1.69
8.7788	2.75	2.01	1.96	2.64	3.22	1.70
8.7916	2.82	2.00	1.94	2.68	3.23	1.72
8.8045	2.89	1.99	1.93	2.72	3.24	1.74
8.8174	2.97	1.99	1.91	2.77	3.26	1.76
8.8303	3.05	1.98	1.90	2.82	3.28	1.78
8.8432	3.15	1.98	1.89	2.88	3.31	1.81
8.8562	3.25	1.97	1.88	2.95	3.34	1.83
8.8692	3.36	1.97	1.87	3.02	3.37	1.85
8.8822	3.49	1.98	1.87	3.10	3.41	1.88
8.8952	3.62	1.98	1.87	3.20	3.46	1.90
8.9082	3.77	1.98	1.86	3.30	3.51	1.92
8.9212	3.94	1.99	1.87	3.42	3.56	1.95
8.9343	4.12	2.00	1.87	3.56	3.62	1.97
8.9474	4.33	2.01	1.88	3.70	3.69	1.99
8.9605	4.56	2.02	1.88	3.87	3.77	2.01
8.9736	4.81	2.04	1.89	4.06	3.85	2.03
8.9868	5.10	2.05	1.91	4.28	3.94	2.04
8.9999	5.43	2.07	1.92	4.52	4.04	2.06
9.0131	5.80	2.09	1.94	4.80	4.15	2.06
9.0263	6.22	2.12	1.96	5.11	4.28	2.07
9.0395	6.70	2.14	1.98	5.47	4.41	2.07
9.0528	7.24	2.17	2.00	5.87	4.56	2.07
9.0660	7.86	2.20	2.03	6.32	4.73	2.07
9.0793	8.55	2.24	2.06	6.81	4.91	2.06
9.0926	9.31	2.28	2.10	7.33	5.12	2.05
9.1059	10.12	2.32	2.14	7.85	5.34	2.03
9.1192	10.92	2.36	2.18	8.31	5.60	2.01
9.1326	11.63	2.41	2.23	8.66	5.89	1.99
9.1460	12.15	2.47	2.28	8.80	6.21	1.97
9.1594	12.35	2.53	2.34	8.71	6.58	1.95
9.1728	12.19	2.59	2.40	8.38	6.99	1.92
9.1862	11.72	2.66	2.47	7.90	7.47	1.90
9.1997	11.04	2.74	2.55	7.33	8.01	1.87
9.2131	10.25	2.82	2.64	6.73	8.64	1.84
9.2266	9.46	2.91	2.73	6.17	9.37	1.82
9.2401	8.70	3.01	2.84	5.64	10.20	1.79

Frequency (Hz)	1D PS-Logging	1D LR = 1.5	1D LR = 2.0	1D LR = 3.0	1D LR = 5.0	2D Mean Azimuth
9.2537	8.02	3.12	2.96	5.18	11.16	1.77
9.2672	7.40	3.24	3.09	4.76	12.25	1.75
9.2808	6.86	3.38	3.24	4.39	13.44	1.73
9.2944	6.38	3.53	3.40	4.07	14.67	1.71
9.3080	5.97	3.69	3.59	3.79	15.81	1.69
9.3216	5.60	3.88	3.80	3.54	16.66	1.68
9.3353	5.27	4.08	4.04	3.32	17.00	1.67
9.3490	4.99	4.31	4.32	3.12	16.73	1.67
9.3627	4.73	4.58	4.63	2.95	15.93	1.67
9.3764	4.51	4.87	4.99	2.79	14.79	1.67
9.3901	4.31	5.21	5.41	2.65	13.54	1.68
9.4038	4.13	5.59	5.88	2.52	12.32	1.69
9.4176	3.96	6.03	6.41	2.41	11.19	1.71
9.4314	3.82	6.53	6.99	2.31	10.20	1.74
9.4452	3.69	7.11	7.59	2.21	9.33	1.77
9.4591	3.57	7.77	8.16	2.13	8.58	1.79
9.4729	3.46	8.52	8.61	2.05	7.93	1.81
9.4868	3.37	9.33	8.84	1.98	7.36	1.81
9.5007	3.28	10.18	8.78	1.91	6.87	1.80
9.5146	3.20	10.98	8.45	1.85	6.44	1.76
9.5285	3.13	11.61	7.92	1.80	6.06	1.70
9.5425	3.06	11.94	7.30	1.75	5.73	1.64
9.5565	3.01	11.88	6.66	1.70	5.43	1.59
9.5705	2.96	11.45	6.06	1.66	5.17	1.53
9.5845	2.91	10.76	5.52	1.62	4.93	1.48
9.5985	2.87	9.95	5.05	1.58	4.72	1.44
9.6126	2.83	9.13	4.63	1.55	4.54	1.40
9.6266	2.80	8.35	4.27	1.51	4.37	1.36
9.6407	2.78	7.65	3.95	1.49	4.21	1.34
9.6549	2.75	7.03	3.68	1.46	4.07	1.31
9.6690	2.74	6.49	3.43	1.44	3.95	1.29
9.6832	2.72	6.01	3.22	1.41	3.83	1.27
9.6973	2.71	5.60	3.03	1.39	3.73	1.25
9.7115	2.71	5.24	2.87	1.38	3.63	1.24
9.7258	2.70	4.93	2.72	1.36	3.55	1.23
9.7400	2.71	4.65	2.58	1.34	3.47	1.22
9.7543	2.71	4.41	2.46	1.33	3.40	1.21
9.7686	2.72	4.19	2.36	1.32	3.34	1.21
9.7829	2.73	4.00	2.26	1.31	3.28	1.20
9.7972	2.75	3.83	2.17	1.30	3.23	1.20
9.8115	2.77	3.67	2.09	1.29	3.18	1.20
9.8259	2.80	3.54	2.01	1.29	3.14	1.20
9.8403	2.83	3.41	1.95	1.28	3.10	1.20
9.8547	2.87	3.30	1.89	1.28	3.07	1.20
9.8692	2.91	3.20	1.83	1.28	3.05	1.21
9.8836	2.96	3.11	1.78	1.28	3.02	1.21
9.8981	3.01	3.03	1.73	1.28	3.00	1.22
9.9126	3.07	2.96	1.69	1.28	2.99	1.23
9.9271	3.13	2.89	1.65	1.28	2.98	1.24
9.9416	3.21	2.83	1.61	1.29	2.97	1.25
9.9562	3.29	2.78	1.58	1.30	2.97	1.26
9.9708	3.38	2.73	1.55	1.30	2.97	1.27
9.9854	3.48	2.69	1.52	1.31	2.97	1.28

Frequency (Hz)	**1D PS-Logging**	**1D LR = 1.5**	**1D LR = 2.0**	**1D LR = 3.0**	**1D LR = 5.0**	**2D Mean Azimuth**
10.0000	3.60	2.65	1.49	1.32	2.98	1.29